THE EFFECT OF INLET SWIRL ON KNOCK LIMITS IN SPARK IGNITION ENGINES

by

C. B. ALLISON

Submitted to the University of Cape Town
in partial fulfilment for the degree of
Master of Science in Engineering

DECLARATION

I, Colin Bidden Allison, submit this thesis in partial fulfilment of the requirements of the degree of Master of Science in Engineering. I claim that this is my original work and that it has not been submitted in this or in a similar form for a degree at an other University.

Signed by candidate

Signature Removed

.....

C. B. Allison BSc.(Eng.) Mechanical

7th day of Feb 1992

ABSTRACT

An investigation was undertaken to determine the effect of swirl ratio on knock limits in spark ignition engines. Initially it was attempted to find a correlation between swirl ratio and Knock Limited Spark Advance (KLSA) for a selection of commercially available engines. A comparison of measured swirl ratios and KLSA indicated that no such correlation could be found. This was put down to the fact that other factors such as combustion chamber shape and spark plug location play a more dominant role in affecting knock limits than swirl level.

Following from this, a single engine with a relatively poor swirl ratio was selected and the swirl level was altered. A novel method of increasing and decreasing the swirl level, with the same pressure drop in each case was developed, and this development is described. This method made it possible to perform dynamometer tests, measuring the KLSA timing for the cases of low and high swirl, while keeping all other parameters such as pressure, temperature, spark plug location and combustion chamber shape constant. All these factors are known to have an affect on the occurrence of knock. In this manner it was possible to determine whether swirl alone has any affect on knock limits. It was found that the high swirl case exhibited higher values of knock limited spark advance above the low swirl case although there was no significant change in torque.

A comparison of rubber castings of the inlet ports of numerous engines was made, and is presented in a photographic form. This was done in order to asses how inlet port geometry affects swirl ratios. It was found that a helically shaped inlet port produced the greatest swirl ratio, non directed ports have average values and multiple inlet valve ports have very low swirl ratios.

Furthermore, a comparison of swirl ratios of an inlet port with and without deposits, demonstrates that deposits have a significant affect on swirl ratios and volumetric efficiency. However, although the volumetric efficiency was reduced, the deposits enhanced the swirl ratios for this particular case. This is contrary to the general belief that deposits reduce swirl.

ACKNOWLEDGEMENTS

The author wishes to thank the following for their invaluable support and assistance:

Professor T. Priede for his exalted supervision, guidance and pertinent ideas.

Professor R.K. Dutkiewicz for his interest, and suggestions.

Mr L. Watkins and the workshop staff of the Energy Research Institute for their prompt assistance and considerable patience.

Dr G.H. Hendricks for participating in useful discussion.

Mr M.I. Gielink for helping with the computer software and taking photographs.

Mr C. Wozniak for building the necessary instrumentation.

Miss B. Wight for assisting with the final presentation.

NOMENCLATURE

Upper case

Hz	Hertz
Nm	Newton meter
Pa	Pascal
V	Volt

Lower case

dB	Decibel
g	Gravitational acceleration
kg/s	Kilograms per second
kW	Kilowatt
mm	Millimeter
ms	Milliseconds
pC	Pico-coulomb
rpm	Revolutions per minute

Greek

α	Angle
γ	Specific heat ratio c_p/c_v
η_t	Thermal efficiency
λ	Stroke/connecting rod ratio r/l
ϵ	Air compressibility
π	Pi
ρ	Density

Other

A_o	Orifice bore area
A_l	Cylinder bore area
C_d	Orifice discharge coefficient
d_v	valve diameter
G	Air flow rate
h_v	valve lift
nd/n	Swirl ratio

GLOSSARY

AVL	Austalt fur Verbrennungskraft maschinen, Professor H. List
BSFC	Brake specific fuel consumption
EDA	Electric Discharge anemometer
EGR	Exhaust gas recirculation
HSC	High swirl combustion
KLSA	Knock limited spark advance
LDA	Laser Doppler anemometer
MBT	Maximum brake torque
SI	Spark ignition
TDC	Top dead centre
TFM	Turbulent flow manifold
WOT	Wide open throttle

TABLE OF CONTENTS

LIST OF FIGURES

LIST OF PHOTOGRAPHS

LIST OF TABLES

1. INTRODUCTION

1.1 Background

Ever since the inception of the Otto four-stroke engine cycle for use in automobiles, continuing attempts have been made to improve its performance. Initially it was the competitive nature of drivers demanding more power that motivated this work. More recently, as oil embargoes and the energy crisis started to become pertinent issues, the emphasis has shifted from performance to fuel economy. Also, an increasing awareness of conservation, brought about by increasing levels of atmospheric pollution, of which the automobile is a substantial contributor, has put pressure on engine manufacturers to reduce engine emissions.

For all its shortcomings, many believe that the spark ignition engine will continue to dominate as the power source for automobiles, and it is therefore important to find ways of increasing efficiency and reducing emissions. One of the attractive avenues of research, is that of lean burn combustion, which permits higher compression ratios, and thus an increased efficiency. Also, lean mixtures improve the thermal efficiency because of a reduction in specific heat capacity.

Compression ratios are limited by the octane rating of the fuel due to the occurrence of knock. For a fuel of a particular octane level, knock depends on temperature, pressure and flame speed. Flame speeds are a critical parameter of SI engine operation. Engines generally operate from 1000 to 5500 rpm, and combustion has to take place within the space of approximately 45 degrees of crank angle. Thus at 2000 rpm combustion must be completed within 3 ms. A typical gasoline mixture has a laminar flame speed such that about 100 ms is required for complete combustion and is therefore not suitable for engine operation. Making the mixture turbulent increases the flame speed enough to permit suitable engine operation. Conveniently, turbulence increases with engine speed so that the decrease in combustion time available with increase in speed, is balanced by the increase in flame speed due to turbulence.

Flame speed is also governed by mixture composition. Lean mixtures have a reduced speed of flame propagation which results in a reduction of Brake Mean Effective Pressure (BMEP) and hence torque. But, as turbulence increases flame speed, it follows that the thermal efficiency of an engine can be improved by lean

operation, without a sacrifice in torque. An additional advantage of turbulence, is that the higher rate of heat transfer through the charge associated with a non laminar flow, eliminates local conditions in the mixture which may result in detonation.

In summary, it can be said that the efficiency and knock limit of an engine can be improved by operating the engine on a leaner mixture, and increasing the turbulence levels within the mixture. This is apparent from figure 1.1.1 below.

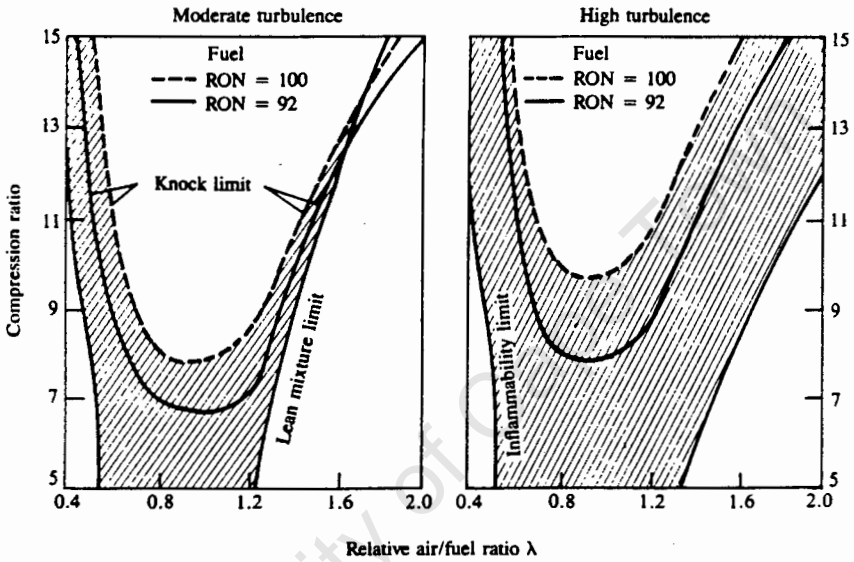

Figure 1.1.1 Knock limits as a function of compression and air to fuel ratio

Turbulence is the variation of a mean flow due to vortices of different sizes which are superimposed upon, and randomly dispersed in the flow. The turbulence of the charge is increased by introducing swirl and squish.

Swirl is usually defined as the rotation of the charge about the cylinder axis and is created by bringing the intake flow into the cylinder with an initial angular momentum. There are several methods of inducing swirl, the main methods being:

(a) The use of a directed port, where the air enters tangentially and is transferred into rotational motion by the cylinder wall.

(b) A pre-swirl port where the air enters the cylinder with an initial angular momentum after passing around a helical passage above the valve.

In addition there are various devices which can be combined with non-swirl or directed ports such as masked valves, swirl plates or swirl crescents. All of the swirl inducing methods restrict the flow and reduce the volumetric efficiency. Consequently a trade off between charge quantity and swirl level must be made.

Squish is defined as the radially inward or transverse gas motion that occurs toward the end of the compression stroke when a portion of the piston face and cylinder head approach each other closely. Squish creates turbulence without reducing the volumetric efficiency.

The effect that swirl and squish have on turbulence levels can be seen in figure 1.1.2 below.

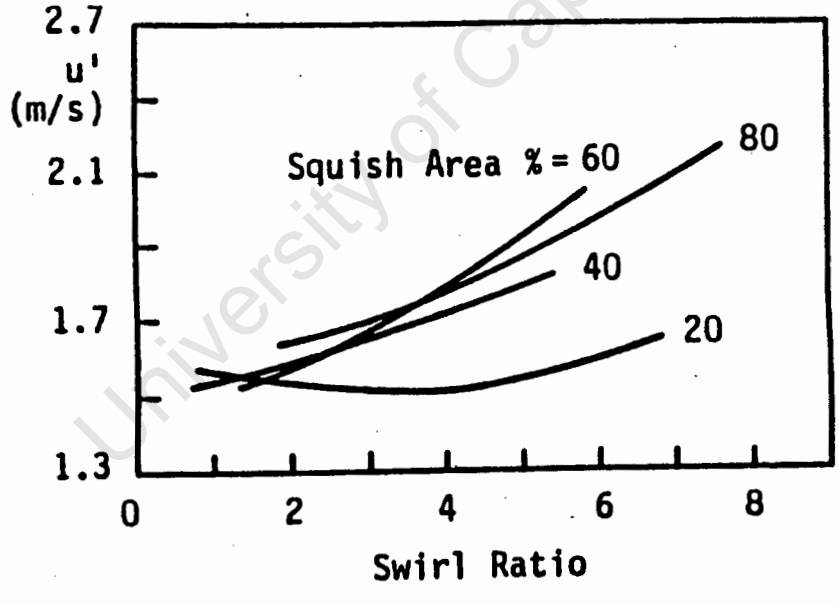

Figure 1.1.2 Turbulence intensity as a function of swirl ratio and squish area

Although it may be intuitively clear that squish promotes turbulence, it is not obvious that the same can be said of swirl. If swirl is considered to be a solid body rotation, then one would expect turbulence levels to be low. However, the author suggests

that it is rather the resultant turbulence which occurs due to piston motion imposed on the swirl once it is initiated, that contributes to increased turbulence levels. Also, the increase in swirl that occurs as the charge is forced into the smaller radius of the combustion chamber due to conservation of angular momentum, and the interference thereof because of combustion chamber irregularities, must result in increased turbulence.

Swirl, plays a vitally important part in the mixing of the air and fuel in diesel engines, and a substantial amount of research has been carried out in order to model the swirl induced by direct injection diesel engine inlet ports. Relatively little work has been carried out, with regard to this aspect, in spark ignition engines.

Swirl levels are compared between engines by defining a swirl ratio. This is normally defined as the ratio of rotational speed of the charge within the cylinder to a fictitious engine speed. The swirl ratio of a particular inlet geometry, is normally evaluated on a steady-flow swirl rig. Here air is drawn steadily through the inlet port and valve assembly in the cylinder head into the equivalent of the engine cylinder. One technique for characterising the swirl inside the cylinder is to use a light paddle wheel pivoted on the cylinder centre line, mounted on a low friction bearing. The rotational speed of the paddle is used as an indication of the air swirl. A superior method is to use an impulse swirl meter which has a honeycomb flow straightener replacing the paddle wheel. This measures the total torque exerted by the swirling flow as it passes through the honeycomb. Both methods result in an approximation of actual conditions because of a constant flow rate and a fixed valve setting. They do however form a useful basis for comparison of swirl turbulence for various engine inlet geometries. The steady-flow swirl rig provides a quick and practical method of developing the required swirl level in diesel prototype engines. Plastic models can be tested instead of the more expensive casting of actual heads.

Techniques also exist such as the use of a Hot Wire anemometer, Laser Doppler anemometer (LDA) or Electric Discharge anemometer (EDA) for measuring velocities during motored engine conditions. These arguably give a more realistic indication of cylinder turbulence.

Up to this point the advantages of increasing swirl and turbulence have been discussed. There is evidence however that the benefit of swirl is limited. Experiments have been carried out which demonstrate how initially, an increase in turbulence promotes rapid combustion, but further increases in turbulence are

progressively less beneficial and ultimately can lead to flame quenching, particularly in the case of lean mixtures.

An alternative approach to looking at the influence of swirl, is to consider the negative effects of engine deposits on swirl. It is understood, that accumulated deposits on the valve and in the inlet port, can substantially reduce the swirl level and decrease the engine performance.

1.2 Objectives

The purpose of this project is to investigate the effect of swirl on knock formation in a spark ignition engine. An attempt is made to find a correlation between swirl ratio and KLSA. Initially this is done by comparing the KLSA of several engines and their corresponding swirl ratios. Following this, the swirl levels of a particular engine are varied, and dynamometer tests are carried out to examine this effect on the engines KLSA.

In addition an attempt is made to obtain an understanding of how inlet port geometry affects swirl ratios. This is done by making a rubber casting of each inlet port tested, which provides a three dimensional visualisation of the inlet port. Also, the change in swirl ratio due to inlet deposits is measured.

1.3 Thesis outline

Chapter 2 is a literature survey which is split into four parts. Part one discusses the advantages and disadvantages of operating an engine on a leaner mixture. This usage gives rise to the term lean or fast burn combustion which is practiced in order to improve engine efficiency and reduce exhaust emissions. Part two reviews what experiments and modelling have been carried out in an attempt to characterise the inlet flow of an engine cylinder, with particular regard to swirl, something that has yet to be fully understood. Part three investigates the possibility that the advantages of swirl have a limiting value. Part four discusses the possibility that inlet deposits have a detrimental effect on swirl levels and engine performance in general.

Chapter 3 describes the experimental procedure and apparatus used in measuring swirl ratios, and describes the internationaly accepted standard of measuring swirl ratios, drawn up by AVL. It describes the trial of various accepted methods of increasing swirl. Also described is the development of a unique method of varying

the swirl ratios of an engine while maintaining the same pressure drop across the inlet port. Finally the method of testing this device on an engine during dynamometer tests is described.

Chapter 4 presents the results of the project along with discussion thereof.

Chapter 5 closes, with conclusions.

2. LITERATURE SURVEY

This chapter presents various observations related to inlet swirl in order to establish the potential benefits from purposely designing swirl into the inlet manifold of a spark ignition engine. Of course, engine designers and researchers[2,3,4,5] are aware of the vital role that swirl plays in the distribution of fuel during the injection period of a direct injection Diesel engine. This employment of swirl has been well researched and documented[14,15,16], however the analogous application in an SI engine has not been as extensively researched. Swirl is thought to have further benefits related to the spark ignition combustion process in addition to better fuel and air mixing.

2.1 The effect of air/fuel ratio and turbulence

As early as 1908, Hopkinson[1] demonstrated that for a given compression ratio, the thermal efficiency of an engine could be improved by running it on a leaner mixture. He attributed this to the variation in specific heat with temperature in a real gas. Heywood[7] proposes that after combustion, the burned gas temperatures of a lean mixture are lower than that of a rich mixture which decreases the burned gas specific heats and effectively increases the value of gamma, in the Otto efficiency equation $\eta_t = 1 - 1/r^{(\gamma-1)}$, over the expansion stroke. The efficiency increases because, for a given volume expansion ratio, the burned gases expand through a larger temperature ratio prior to exhaust; therefore, per unit mass of fuel, the expansion stroke work is increased. If the charge were a perfect gas with no variation in specific heat capacity then the thermal efficiency of the ideal Otto cycle would be a function of compression ratio, limited only by octane rating of the fuel as shown by Clerk[1].

Thus the thermal efficiency of a real engine increases with lean mixtures and high compression ratios. Coincidentally, higher compression ratios can be used with lean mixtures before knock occurs. This is due to lean mixtures having lower heating values, resulting in lower combustion temperatures. Also, lower temperatures of combustion reduce the volume of nitric oxides emitted as verified experimentally by a number of authors[17,19,12,13]. In order to exploit the fact that lean mixtures reduce emissions, some engines employ exhaust gas recirculation (EGR) which effectively dilutes the intake mixture.

Unfortunately, a consequence of lean mixtures, is a reduced speed of flame propagation. This adversely effects combustion stability and increases cycle to

cycle variation culminating in reduced torque and higher specific fuel consumption, as well as increased hydrocarbon emissions. The flame speed can be increased by intensifying turbulence levels in the charge which in turn promotes flame straining(6). Flame straining is the process of increasing the flame front exposed to fresh charge by "stretching" it. Thus in order to capitalise on the benefits of lean mixtures, it is necessary to introduce measures which increase turbulence. This is normally done by designing inlet ports to enhance swirl, or designing combustion chambers to promote squish.

How swirl is beneficial in increasing turbulence, is explained by Amann[1]. He maintains that swirl introduces a component of kinetic energy into the cylinder that tends to degenerate into turbulence through shearing action caused by the piston during the compression stroke.

In order to determine whether swirl is beneficial, it is necessary to assess which factors swirl is likely to influence, and then draw comparisons between standard and swirl implemented settings. For example, the speeds of flame propagation could be compared or the levels of NO_x emissions, between engines with low and high swirl. One belief is that swirl reduces the tendency of the engine to knock. Inoue et al[26] measured the KLSA of engines with low and high swirl and combined swirl and squish. He then plotted the difference between Maximum Brake Torque (MBT) timing and KLSA against engine speed as shown in figure 2.1.1 below.

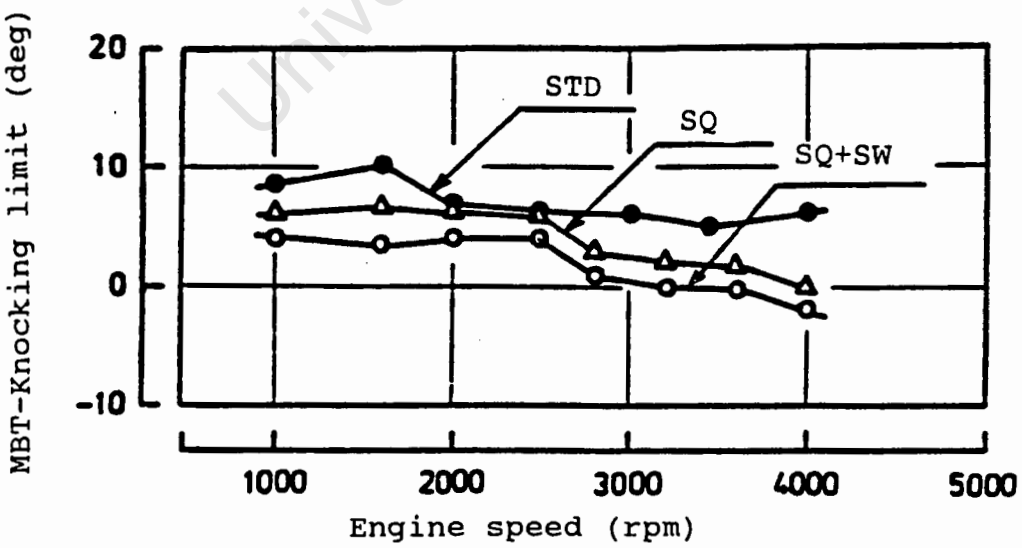

Figure 2.1.1 Effects of Swirl and Squish on MBT - KLSA, Inoue[26]

For the case of swirl plus squish, this difference is smaller than that of the standard case over the whole speed range, and especially above 3000 rpm, becomes negative. This means that the engine with swirl and squish can operate at MBT above 3000 rpm which is not the case of the standard engine. He therefore concludes that swirl and squish "certainly improve the knock limit".

Agnew[20], using a theoretical approach, calculated the effect of swirl on mass burn rates. In his calculations, he makes the assumption that swirl can be considered as either a free or forced vortex, as opposed to solid body rotation. Since this assumption effects the choice of appropriate initial velocity estimates and boundary conditions, caution should be employed in assessing the results as being representative of the real situation. Nevertheless, Agnew's results indicate a definite increase in flame speed with increased swirl.

Marsee[17] points out that lean mixture operation has traditionally been associated with poor driveability as evidenced by surge and stumbling. These problems are due to poor cylinder-to-cylinder fuel distribution, which produces differences in the air to fuel ratio between cylinders. Figure 2.1.2 shows that any variation in the air/fuel mixture in an engine operating at a stoichiometric or rich condition results in small fluctuations in torque. By comparison, the same variation in air/fuel ratio during lean mixture operation produces large fluctuations in torque which are felt as surge. Stumbling occurs when poor mixture distribution causes the leanest cylinder to drop below the flammability limit with resultant misfire.

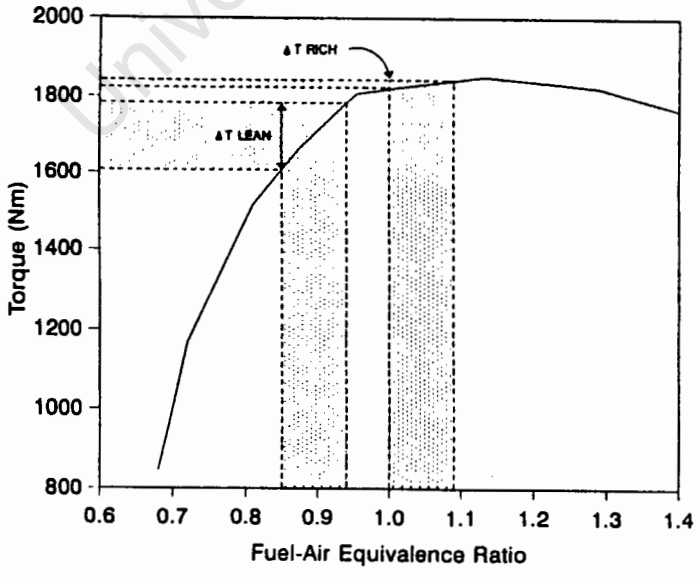

Figure 2.1.2 Effect of Equivalence ratio on Engine Torque

Although improvement in mixture distribution does not permit any given cylinder to operate at a leaner then stoichiometric condition, the engine can be operated at a relatively more lean composite mixture if all of the cylinders operate near the same air/fuel ratio. Figure 2.1.3 demonstrates this effect. It can be seen that the leanest cylinders of a standard and a turbulent engine operate at the same air/fuel ratio but in the standard engine there is a large variation between the richest and leanest cylinders and a small variation in the turbulent engine. The average air/fuel ratio of the turbulent engine is substantially higher then that of the standard engine.

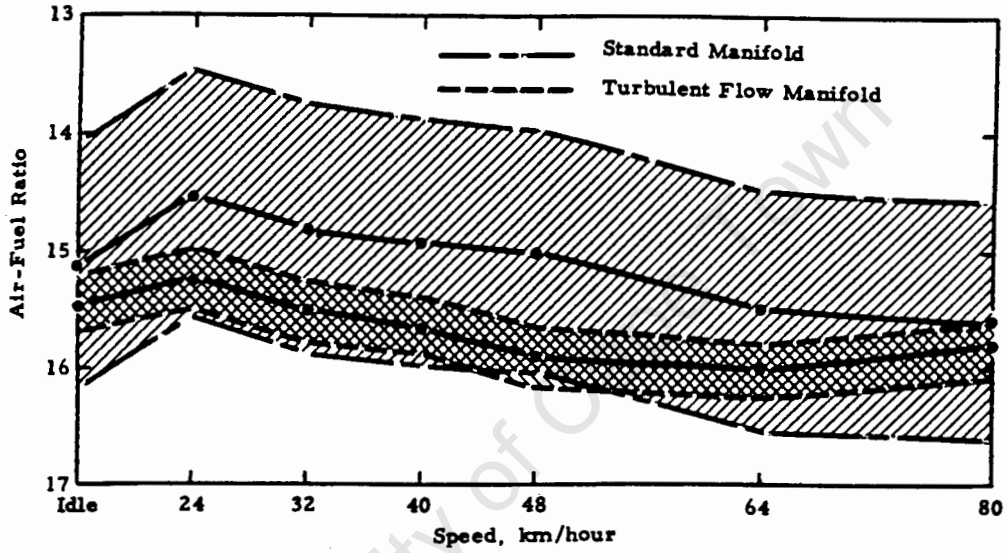

Figure 2.1.3 Air/fuel ratios for standard and turbulent engines

Marsee reports that fitting a Turbulent Flow Manifold (TFM) to a 1.3 litre engine increased the burn rate and improved the Exhaust Gas Recirculation (EGR) tolerance. He designed a simple experiment to determine whether swirl would offer the same benefits. Swirl was created by recessing part of the valve seats, which not only decreased the compression ratio but also had a throttling effect on the air flow and ultimately resulted in a small power loss. To partly compensate for this, the compression ratio was increased. The final result was a reduction in fuel consumption of 6.2%. The amount of swirl introduced was not quantified, however he indicates that further increases in swirl would attain further reductions in fuel consumption. It is possible, that the reduced fuel consumption in this case could be attributed to other factors, and not necessarily swirl. For example there could be an increase in thermal efficiency due to a higher compression ratio.

Lenox[12] describes the development of a Ford 2.3 litre High-Swirl-Combustion (HSC) engine. The engine was developed in order to meet stringent emission standards and improved fuel economy using the fast burn principle. The engine was designed for automatic transmission with a greater emphasis on low down torque and part throttle performance. The inlet manifold was designed to achieve the maximum flowrate. Swirl was induced via methods external to the inlet ports, allowing closer control of swirl parameters between production engines by means other then casting tolerances within the cylinder head. Two methods of inducing swirl were tried, these being air-flow control vanes and masked valves. The air-flow control vanes were orientated in each port such that the flow through each port was biased toward the cylinder wall to create the desired swirl within the cylinder. The mask located on a valve effectively blocked inlet airflow from circulating counter to the desired swirl path. Masked valves were chosen because of more accurate control of the swirl design parameter possible due to a machining operation and also because maximum airflow at the desired swirl intensity was attained. The outcome of the project was not adequately quantified, however it was stated that the objectives for fast burn were achieved and vehicle performance was at the "objective level".

Significant work has been performed by Nagayama[13] in order to determine the relative benefits of both swirl and squish on SI engine combustion and emission. The effect of intensified swirl and squish was studied using a 1.4 litre engine. Swirl was increased by modifying intake port angle, and squish was controlled by changing squish area and clearance. The overall outcome of the investigation indicated that swirl, or squish, or a combination of both, were highly effective in increasing burning velocity, decreasing cycle to cycle combustion fluctuation, while improving fuel economy and driveability. In determining the swirl ratios, the flow in the cylinder was assumed to be a solid vortex flow. The swirl ratio was then expressed as the tangential velocity of a paddle wheel anemometer divided by the axial velocity calculated from the air flowrate. The velocities were also measured during motored conditions using the Electric Spark Discharge Anemometer (EDA) method, in order to examine how velocities were effected by the compression process. Squish velocity was characterised by a function containing variables such as piston speed, clearance, squish area and crank angle.

Nagayama analysed his results on the basis of lean misfire limit, combustion duration and flame velocity as well as on emission level and fuel consumption. In particular, intensified swirl extended the misfire limit towards leaner air/fuel ratios by

1.0, intensified swirl and squish extended it by 1.5 whereas intensified squish only extended it by 0.4. This indicates that swirl is more beneficial than squish in the beginning stages of combustion when flame initiation takes place, and swirl prevents flame quenching in the leaner mixtures. Squish only increases turbulence levels towards the end of the compression stroke and therefore cannot be beneficial in preventing flame quenching. Furthermore, after analysis of mass burnt rates, it was determined that swirl decreased the initial combustion period where between 0% and 10% of the mass is burnt, whereas squish reduced the main combustion period where between 10% and 90% is burnt. Torque was significantly increased by squish in lean mixtures and by swirl in even leaner mixtures. Both swirl and squish together increased the torque throughout the mixture ranges tested. The improvements in fuel consumption exhibited the same characteristics as that of the improved torque. However due to increased flame speeds resulting in higher combustion pressures, the NO levels were increased at near stoichiometric conditions. At lean mixtures the NO levels were equivalent to standard conditions when swirl and squish were increased. Similarly an increase in HC emissions resulting from misfire at lean mixtures was reduced when swirl and squish or both were intensified.

It is Nagayama's opinion that swirl produced in the intake stroke effects better mixing of the fuel and air by stirring and expediting the evaporation process. Furthermore, the swirl velocity effect reduces the initial flame propagation time, thus the certainty of ignition is increased. Since maximum squish velocity occurs directly before TDC, flame velocity is increased during the main combustion stage because of increased turbulence, leading to an improvement in torque. A simultaneous increase in swirl and squish, each of which have major effects during different stages of combustion, improves the misfire limit and increases torque while decreasing cycle to cycle fluctuation, ultimately leading to an improvement in driveability and fuel consumption.

Kumar[22] performed tests to determine the effect of swirl on combustion, by measuring flame speeds. He used a research engine with a quartz piston through which photographs of the combustion process could be taken. Inserted into the inlet port was a rotatable sleeve which had the effect of biasing the flow onto the back of the inlet valve, thus producing enhanced or diminished levels of swirl. However no account was taken of the pressure drop across this sleeve which would result in lower initial pressures and temperatures in the combustion chamber. Normally, throttling results in lower speeds of flame propagation and therefore a measured increase in flame speed would indicate that swirl has a dominant effect on increasing flame speed. It was established that in low speed tests the flame travel

time was reduced by 7% in stoichiometric mixtures and 25% in lean mixtures. Tests at other speeds produced similar reductions in flame travel time.

The above results are in line with the findings of Inoue[26] who compared flame propagation patterns of swirling gas motion with no swirling motion but with turbulence. He found that swirl and squish are effective in combustion improvement especially with lean mixtures or higher Exhaust Gas Recirculation (EGR) rate. Inoue also found that turbulence with swirl lasts longer then turbulence without swirl. Thus it can be expected that turbulence generated in the induction stroke may be maintained into the combustion period.

A paper by Benjamin[19] describes the development of a combustion system capable of operating with high levels of charge dilution. Numerous design concepts were evaluated and finally four were assessed as suitable for trials. Among these were a four-valve head and a high swirl chamber. In the four-valve head he identifies the presence of a tumbling motion or barrel swirl as opposed to the conventional axial swirl. Axial swirl is the rotation of charge about an axis concentric to the cylinder axis, while barrel swirl has the axis perpendicular to the cylinder axis. He chooses to compare the engines on the basis of each engine's predominant swirl axis. He established that the characteristics of the swirl curves are quite different, presumably because they are being measured in different planes. The results of his measurements indicate that the four-valve head was capable of stable operation at lean mixture conditions with large improvements in BSFP. On the contrary, the high swirl head showed poor lean burn capability and inferior economy. He attributes this to the high mean velocities associated with high swirl at the point of ignition which prove detrimental to flame growth at weak mixture ratios. Compare this finding with that of Nagayama[13] who believes that swirl is beneficial in preventing flame quenching during flame initiation in lean mixtures. Benjamin suggests that the swirl energy available in the four-valve head is somehow dissipated by the time of ignition and this restructuring of the swirl field may in some way be providing the optimum flow field.

2.2 Inlet flow characterisation

It is clear that the flow of charge into the cylinder of an engine during the induction period is extremely complex and difficult to characterize. Moreover it is most probable that the flow character changes with engine speed and valve opening. Numerous flow measurements within the cylinder have been taken by various

researchers using a variety of techniques. In addition, computer software based on numerical computational methods has been developed in order to simulate and model the flow structure within the cylinder. Unfortunately, a complete understanding and characterisation of this flow has not yet been accomplished. However, some significant findings have been made, and isolated flow structures have been identified.

According to Brandstatter[11], it would appear from theoretical studies that the swirl structure in an engine is of similar importance to the swirl level. He undertook a combined experimental-theoretical investigation into the intake flow produced by a helical inlet port. The study consisted of two major parts. In the first stage, 3 orthogonal velocity components were measured in the valve gap under steady-flow conditions using LDA. Prior to the second stage, an unsteady gas-dynamics calculation was performed to determine the thermodynamic conditions upstream of the valve and the mass flow rate. The second stage consisted of combining the measured data and gas dynamic calculations into "quasi-steady" velocity profiles which were used as boundary conditions for a 3-dimensional calculation of the in-cylinder flow during the intake period.

The results of the study show that the flow within the cylinder is highly complex with regions of circulation that are difficult to explain. However, there were some general patterns that are worth noting. Firstly it was observed that although there was a major swirl circulation within the cylinder in one direction, there was an additional swirl circulation directly below the valve in the opposite direction. This latter swirl is due to expansion of the intake jet in the circumferential direction as it impinges upon the cylinder wall. Secondly, the highest swirl speeds were found to exist within the valve gap and immediately adjacent to the piston with a reduced amount of swirl towards the middle of the cylinder. This implies that the swirl structure develops from the piston upwards as opposed to the commonly held belief that the flow spirals down into the cylinder. Thus any swirl measurements made on a steady flow swirl rig using a paddle wheel anemometer would produce lower swirl results since the paddle is located approximately where the swirl is lowest. Also, it appears that the piston surface is required for adequate swirl development and this is absent in steady-flow swirl rigs.

Seppen[10] used EDA to measure velocities in a motored and fired engine with the intention of using the results to check the calculations of in-cylinder air flow from a mathematical model known as PHOENICS. A variety of cylinder heads and piston

crowns were used, including a four-valve cylinder head. The measured and calculated velocities appeared to agree well. Like Brandstatter, his results inferred that the direction of rotation in the inlet port is opposite to that in the cylinder space. He found that the flow pattern during a motored and fired engine did not differ substantially. In the case of the four-valve head, measurements indicated that during the compression stroke the air motion did not resemble an axial symmetric flow field. The flow field could be explained by assuming both a tumbling and swirling motion. An initial value of tumbling motion, chosen on the basis of the measured values, was used in a three-dimensional simulation of the flow field. The results of this indicate that due to dissipation, the tumbling motion is suppressed during compression. This is opposite to the findings of Benjamin[19] who reports that tumbling motion is accentuated during compression due to conservation of angular momentum.

In addition, Seppen used the computer model to simulate the air flow in a steady-flow test rig in order to calculate the swirl ratio. Here again his measured and calculated values agree well, implying that the model can be used in the early design stages for predicting swirl ratios in place of the steady-flow rig. However, if any tumbling motion exists, he suggests that it will be suppressed during compression and can therefore be neglected. Thus he has not accounted for the fact that the tumbling motion may be enhanced during compression. It is clear that tumbling motion can not be measured with a conventional paddle wheel anemometer, but if energy is used up to create tumbling motion then there is less energy available for axial swirling motion and this would be reflected in measurements. A model which simply ignores this factor will be less likely to produce accurate results.

Nagayama[13] used a novel method of determining the relative contributions of swirl and squish near TDC of the compression stroke. The surface of the piston was coated with a layer of vaseline and tungsten disulfide. After motoring for a few minutes observations were made of the flow pattern of this coating generated by the surface gas movement. He found that with a swirl intensified head the pattern was entirely spiral. On the other hand when both swirl and squish were intensified then the pattern consisted of radiating straight lines due to the squish velocity exceeding the swirl velocity.

Kajiyama[14] measured the swirl ratios of a Diesel engine with a variable inlet geometry, but identical in every other respect. The swirl ratios were measured on a steady-flow swirl rig although the valve lift was kept constant at 11 mm and therefore

does not conform to standard measurement procedures. He chose to compare the engine performance with swirl ratios of 2 and 3.5. His results indicated that the higher swirl resulted in a better BSFC and lower smoke emission. Interestingly enough, the volumetric efficiency was approximately equal for the two cases. He also measured velocities at various points within the glass cylinder of the steady-flow rig using LDA and used an interpolation method to characterise the flow. This was presumably done in order to verify results from the vane anemometer method. It was established that whether the swirl was characterised by angular momentum flux or turbulence kinetic energy, the results were the same. The swirl varied with distance along the cylinder and therefore he believes that it is important to measure the swirl near the valves as well as lower down the cylinder. However, he only measured swirl during an intake stroke and thus failed to show how the swirl influenced the flow near TDC where it is more important for the combustion process.

Duggal[15] used a computer programme known as PICALO to compute the in-cylinder flow field of a Diesel engine. His results showed that high swirl brings about greater mixing of the fuel and air, therefore the peak local equivalence ratio is lower at high swirl then at low swirl. Also, the increased swirl velocity during compression distributes the temperature field further downstream in the circumferential direction i.e. there is a more even spread of temperature eliminating local conditions which may cause detonation. Thus it would appear that the initial swirl momentum has a significant effect on the mixing process of liquid and vapour fuels.

Tanabe[16] used a Diesel engine to measure swirl speeds during motored and fired conditions and these were compared with those measured in a steady-flow test. Swirl, was varied by rotating the position of shrouded valves. He found that during combustion, swirl speeds are the same during firing and motoring. Also, there is a linear correlation between swirl speed predicted from steady-flow tests and that measured at TDC in motoring. Contrary to other findings, he discovered that there was a decrease in swirl during compression. Unlike Brandstatter[11] who calculated that minimal swirl occurred toward the centre of the cylinder length, Tanabe found that the maximum swirl occurred at a distance of 1.52 times the cylinder bore from the cylinder head.

Arcoumanis[18] took measurements of flow during motored conditions. He found that depending on the initial swirl strength and distribution, precession of the centre of rotation may take place but its magnitude diminishes towards the end of the compression stroke, and remains a localised phenomenon. He believes that since

solid body rotation corresponds to a condition of zero internal shear stress, it is the most energy conserving flow structure and as such may lead to a reduction of turbulence.

Recently, multiple intake valves have been used to improve performance by increasing the amount of intake charge due to the larger inlet area. It is not easy with this type of engine to generate the induction swirl necessary for suitable combustion. The gas motion is much more complex than that of a single inlet valve engine. The swirl characteristics of a multiple intake valve engine were modelled by Wakisaka[21] who used a three-dimensional numerical simulation technique to calculate the in-cylinder air motion. The results of the calculations imply that in the space between the two valves the collision of the two intake jets produces a strong flow descending towards the piston and this flow is prevalent above any swirl motion. He reasons that the reduction in swirl is not due to the collision of the two jets but rather the decrease in total angular momentum flux through the two valves. This reduction in angular momentum could manifest itself in more turbulence due to the colliding intake jets. It could furnish a short cut of the process of swirl development and subsequent decay into turbulence. It is suggested by Benjamin[19] that the benefit from swirl is derived from the fact that, the associated higher energy levels, and consequent dissipation and restructuring into turbulence of the initial swirl, provide for the optimum flow field. Further results of Wakisaka's calculations show that the swirl is strongest near the piston and is further intensified if there is a cavity in the piston. This is in agreement with the findings of Brandstatter[11] who also used a computer model to show that the swirl develops upwards from the piston rather then spiralling down into the cylinder.

Wakisaka also varied the velocity distributions issuing from the valve circumferences of the two ports. The velocity distributions were those associated with helical and directional ports. He found that the velocity distribution of the upstream port characterises the flow development. He states that changes in the velocity distribution between the two valves causes large variations in the cylinder air motion. It is unfortunate that he was unable to identify a combination of velocity distributions which would result in the optimum swirl development.

Wakisaka did not detect any barrel swirl during his simulations and this is contrary to the findings of Benjamin[19], who measured swirl ratios in an engine with two inlet valves and identified the strong presence of barrel swirl. Benjamin maintains that barrel swirl is more prevalent in a multiple intake valve engine then axial swirl.

Furthermore the benefits derived from axial swirl are accentuated in the case of barrel swirl and further enhanced if both types of swirl are present. He identified three distinct phases of charge motion during the induction and compression process:

Phase 1 is the generation of a barrel swirling motion, the intensity of which is governed by the design of the ports and chamber. The swirl is generated when the incoming gas becomes detached from the port floor and subsequently flow over the top of the valve. See Fig 2.2.1 below.

Phase 2 consists of the compression of the barrel swirl vortex and subsequent enhancement known as spin-up, through conservation of angular momentum.

Phase 3 occurs as the piston nears the top of its stroke and the barrel swirl vortex begins to distort as it is forced into a shape incompatible with its structure. At this point shearing effects are high and the whole structure breaks down.

Benjamin further used a computer simulation to verify the presence of the barrel swirl concept, and its characteristic development as described above.

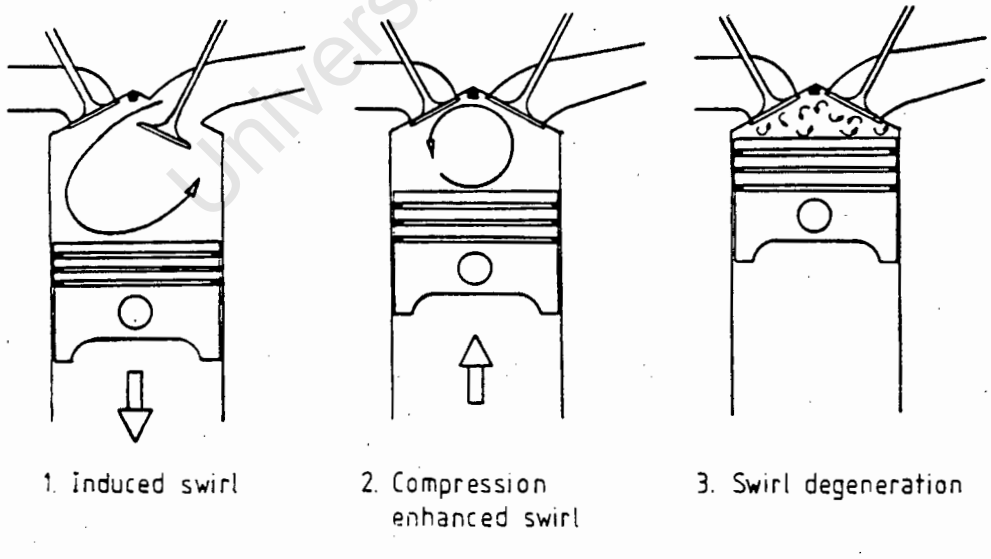

Figure 2.2.1 Schematic of barrel swirl behaviour

Uzkan[25] used a number of different techniques including steady-flow measurements, hot-wire measurements and water flow simulation, in order to characterise high-swirl port flows. His first important discovery was that flow regimes sometimes exhibit hysteresis. In other words, the flow coefficient of an inlet port at a particular valve lift is different if the lift position is approached from a higher lift direction than a lower lift direction. He determined that helical ports provide higher swirl at lower and medium valve lifts whereas directed ports are capable of producing higher swirl at large valve lifts. Contrary to the findings of other researchers, he found that swirl decreased with distance from the cylinder head due to friction torque along the cylinder wall. In addition, he provided reasons as to why steady-flow tests are not an ideal representation of actual operating conditions, namely:

(a) Because of flow unsteadiness and gas inertia, the flow response to the moving valve tends to lag behind the instantaneous valve motion.

(b) Although flow is measured in a steady-flow rig with pressure ratios across the valve of about 0.97, an operating engine encounters pressure ratios as low as 0.5. The pressure ratio effects the flow through two mechanisms, one of which is compressibility and the other is Reynolds number. In fact it has been found that the flow coefficient increased by 20% when the pressure ratio decreased from 0.8 to 0.5.

2.3 Limitations to swirl benefits

Up to now, the positive aspects of swirl have been reported, and it might be automatically assumed that the greater the swirl, the greater the benefits. However, indications are that up to a point increased turbulence is worthwhile but beyond this, the effects are actually negative resulting in poorer engine operation.

Bradley[6] used a correlation of turbulent burning velocities based on experiments, in a thermodynamic engine combustion model. The results demonstrate that initially an increase in turbulence improves engine efficiency due to more rapid combustion. However further increases in turbulence are progressively less beneficial and ultimately can lead to flame quenching, particularly in the case of lean mixtures.

Gajendra Babu[23] undertook some experiments to determine the effect of turbulence generated in the inlet manifold on engine performance. He used blades

and delta-wings inserted in the inlet port to create turbulence. The combustion chamber was disc-shaped providing good antiknock quality with very little squish. Thus any changes in performance would be attributed to the turbulence generated in the inlet manifold and not as a result of squish towards the end of the compression process. He found that the blade-type turbulence generators create a significantly larger amount of turbulence, leading to a loss of engine power compared with the delta-wing shaped generator. However, it was noticed that a slight improvement in performance was obtained when the delta-wing type turbulence generator was used compared with the conventional engine. Furthermore this increase in power took place in the lower speed range where naturally induced turbulence levels are not that high. At higher speeds turbulence levels are higher and therefore an increase in turbulence might not be as significant. In fact, at higher speeds the standard engine had more power demonstrating that very high levels of turbulence are not beneficial. Whereas at lower speeds higher turbulence increases the flame speed and hence increases the engine power, at higher speeds higher turbulence increases the heat losses and hence reduces the flame speed, which reduces the engine power. Although these arguments appear to be sound, he fails to account for the effect that the increased pressure drop across the turbulence generators would have on flame speed and hence power output. Similarly although he acknowledges the fact that turbulence generators tend to decrease the volumetric efficiency, he neglected to associate the effects of this on his results.

Along with increased turbulence, increased swirl velocities also have a limiting effect. Benjamin[19] compared the effects of different types of combustion chambers on engine performance with specific regard to lean mixtures. Among the various chambers tested was a high swirl head, with unfavourable results. The high swirl chamber maintains a high velocity throughout the burn period and these high velocities at or near the point of ignition prove detrimental to flame growth especially at weak mixture ratios, accounting for a poor lean burn potential.

2.4 Swirl reducing deposits

Although it seems quite conceivable that considerable inlet port deposits might adversely effect engine breathing, reducing volumetric efficiency and resulting in a loss in power and even increasing emissions, it is not clear how the intake generated swirl might be effected. It is known that measures taken to increase swirl, normally result in a decrease in volumetric efficiency, but is the converse true? Will factors

that decrease the volumetric efficiency result in increased swirl? One of the ways of inducing swirl, is by causing a biasing of the flow to one side of the valve. Thus it could be possible that deposits which are irregular in nature may cause a similar biasing of the flow and result in increased swirl.

Gething[24] conducted a comprehensive programme to evaluate the effects of intake valve and port deposits on engine performance and swirl levels. Real as well as synthetic deposits were used. Generally, as may be expected, the performance of the engines tested was reduced. It was found that in a high-swirl fast-burn engine the overall swirl was reduced by 14% with real deposits, although one cylinder showed an increase in swirl. When synthetic deposits were used, the swirl levels decreased by up to 40%. In an engine which was not a high swirl fast burn engine, it was found that deposits did not affect the swirling appreciably.

3. EXPERIMENTAL PROCEDURE

3.1 Introduction

As has been discussed, it is believed that an increase in swirl level increases the knock limit of an engine. In order to measure the "mean swirl ratio" of an engine, a steady-flow swirl rig was built, of which the method and operation is described below. As far as possible, the swirl ratio measurements and calculations were carried out in accordance with an internationally recognised standard, drawn up by the Austrian automotive research company AVL. A brief summary of this mean swirl ratio calculation procedure can be found in Appendix D. Thus a swirl ratio comparison with the knocking propensity of several engines could be achieved, with the intent of proving whether a correlation exists. The knocking propensity can be assessed by various techniques. It was decided to relate this on the basis of KLSA. The knock limit of an engine is influenced by a number of factors which make the comparison of swirl ratio and knock limit between several engines fraught with complications. An experiment was designed to eliminate all of these variables so that an objective comparison between swirl ratio and knock limit could be realised. This involved altering the swirl ratio only, of a particular engine as verified by measurement on the steady-flow swirl rig. Dynamometer tests were then conducted to establish the KLSA for each level of swirl ratio.

3.2 Measurement of Swirl Ratio

3.2.1 Apparatus

A steady-flow swirl rig using a paddle wheel anemometer was set up for the purpose of swirl ratio measurement, using existing equipment which had been previously used for a similar project. The rig was constructed in such a manner as to comply with the AVL measurement standards as closely as possible. A schematic diagram of this rig is shown in figure 3.2.1, along with a photograph of the equipment.

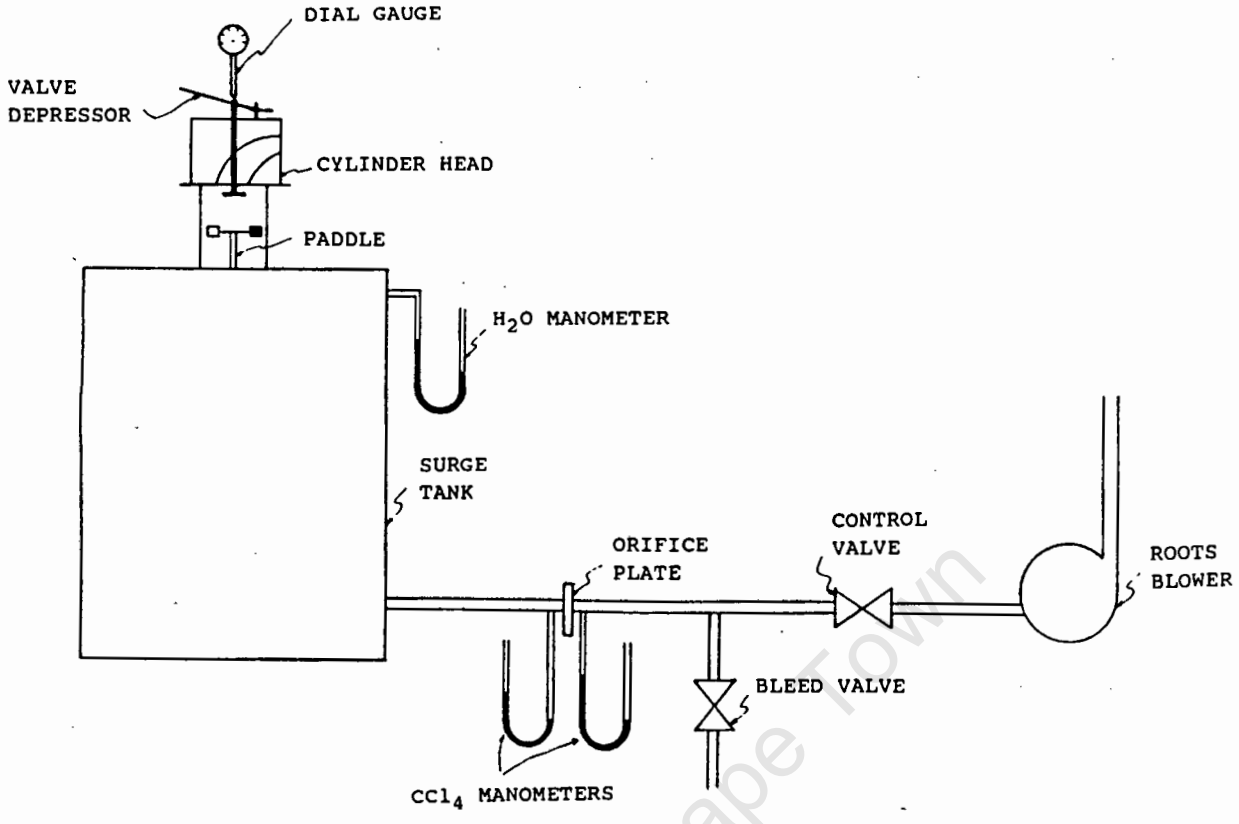

Figure 3.2.1 Schematic arrangement of steady-flow swirl rig

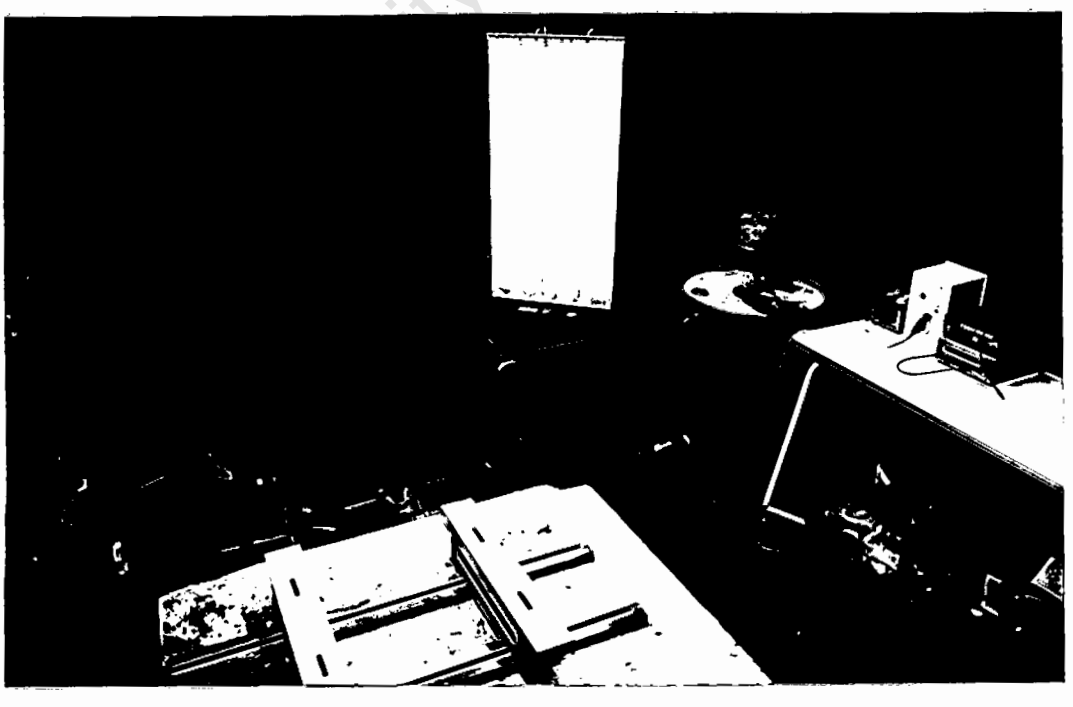

Plate 3.2.1 Steady-flow swirl rig

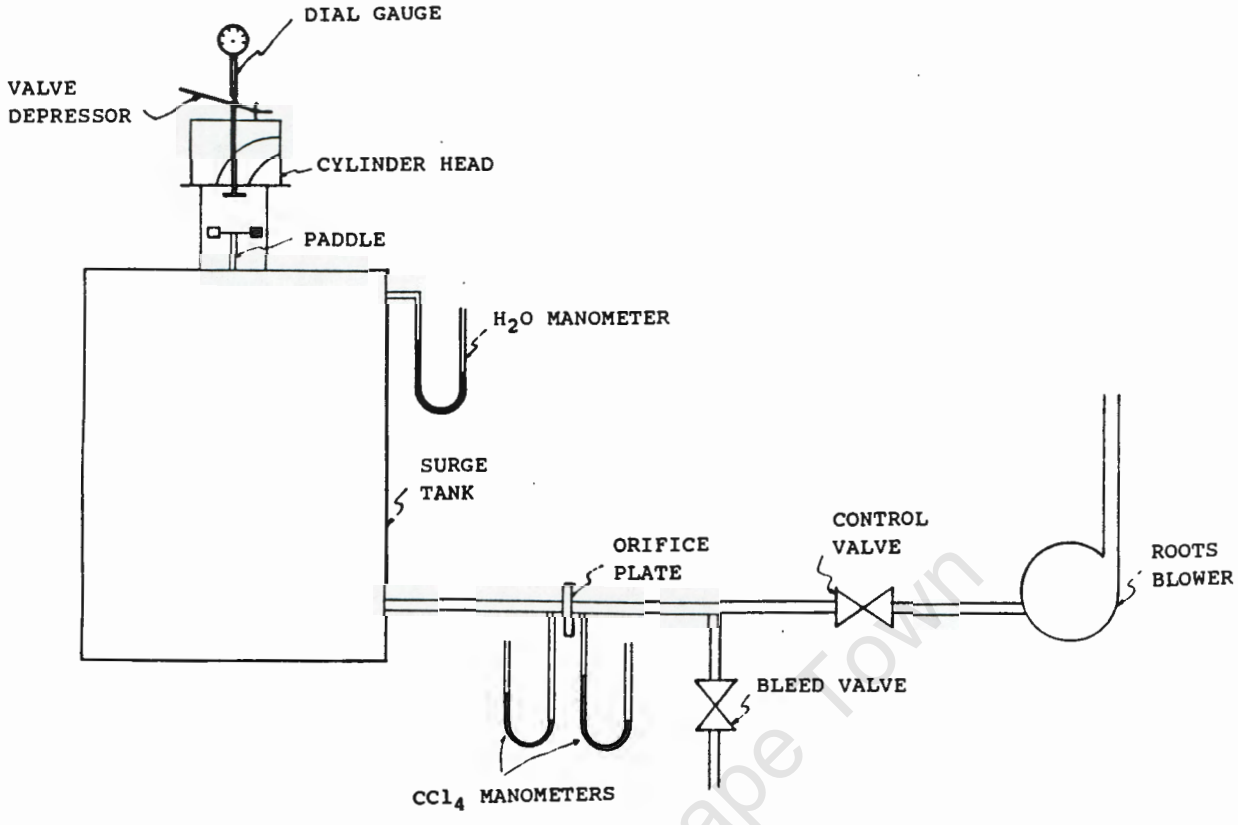

Figure 3.2.1 Schematic arrangement of steady-flow swirl rig

Plate 3.2.1 Steady-flow swirl rig

Since most of the engines to be tested have similar bores, one perspex tube of 80 mm diameter and 200 mm long was used, upon which the cylinder heads were mounted. Strictly speaking, the diameter of the tube should correspond exactly with the bore of the engine to be tested, in order to simulate actual conditions. This would have meant using several different sized tubes and several different sized paddles. It was felt that the extra expense and effort required to implement this were not justified in this case. Moreover, the dimensions of the paddle previously constructed, did not conform identically to those suggested by the AVL measurement standard, but the slight discrepancy was deemed to be insignificant. However in the case of the 3 litre Ford engine which has a 93.67 mm bore and the Toyota 22R engine which has a 92 mm bore, a 94 mm diameter tube was used with a correctly sized paddle complying with AVL standards.

The paddle was mounted approximately 1.5 times the tube bore from the cylinder head on a low friction cylindrical bearing. The base of the cylinder forming the bearing was fitted with a teflon cone so that it rode on the cone fulcrum. This minute contact area further reduced friction.

The perspex tube was mounted on a 45 gallon drum which proved ideal for the purpose of damping out pressure pulses. A pressure tapping in the side of the drum allowed the measurement of pressure across the inlet port, using a water filled manometer.

As is common practice with steady-flow rigs, a roots type air compressor was used to draw air through the inlet port. This was a Dresser roots blower model 2506J driven by a 3kW motor. A bleed valve system was incorporated which allowed for fine adjustments of the air flow at any particular valve lift. Air flow measurement was accomplished by using a sharp edged orifice plate. The manometers across the orifice plate were filled with carbon tetra chloride which, having a density 1.5 times greater then water, allowed a greater range of pressure measurement for the same length of manometer.

The speed of the paddle was measured using a stroboscope. This consisted of a Snap-On variable advance magnetic pick-up car timing light, model MT241A. The magnetic pick-up received amplified pulses from a King Instrument function generator, model# FG2512F. A separate amplifier was constructed to convert the voltage signal to a current square wave signal of 1 amp. This provided the necessary signal strength for the magnetic pick-up. An HC multi-function counter,

model# HC-LF100, was used to measure the frequency supplied by the function generator, providing a digital frequency readout. The counter gate time was set at 10 seconds providing maximum display resolution. This equipment arrangement is shown schematically in figure 3.2.2 below.

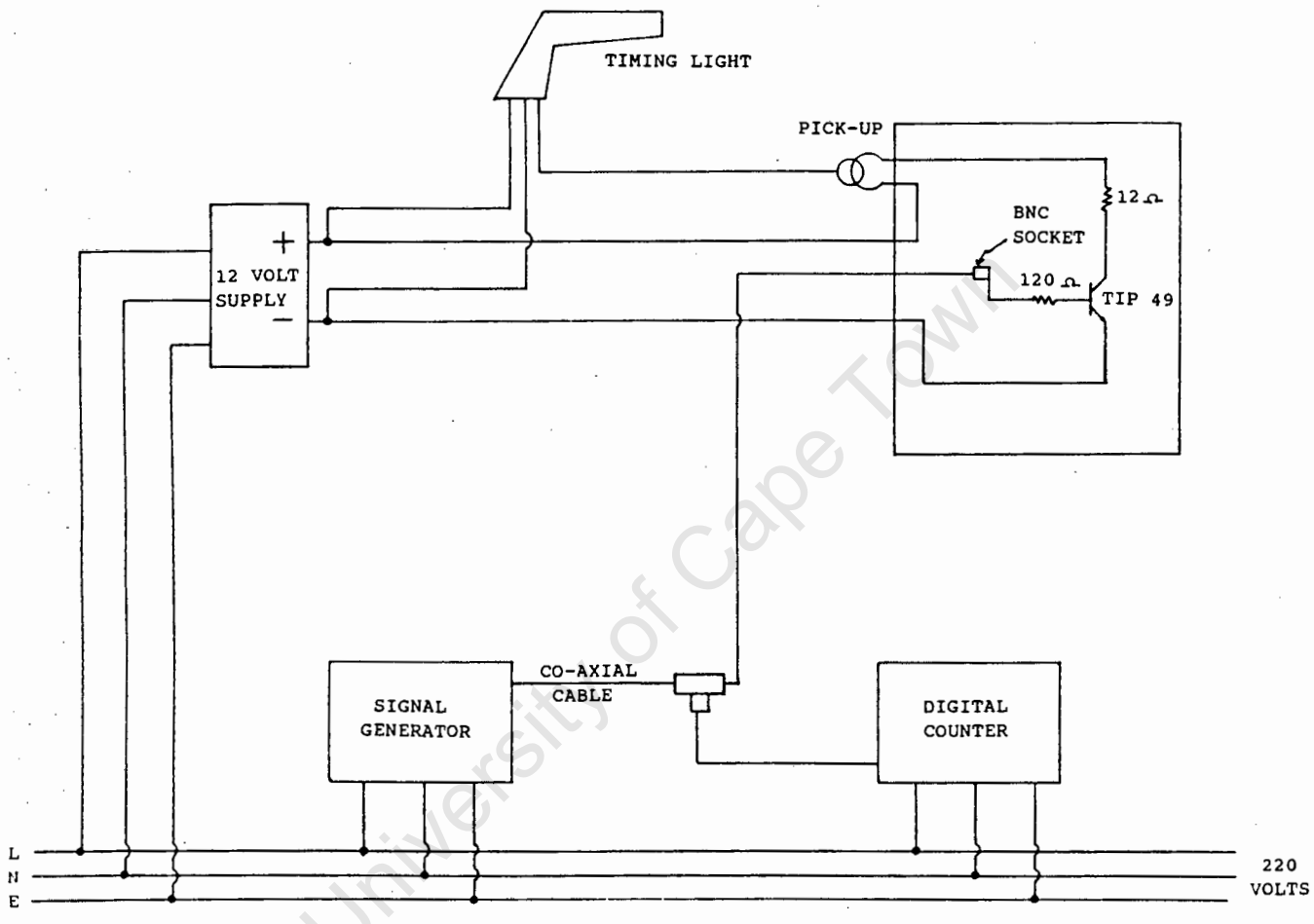

Figure 3.2.2 Schematic arrangement of stroboscope

In addition to the stroboscope, a Lutron digital tachometer model# DT-2234A was used to verify the speed measurements. Due to the fluctuating speed of the paddle, it was not possible to simply use the tachometer because of varying readouts, but it was useful for determining the speed range of the paddle. This prevented measurements of speeds which would be multiples of the true speed. If the speed of the paddle was low then the strobe frequency was doubled or even quadrupled in order to "freeze" the paddle at a particular speed. Alternatively, if the speed of the

paddle was so low that the stroboscope could not be used, then the number of revolutions of the paddle in a certain time were counted.

The valve lift was measured with a dial gauge indicator calibrated in ten thousands of an inch (0.254 mm) allowing an accurate measurement. The maximum travel of the follower was approximately 15 mm, but since the maximum valve lift of all the engines was about 10 mm, it was not necessary to measure the swirl ratio at lifts greater then 10 mm. Various methods of depressing the valve were used, depending on the cylinder head. For multiple intake valve engines the whole cylinder head with cam-shaft was mounted on supports spanning the perspex tube so that the valves could be opened by turning the cam-shaft.

In order to calculate the mean swirl ratio of single intake port engines, the valve lift profile of the engine was required. In this case the valve lift profile was measured since this data was unavailable. The valve lift profiles of these engines as measured is plotted for comparison purposes below. As can be seen, these engines have very similar valve lift profiles.

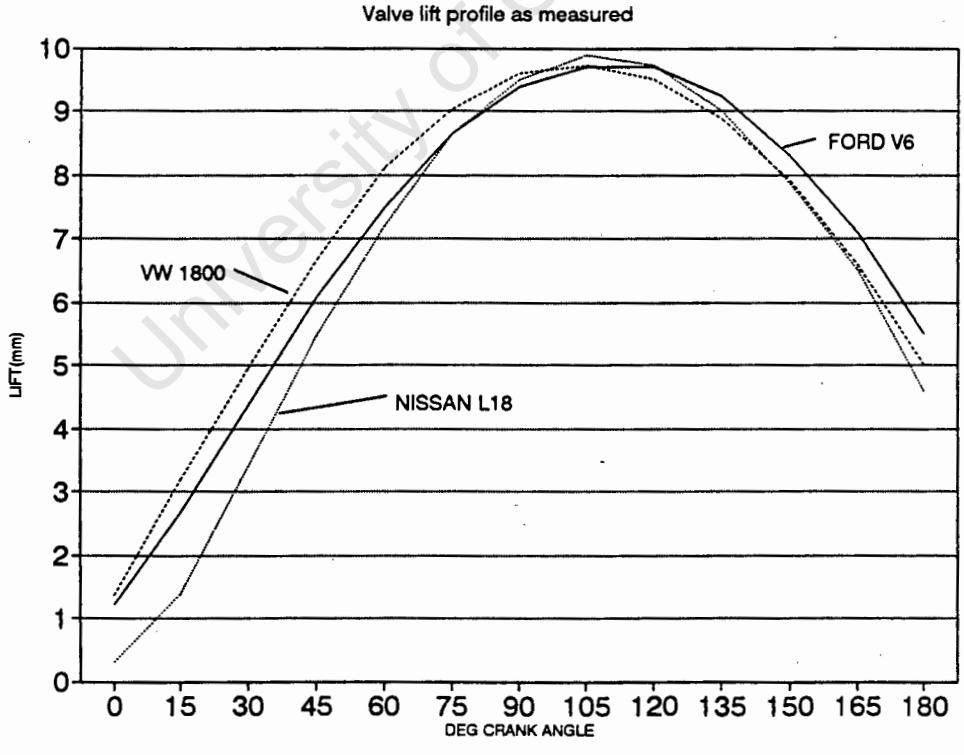

Figure 3.2.3 Measured Valve Lift profiles of test engines

3.2.2 Measurement Procedure

(a) Single intake valve engines

The AVL standards state that a normalised valve lift should be used when measuring swirl ratio. The valve lift is normalised by dividing the lift by the valve diameter. This ratio should then vary from 0.04 to 0.4, incrementing by 0.04. Thus the first step was to determine the valve lifts depending on the valve diameter that would produce these ratios. As flow-rate depends on atmospheric pressure, the pressure was measured using a dial gauge barometer calibrated in hectapascals. Dry bulb and wet bulb temperatures were recorded using alcohol thermometers. This enabled the humidity and density of the air to be calculated.

Once the valve lifts pertaining to a particular head were known, the smallest valve lift was selected and the air flow adjusted to give a pressure drop of 250 mm of water across the valve. Once the paddle speed, and the manometer readings had been recorded, the valve was opened to the next lift position, taking care not to exceed the new lift position. Thus the valve was only moved in one direction. It was hoped that this precaution would eliminate the occurrence of any flow hysteresis, should the lift be approached from the opposite direction. Likewise, as it was necessary to increase the flow once the valve had been opened in order to maintain the 250 mm of water pressure drop, it was attempted to keep this adjustment to one direction.

(b) Multiple intake valve engines

The AVL procedure does not make allowance for multiple intake valves which may or may not open simultaneously, and which may be of differing size. It was decided that these engines would be tested at particular crank angles rather then particular valve lifts, which meant that the cam shaft as well as valve followers had to be left in place. The advantages of this are twofold. Firstly, as the mean swirl ratio is usually calculated using Simpsons Rule, with intervals corresponding to 15^{o} of crank angle, measuring the swirl at these positions eliminated the necessity of interpolating swirl from a valve lift position to a crank angle position. Secondly, following from this, it was then unnecessary to measure the cam lift profile of the engine for the purpose of interpolation. Thus the swirl was measured from 0^{o} to 90^{o} at intervals of 7.5^{o} since the cam shaft rotates at half the speed of the crank shaft. This method also applies to engines with two cam shafts.

Apart from this, the procedure of measuring swirl was identical to that described for single intake valve engines.

3.2.3 Measurement Repeatability

The testing of a particular head was repeated several times, in order to examine the repeatability of measurements. It was found that the Carbon tetra-chloride manometer readings were repeatable to within three or four mm. This accounted for a discrepancy between readings of approximately 1.5 percent. The measurement of paddle speed between subsequent tests was repeatable to within 0.6 Hz or 36 rpm at about 250 rpm. This accounts for a discrepancy between readings of approximately 15 percent. At a paddle speed of about 500 rpm the speed measurements were repeatable to within 0.4 Hz or 24 rpm, a discrepancy of 5 percent. The final discrepancy in calculated swirl ratios assuming the worst case is only about 8 percent. This is demonstrated in Appendix D.

3.2.4 Computer Software

The repetitive and time consuming nature of the necessary swirl ratio calculations justified the use of a computer spreadsheet. A Quatro Pro spreadsheet was set up to make data analysis easier. If the engine valve diameter was input, the applicable valve lift positions were given. From the atmospheric data such as pressure and temperature, the humidity was calculated. This was used for correcting air density calculations for each valve lift. The orifice discharge coefficient, and air compressibility values were read off a graph from AVL standards, and used in the flowrate calculations, along with the pressure ratios calculated from the manometer readings. The mean piston speed could be calculated from the input stroke and connecting rod length. The instantaneous swirl ratio was calculated for each valve lift, and a plot of swirl ratio and flow rate versus normalised valve lift could be produced. The expressions used for these calculations, along with sample calculations are given in Appendix D.

A Basic program was written which linearly interpolated swirl ratios at crank angle positions from the instantaneous swirl ratios at the specified valve lifts. The inputs to this program were the cam lift profile, and the instantaneous swirl ratio. From the stroke and connecting rod length, the program calculated the instantaneous piston speed at any particular crank angle. Thus the swirl and corresponding piston speed at a particular crank angle were used to calculate a mean swirl ratio using Simpsons Rule. The listing of this program is given in Appendix E.

For the sake of thoroughness, the interpolated swirl ratios calculated from the Basic program were input into the spreadsheet along with the valve lift profile and a similar calculation of mean swirl ratio was possible. The data measured and the calculation results are presented in Appendix F.

3.3 Casting of inlet ports

In order to assist with the visual interpretation of each type of inlet port, a rubber casting was made of it. The rubber used was a low temperature melting compound known as Binamould. This compound proved relatively easy to use and even fairly intricate inlet ports could be cast without difficulty. In the case of multiple intake valve heads, the casting had to be made in two sections which were then joined together using an all purpose adhesive. In the case of the head with extensive deposits, removing the casting proved somewhat challenging. The use of liquid soap made this task slightly more tolerant. Finally, photographs of these castings were taken and are displayed in chapter 4.

3.4 Detection of Barrel Swirl

Some rough tests were performed in order to detect the presence of barrel swirl. A circular piece of gauze the same diameter as the perspex cylinder was fitted with strips of cotton and inserted into the cylinder above the paddle. These tests were not intended to provide an in depth analysis of the flow, but to gain an insight into any flow patterns that may exist. Unfortunately, the billowing strips of cotton made it difficult to gauge between levels of swirl, but did reveal if there was an upward flow, indicating barrel swirl.

3.5 Swirl Ratio comparison with KLSA data

Four engines were selected which were approximately of the same bore, but with varying combustion chamber types. The engines selected are as follows:

Ford Essex - 3.0 litre V6
Nissan L18 - 1.8 litre
Volkswagen - 1.8 litre
Toyota 4AF - 1.6 litre

The technical specifications of these engines can be found in Appendix B.

The KLSA data for these engines had been previously accumulated for a range of test fuels. Once the mean swirl ratios of all four engines had been measured and calculated, these were compared against the existing KLSA data. The KLSA data was presented in terms of degrees before TDC, and these values varied with engine speed. A correlation was attempted between mean Swirl Ratio and KLSA for the test engines.

3.6 Swirl comparison with deposits

Tests were performed to determine the influence of inlet port deposits on swirl ratio. A Toyota 1300 cc engine with two inlet ports was used, simply because it had extensive carbon deposits in the port and on the valves which were of natural origin, as opposed to being synthetically created.

Initially the head was tested with inlet port and valve deposits. Then the valves were removed and the deposits in the inlet port cleaned off. The valves with deposits were replaced and the head was retested. Finally, the valves were cleaned of any deposits and the head was tested with a clean inlet port and valves.

3.7 Design of swirl increasing device

In order to isolate the effect of swirl alone on knock limits, it was intended to increase the swirl ratio of a standard engine by artificial means, and then perform dynamometer tests to determine any resultant effect on Knock Limits, by measuring the knock limited spark advance. Two methods of increasing swirl were tested on the steady-flow swirl rig and assessed for suitability of use for dynamometer tests.

3.7.1 Shrouded valves

The Nissan Cylinder head was used for swirl measurements with a shrouded valve. The shroud used was 10 mm high and encompassed 120° of the valve circumference as shown overleaf.

Plate 3.7.1 Shrouded valve

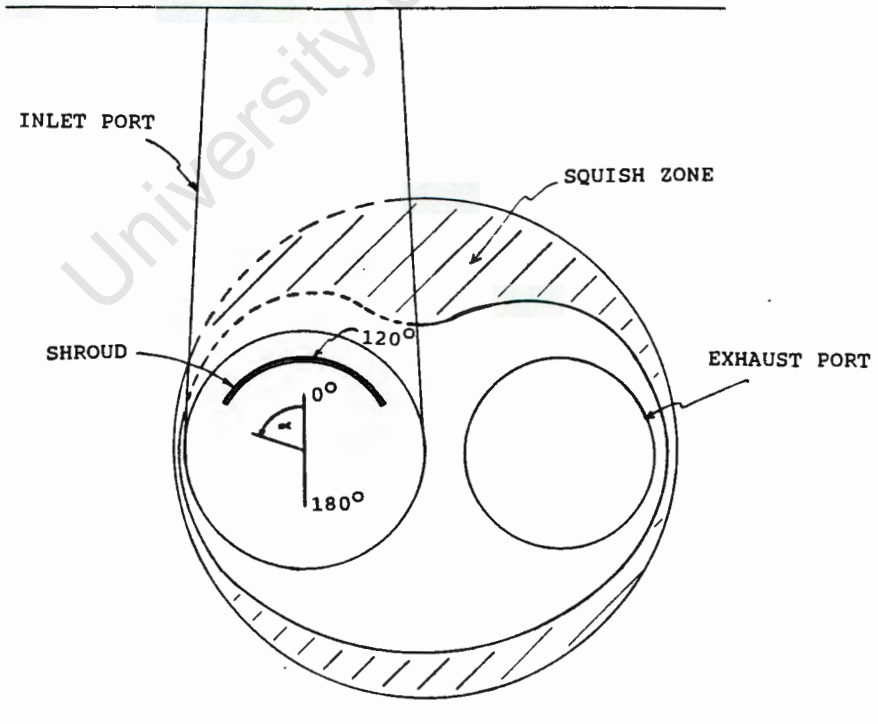

Figure 3.7.1 Plan of shrouded valve arrangement

The swirl ratio of the shrouded valve was measured at valve rotations of 30 degree intervals, between 0 and 180 degrees. It was noted that the highest swirl occurred at 0 degrees and then decreased almost linearly with valve rotation until 180 degrees whereupon the swirl direction reversed, as can be seen in figure 3.7.2 below.

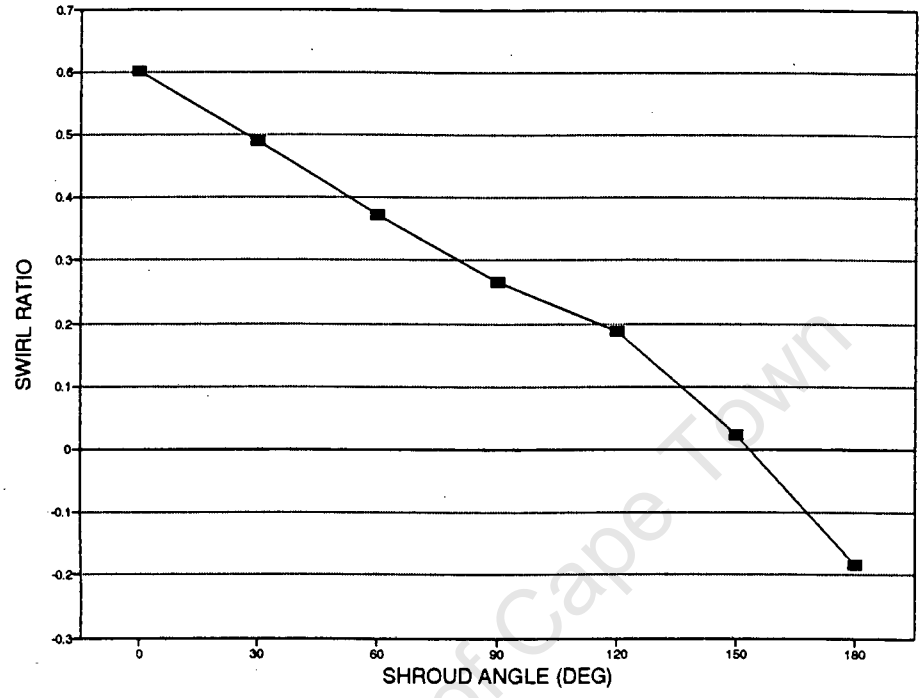

Figure 3.7.2 Swirl ratio variation with shroud angle

The shrouded valve evidently offers a suitable spread of swirl ratios and for this reason would appear ideal for implementation on the test bed engine. However, it was considered impractical to undertake this measure for the following reasons. Since all four inlet valves would need to be shrouded, some method of coordinating the position of the valves would have to be sought. Each valve would have to be prevented from rotating during engine operation but be capable of rotation to subsequent shroud positions. Furthermore, welding the shrouds in place may have caused valve distortion. Alternative methods of fixing the shrouds in place such as silver solder led to concern over the shrouds coming adrift during engine operation with subsequent engine damage. In addition the shrouded valve caused a large decrease in flowrate. Thus an alternative method of increasing swirl had to be found.

3.7.2 Deflection plates

The use of deflection plates to increase swirl is not particularly common, although this method has been used in research. The idea is to insert a gasket, with deflection plates attached, in the inlet manifold. This causes a biasing of the flow to one side of the inlet port.

(a) Nissan

Initial tests were carried out with a loose piece of plastic to determine on which side of the inlet port the deflection plate should be positioned for increased swirl, and to obtain a rough idea as to what increase could be expected. As a substantial increase in swirl was produced, a prototype gasket was designed. This consisted of 0.5 mm aluminium sheet with a circle of the same diameter as the inlet port cut into it, except for a 10 mm segment, so that this so formed circular flap could be bent open. The flap was bent open to two different positions and the swirl ratio measured on the steady-flow swirl rig.

The swirl ratio increased for both positions by approximately the same amount. This indicated that obtaining a broad range of swirl ratios was not possible using deflector plates. A second prototype was made with the intention of increasing the flap size and reducing the amount that the gasket restricted the air flow. With this in mind, the circular opening was cut with a diameter 5 mm larger then the inlet port diameter. In order for the flap to pass through the inlet port opening, it had to be contoured but this was considered preferable to a flat flap. The flap was opened to an angle of 60^{o} and this assembly was tested. The swirl ratio increased almost linearly with increasing valve lift and resulted in a mean swirl ratio of approximately three times that of standard conditions. This was considered satisfactory for drawing a comparison of KLSA on the test bed engine.

Thus a final model was constructed using 1.2 mm thick aluminium plate to make it more rigid, and a final test was performed. Surprisingly, the calculated swirl ratio was lower for the deflector made from thicker material. It was noted that at low valve lifts, the swirl speeds were the same. However, as the valve lift increased, the swirl speed of the deflector made of thinner material increased at a faster rate. It was also noted that at low valve lifts, the flow through both deflectors was equivalent, but as the valve lift was increased, the flow increased at a faster rate through the one made from thinner material. This was attributed to the increasing flow bending the thinner

flap further open in an attempt to create as little pressure drop as possible across the flap, resulting in an increase in swirl speed.

This indicated that a fixed angle of 60° was not optimum for high flow rates and it was therefore increased to 65° in the thicker material and retested. In this instance the swirl speed was slightly lower at low valve lifts but virtually identical to that of the thinner material at high valve lifts. Thus it was felt that the optimum deflector design had been obtained. Figure 3.7.3 is a schematic diagram demonstrating the mounting of the deflector plate in the inlet port, and plate 3.7.2 is a photograph of the final design.

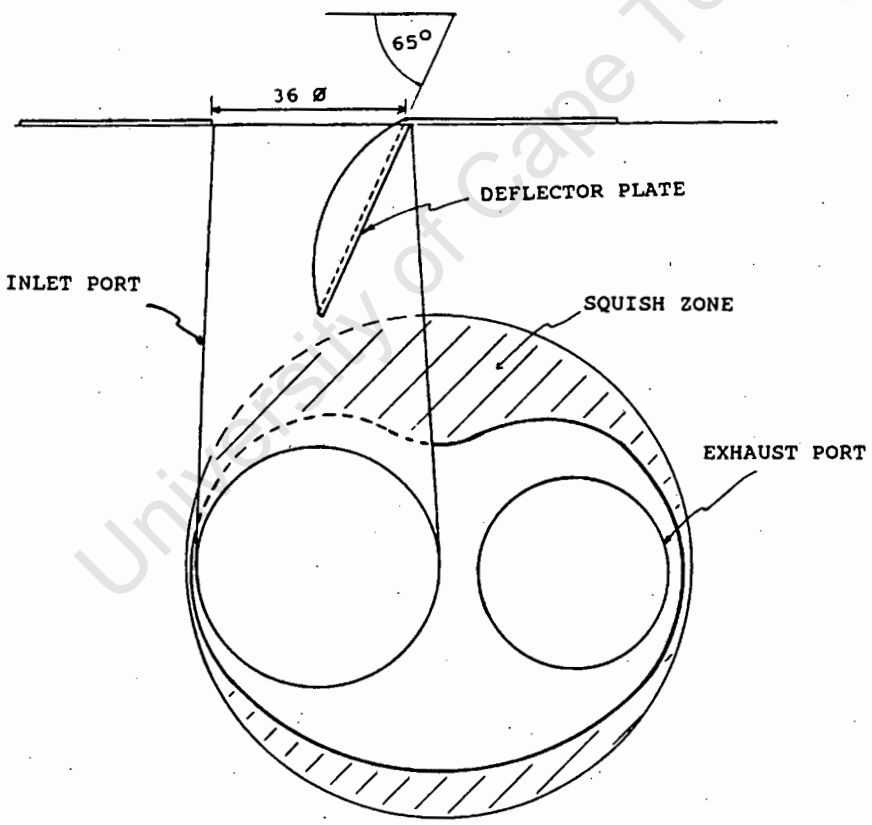

Figure 3.7.3 Mounting of deflector plate in the Nissan engine

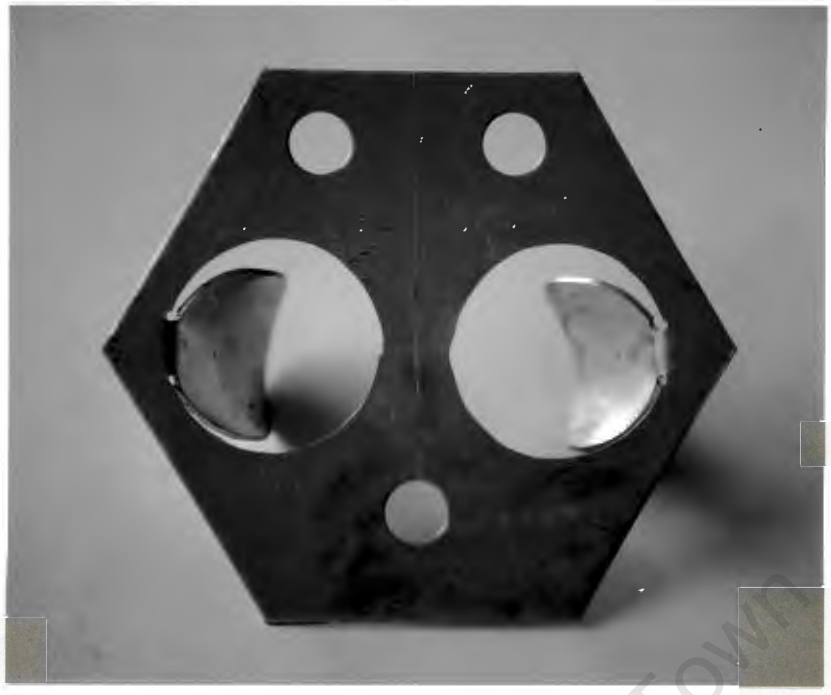

Plate 3.7.2 Swirl inducing deflector plate

Finally a comparison of swirl ratio and flow rate with and without the deflector plate is shown below in figure 3.7.4 and 3.7.5.

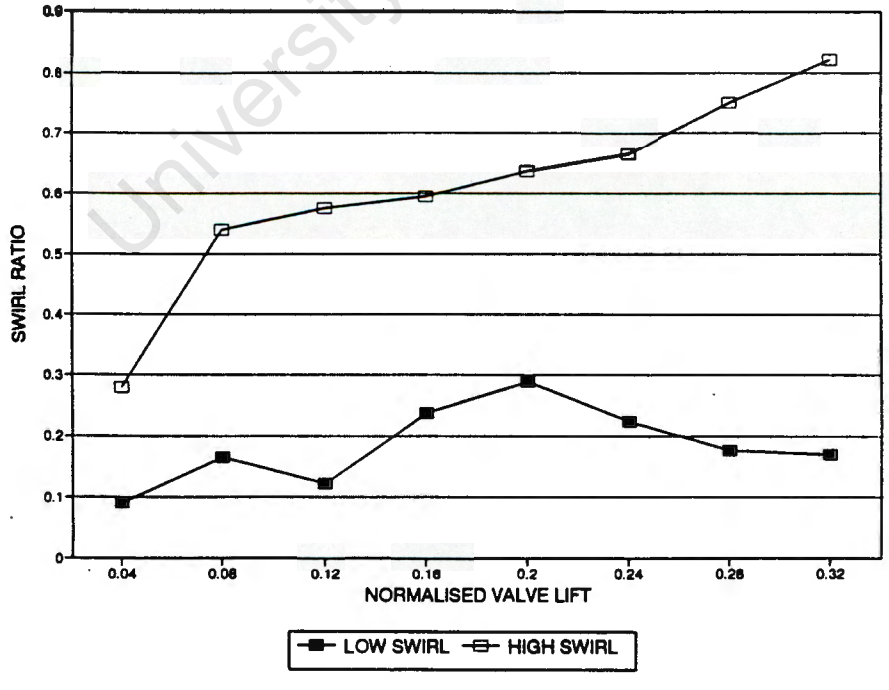

Figure 3.7.4 Swirl ratio comparison with deflector plate in the Nissan engine

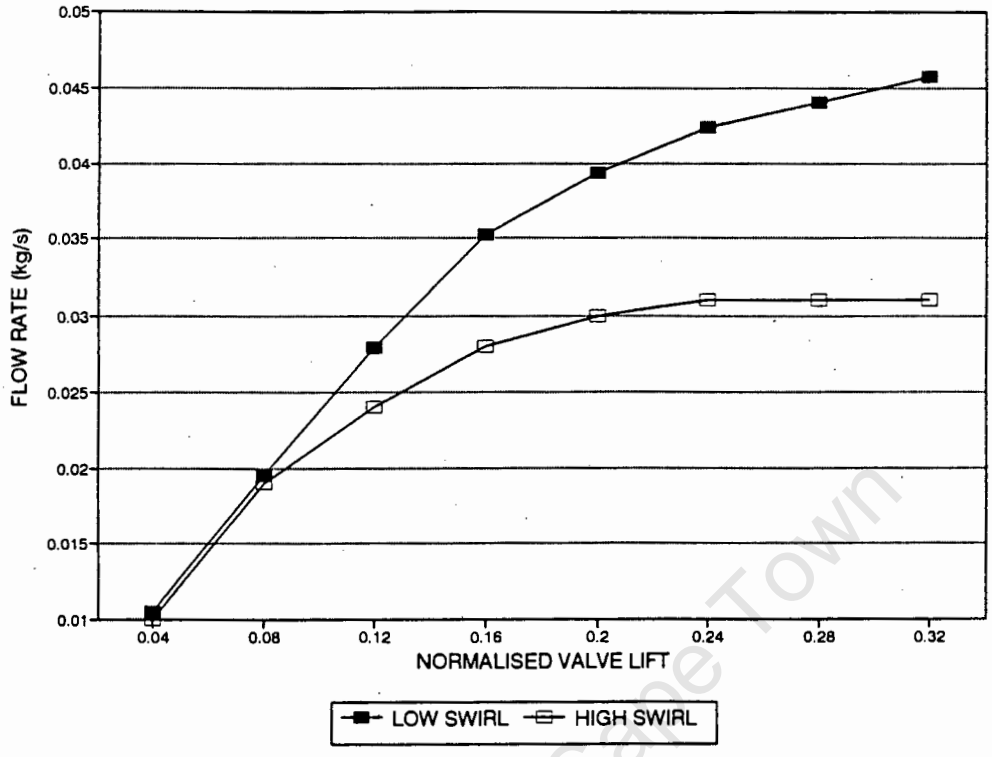

Figure 3.7.5 Flow rate comparison with deflector plate in the Nissan engine

(b) Volkswagen

During dynamometer tests of the Nissan engine, one of the aluminium deflector plates broke loose and passed into the cylinder. Fortunately, as aluminium is soft, no damage was done to the engine. In order to prevent a similar occurrence when testing the VW engine, it was decided to make the deflector plates out of spring steel. Thus 0.6 mm spring steel plate was used to fashion the following batch.

Unfortunately, the VW 1800 head was no longer available for tests on the swirl rig. However, a VW 1600 head which is very similar to that of the 1800, was used to develop a deflector plate design. Beforehand, the standard swirl ratio of the 1600 engine was measured and compared with that of the 1800 in order to asses its suitability as forming a basis for increased swirl design for the 1800 engine. Overleaf is a plot of the swirl ratios of the two engines.

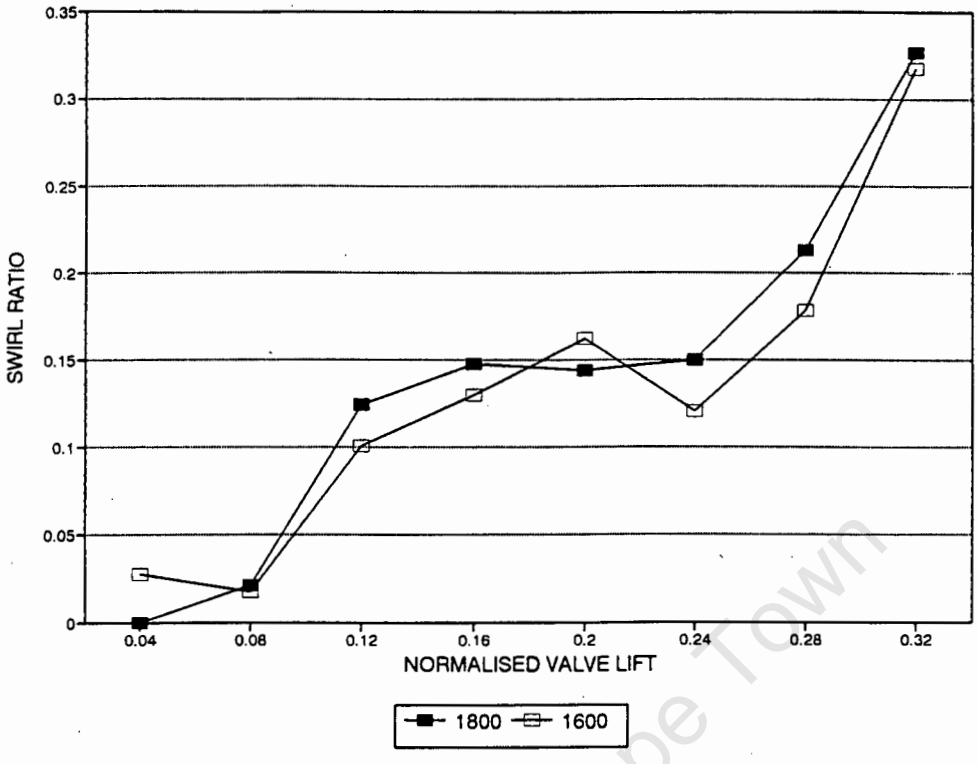

Figure 3.7.6 Swirl ratio comparison between VW 1800 and 1600 engines

The actual swirl speeds of the 1600 engine were slightly less then those of the 1800 at equivalent valve lifts. Similarly, although the port shape of the two heads is similar (see plates 4.1.4 and 4.1.5), the 1600 had a lower flowrate. This resulted in the calculated swirl ratios of the 1600 being equivalent to those of the 1800 engine as is seen from figure 3.7.6. Thus any device increasing swirl on the 1600 head could be expected to increase swirl on the 1800 head by the same amount.

As in the case of the Nissan engine, a piece of plastic was used to determine which side of the port the deflector plate should be located. Drawing from the knowledge accumulated from tests with the Nissan engine, it was assumed that the deflector plate angle should be 65^{o}. Designing the shape of the deflector plate was not as simple as that for the Nissan engine because unlike the Nissan which has a horizontal inlet port, the VW inlet port sloped downwards from the inlet manifold. This can be seen from a comparison of plates 4.1.2 and 4.1.5. Thus the roof of the inlet port formed an obstruction for the deflector plate. The final deflector plate shape was not geometrical as in the case of the Nissan engine, but was more complex. This can be seen in plate 3.7.3. Figure 3.7.7 shows how the deflector plate was mounted in the inlet port.

Plate 3.7.3 VW Deflector plate

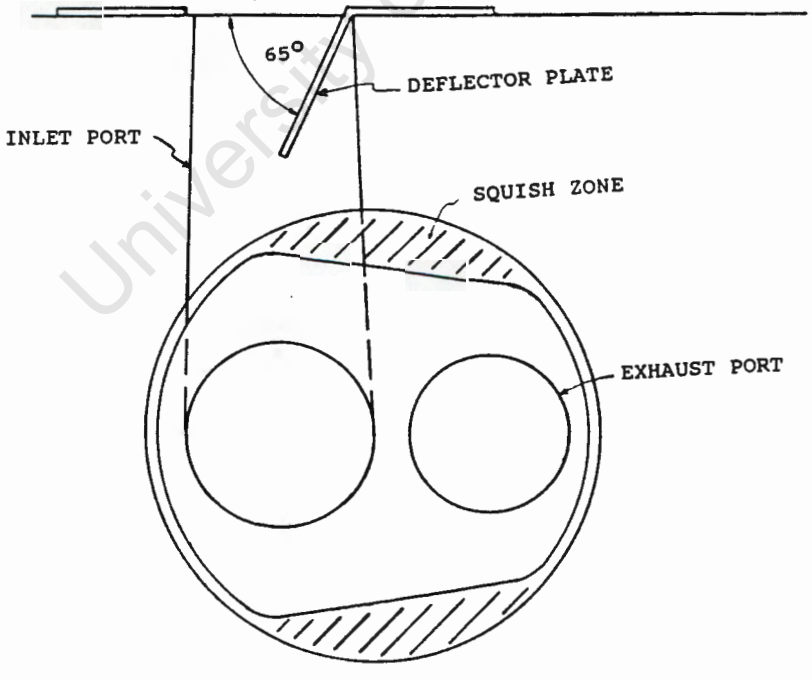

Figure 3.7.7 Mounting of deflector plate in the VW engine

In spite of the difficulties encountered, the final deflector plate design resulted in an increase of mean swirl ratio to roughly 6 times that of the standard engine. Figures 3.7.8 and 3.7.9 are comparisons of swirl ratio and flow rate respectively, expected in the 1800 engine. The predicted flow rates for the high swirl case have been increased from those measured in the 1600 engine by a percentage equivalent to the percentage drop in flowrate exhibited by the 1600 engine in comparison to the 1800 engine.

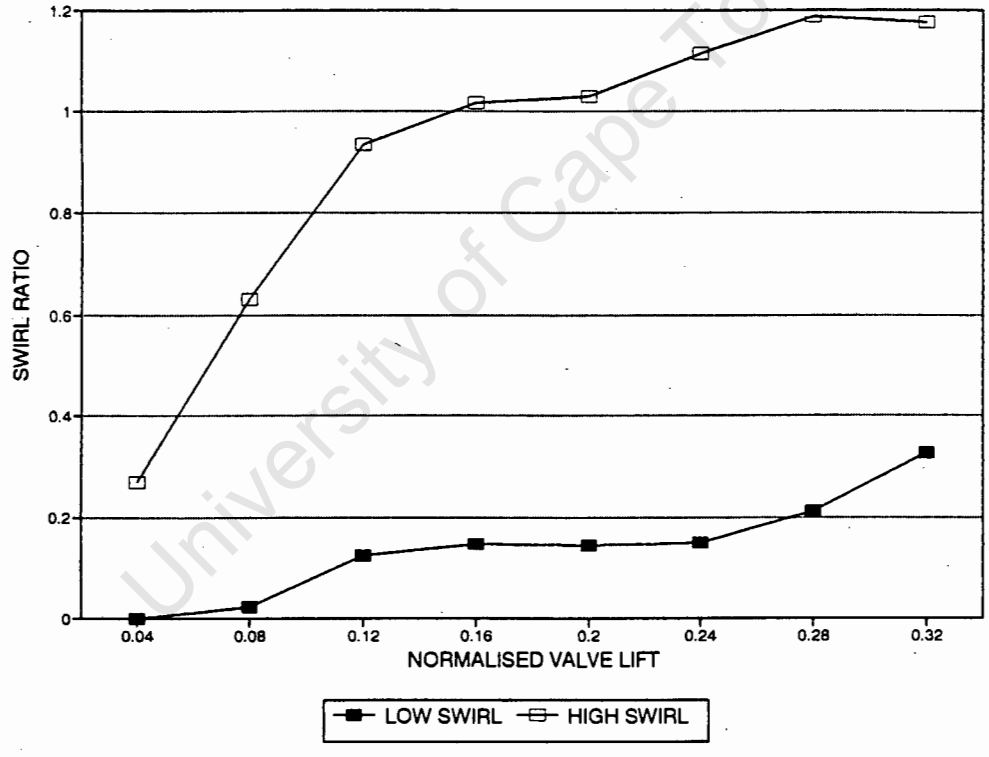

Figure 3.7.8 Swirl Ratio comparison of VW 1800 engine with deflector plate

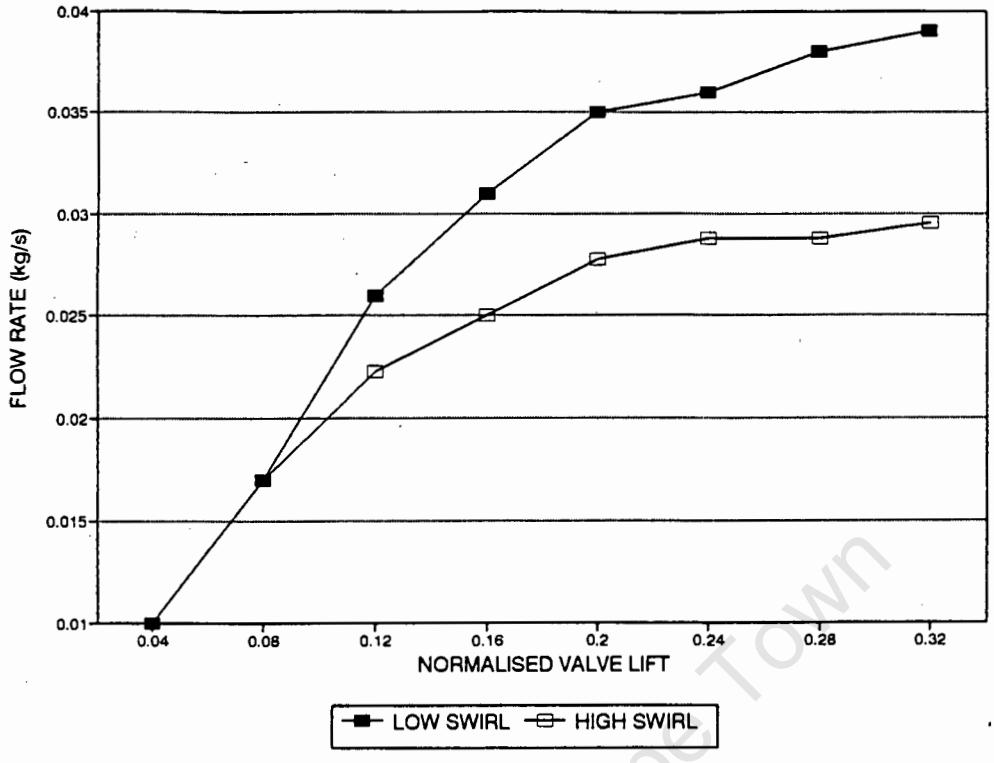

Figure 3.7.9 Flow rate comparison in VW engine with deflector plate

3.7.3 Baffle plates

As mentioned earlier, it was hoped to avoid the deflector plates breaking off and damaging the engine, by making them out of spring steel. Unfortunately, in spite of this precaution, two of the deflector plates broke loose. One of them became wedged in the inlet port but the other entered the cylinder and did considerable damage. Surprisingly, the two plates which did not break off were found completely pushed back against the flow. In other words the original angle of 65^{o} was reduced to about 10^{o}. Thus the plates were only throttling the flow with presumably no increase in swirl. As a result, the engine torque was drastically reduced. Ironically, had the plates been made out of aluminum, they still would have failed, but the engine would have suffered less damage. As it turned out, a new piston was required.

The next course of action amounted to two options. One was to strengthen the deflector plates by making them out of 3 mm plate steel. The other was to find an alternative method of increasing swirl by a means allowing no chance of foreign metal inserts entering the cylinder.

The first option was thought impractical as thick plate would be difficult to cut and it would restrict the flow considerably. Also, there would be difficulty in mounting it between the cylinder head and inlet manifold.

An interesting discovery was made while experimenting with the VW 1600 cylinder head on the steady-flow swirl rig. If a flat plate was used to block off one side of the inlet port, a change in swirl speed resulted. Blocking off one side of the port increased the paddle speed while blocking off the other side reduced the paddle speed. An arbitrary but large valve lift position was selected and a deflector plate was inserted, and the resulting pressure drop across the port and the paddle speed was measured. Then the deflector plate was removed and one side of the port was progressively blocked off until the pressure drop across the port was equal to that experienced with the deflector plate. At this point the paddle speed was slightly less then the deflector plate equivalent. If the port was blocked slightly further the paddle speed did increase, but it was felt that the resultant pressure drop was too drastic. This procedure was repeated at various valve lifts and by trial and error an optimum position was chosen. This position occurred when just less then half the port was covered. Below is a comparison of swirl ratios and flow rates as seen by the VW 1600 between deflector and baffle plates.

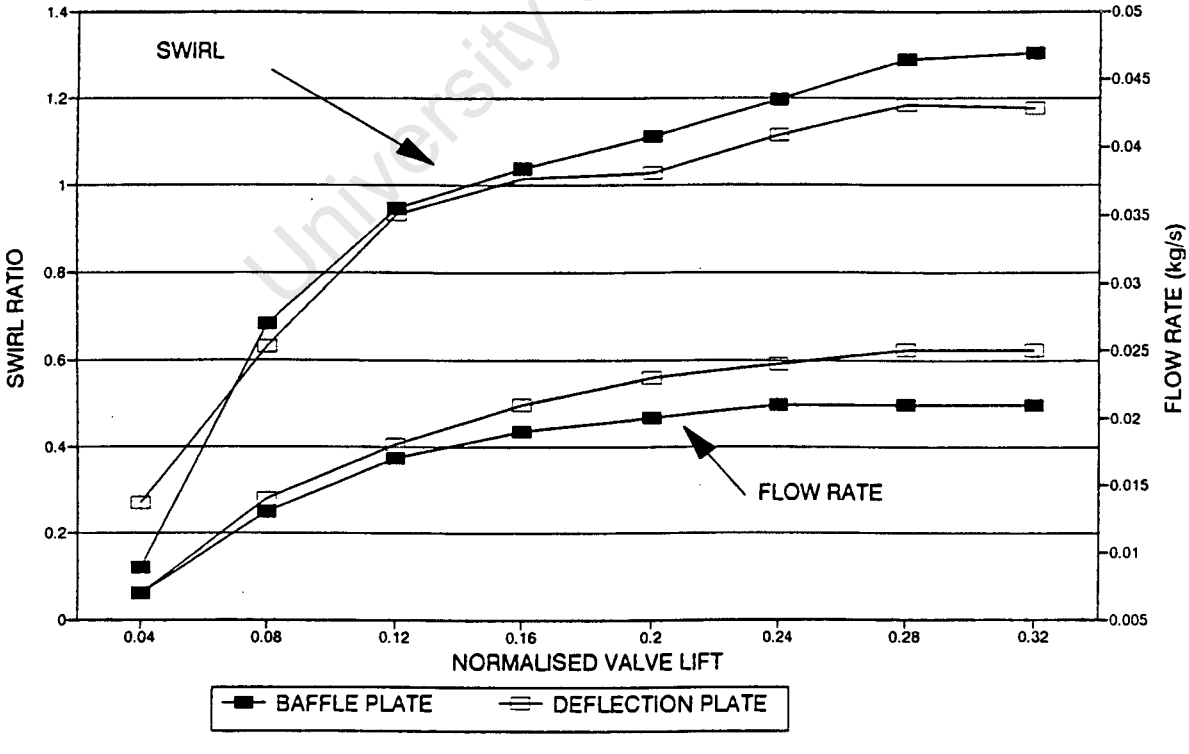

Figure 3.7.10 Swirl and flow comparison with deflector and baffle plates

As expected, the flow rate is less with the baffle plate. However because the flow rate is less, the resultant swirl ratios for the baffle plate are higher. This gave a mean swirl ratio of approximately 7 times that of the standard engine.

When the other side of the port was blocked off by the same optimum amount, the swirl ratios measured were extremely small and in most cases negative. By negative, it is meant that the swirl direction has reversed. Although it is appreciated that swirl direction is probably unimportant in its effect on engine combustion, it is considered important in the calculation of mean swirl ratio if the swirl direction reverses between subsequent valve lifts. This is because at some point between the two valve lifts the swirl speed must be zero which will reduce the total swirl momentum. Below is a diagram and a photograph illustrating the mounting of the baffle plates for increased and decreased swirl.

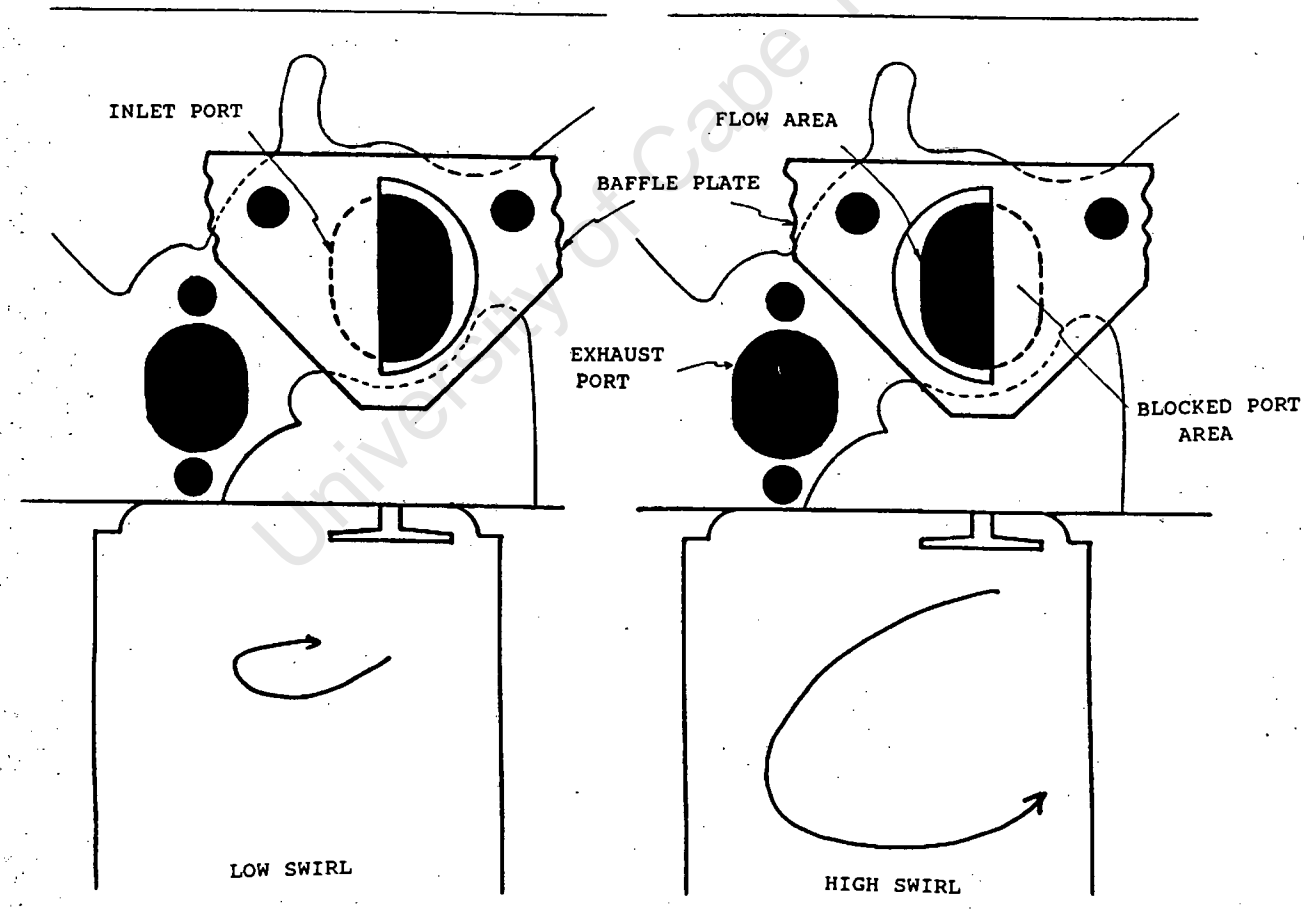

Figure 3.7.11 Baffle plate mounting on VW 1600 engine

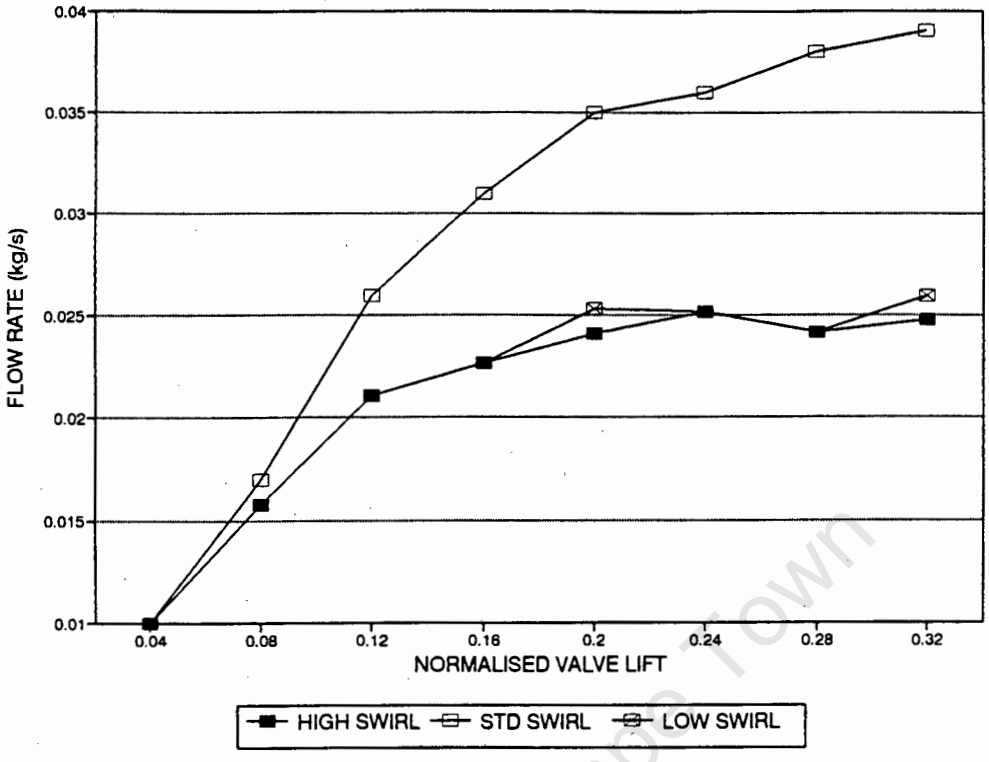

Figure 3.7.13 Flow rate comparison in VW 1800 engine with baffle plate

It can be seen that there is an enormous difference in swirl ratios between the two different positions of baffle plate, but the flow rates are practically identical. This method of varying the swirl is beneficial for the purpose of measuring KLSA since it creates the same pressure drop in each case. Although this pressure drop is high and may result in a drop in torque, it is only the change in KLSA that is of interest.

Some rough tests were performed in an attempt to determine the influence of the inlet manifold on swirl speed. This was done by holding a 10 cm long tube of approximately the same diameter of the inlet port in front of the port. Only small changes in paddle speed were observed, and the pressure drop hardly varied. It was assumed from this that the inlet manifold would not significantly alter the swirl level.

Finally, it can be said that the manufacture of these baffle plates is simple and they are not subject to the same stresses suffered by deflector plates. Thus they were cut from 1.2 mm aluminium sheet, as they were considered unlikely to fracture.

3.8 Dynamometer Comparison of KLSA

3.8.1 Apparatus

The engines used to perform these tests were the Nissan L18 and Volkswagen 1800. The engines were fitted onto cradles and connected via a drive coupling to a Heenan & Froude Mark 1 eddy current dynamometer. This type of dynamometer is suitable for constant speed operation as well as rapid cycling. The specifications for the unit are as follows:

Speed range: 0 - 10000 r/min
Torque range: 0 - 200 Nm
Power range: 0 - 150 hp

The inlet air temperature supplying each engine could be maintained at a selected temperature above ambient by passing it through a plenum fitted with a set of heating coils.

Each engine had a Piezo-electric pressure transducer fitted into one of the combustion chambers, flush with the chamber wall. In the Nissan this was an AVL 8QP pressure transducer with a sensitivity of approximately 12 pC/bar. In the Volkswagen a Kistler 6121 pressure transducer with a sensitivity of approximately 14 pC/bar was used.

The signal from each pressure transducer was fed to a RC Electronics computerscope via a PCB-F462A charge amplifier with an output of 10 bar/volt. The Computerscope was loaded on an IBM XT personal computer fitted with a 12 bit analogue to digital converter, with 16 input channels. During tests two channels were allocated as follows:

Channel #1 : Cylinder pressure traces
Channel #2 : TDC and spark pulses

3.8.2 Test Procedure

This part of the experiment consisted of two parts, namely measuring the KLSA of the test engine, with and then without the swirl improving device.

(a) Nissan L18 : Deflector plates

To begin with, the deflector plates were mounted in the inlet ports. It was important to keep the inlet air temperature constant since knock limit is a function of temperature. Thus the engine was run with the inlet air temperature set at 45°. It was appreciated that the deflector plates would create a lower pressure in the cylinder and therefore bias the results in favour of swirl. It was intended to measure the inlet port pressure, at each speed when the deflector plates were inserted, and then create the same pressure drop by throttling the inlet air flow during tests without the deflector plates. However due to technical difficulties, this was not possible. The engine was run on 93 octane petrol in order to encourage it to knock more readily. Care was taken to ensure that the same batch of petrol was used for all tests.

Initially the spark timing was set at the standard setting of 10° BTDC. At a speed of 1500 rpm, and wide open throttle, the ignition timing was advanced by manually turning the distributor until trace knock could be detected by ear. At this point, the timing was measured with a strobe light and the output torque was recorded. The computer scope was used to record pressure traces for later analysis.

Measurements were taken at incrementing speeds of 500 rpm up to 4500 rpm at which point a high level of engine noise made the detection of trace knock impossible. The tests were duplicated, in order to check for repeatability. It was found that the spark advance readings were repeatable to within 1 - 2 degrees and the torque readings to within 2 Nm. At 1500 rpm this results in a 15% error in spark advance measurement, however at 4500 rpm this error is only 4%. The error in torque measurement is at most 2% throughout the speed range.

The deflector plates were then removed and the entire set of tests repeated. The pressure traces of the two cases at equivalent speeds were then superimposed on one diagram for comparison.

(b) Volkswagen : Deflector plates

The procedure for testing this engine was similar to that of the Nissan engine. However, in this case an oscilloscope was connected in parallel with the computerscope to the output of the pressure transducer and was used for detecting

trace knock. The oscilloscope produced real time pressure traces as opposed to the delay in data capture using the computerscope. With this arrangement, it was possible to also detect knock at higher speeds. Consequently, the measurements were made up to 5000 rpm.

(c) Volkswagen : Baffle plates

The same procedure as above was used for these tests. However, in order to improve the knock detection method, the oscilloscope was used in the digital storage mode rather then the real time mode. This meant that the signal was frozen for one period, until the next pulse retriggered the scope. This made the display less confusing. The engine was tested with the baffle plates inserted for high swirl, and then with the plates reversed for low swirl.

4. RESULTS AND DISCUSSION

4.1 Comparison of inlet port geometry

Following are photographs of the castings of the various inlet ports used in the comparison of swirl ratios.

Plate 4.1.1 Casting of Ford V6 inlet port

Plate 4.1.2 Casting of Nissan L18 inlet port

Plate 4.1.3 Casting of Toyota 16 valve inlet port

Plate 4.1.4 Casting of VW 1800 inlet port

Plate 4.1.5 Casting of VW 1600 inlet port

Plate 4.1.6 Casting of Toyota 22R inlet port

According to the shape of the inlet ports, none of these engines, apart from the Toyota 22R which has a helical pre chamber, should exhibit very high swirl ratios. It has the highest swirl ratio of 0.951. The Ford engine which has an S-bend in the port has a ratio of 0.453. The Nissan and VW engines, which have non-directed ports, have medium swirl ratios of about 0.25. The Toyota 16 valve and 12 valve engines both have low swirl ratios of about 0.015. It is apparent that multi-inlet valve engines, typically have low swirl ratios. A table of all the swirl ratios measured during the project, can be found in Appendix A.

Figure 4.1.1 overleaf shows the comparison of instantaneous swirl ratios as a function of crank angle for the above engines.

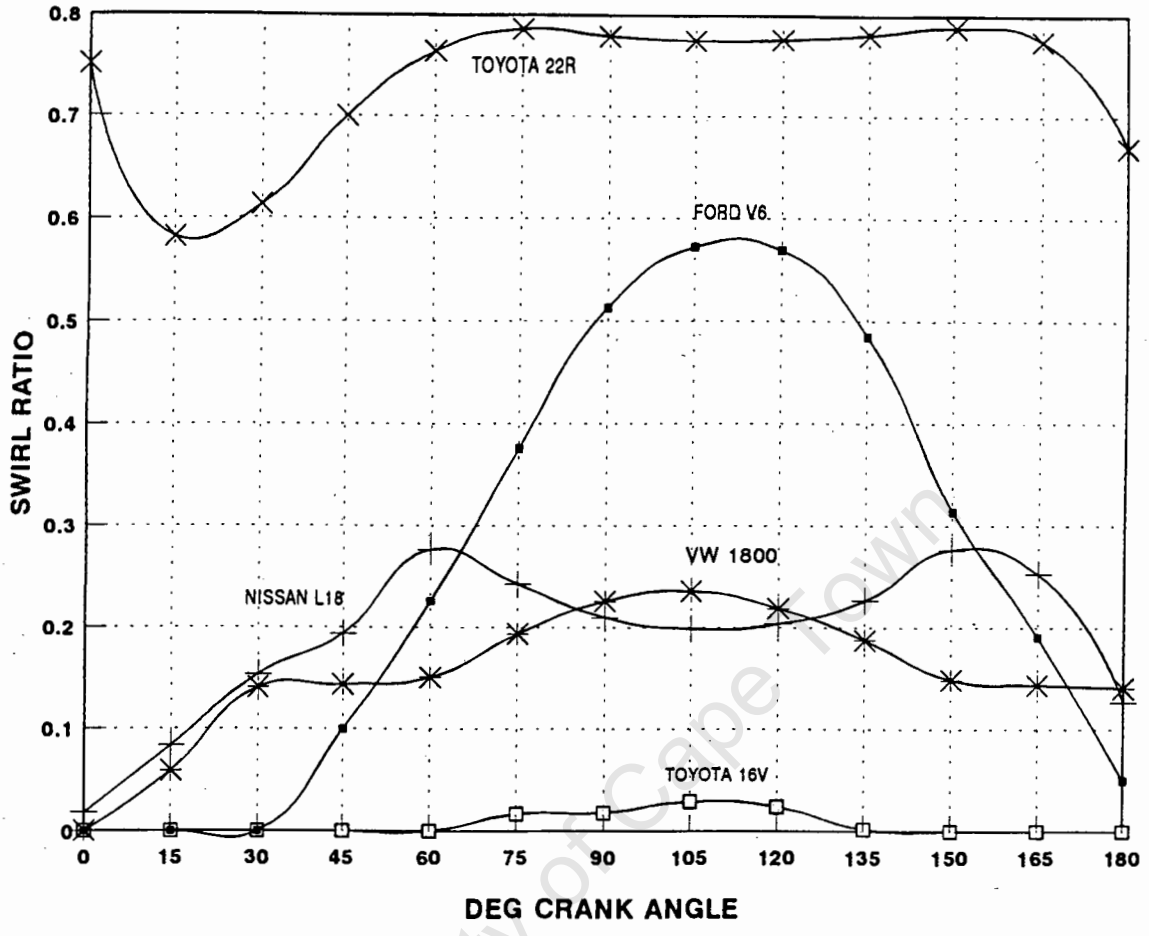

Figure 4.1.1 Swirl ratio comparison of engines as a function of crank angle

4.2 Detection of Barrel Swirl

As previously mentioned, the technique used for the determination of barrel swirl did not provide a sufficient characterisation of the flow field and thus no qualitative results could be obtained for the purpose of formulating comparisons between the various engines. It is included here however as a point of interest rather then an attempt to draw any significant conclusions. The only engine which could be positively classed as having barrel swirl, is the Nissan 1800 engine. The barrel swirl detected in this case was surprisingly strong, even though it is a single inlet valve engine. Also, this swirl was detected in the steady-flow swirl rig which unlike a real engine, does not have a piston surface upon which barrel swirl may be more likely to develop.

4.3 Swirl Comparison with Knock Limited Spark Advance data

Below is a table summarising the measured mean swirl ratios for the four engines used in this study.

Table 4.3.1 Mean swirl ratios of selected engines

ENGINE	SWIRL RATIO
FORD V6	0.453
NISSAN L18	0.274
VW 1800	0.235
TOYOTA 1600	0.015

In an attempt to find a correlation between swirl ratio and KLSA of these engines, graphs were plotted of KLSA versus mean swirl ratio and engine speed, for 97 octane fuel[27] are shown in figures 4.3.1 and 4.3.2.

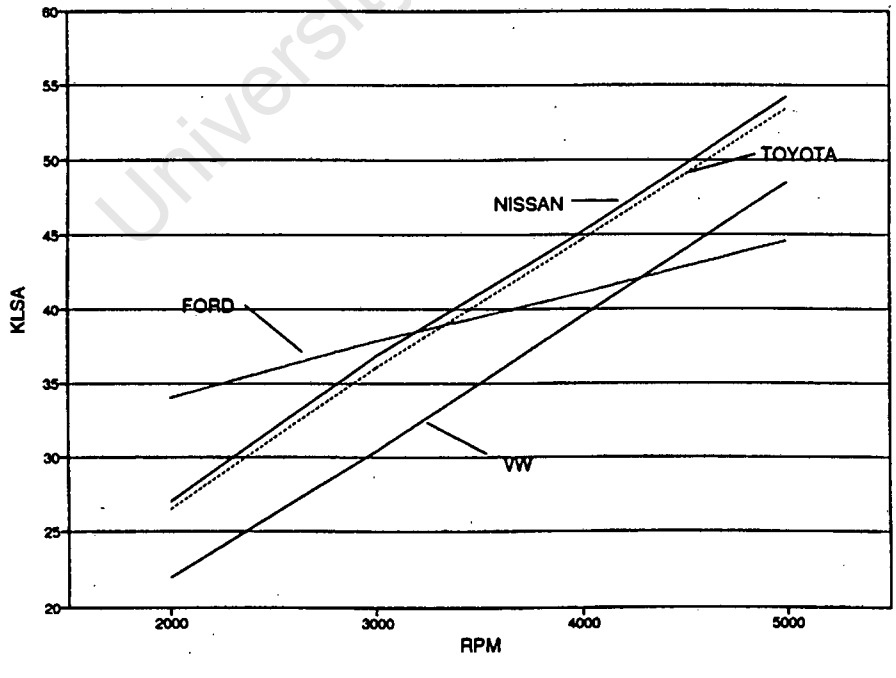

Figure 4.3.1 KLSA data vs Engine speed

It can be seen that KLSA increases at the same rate for all the engines except the Ford which exhibits high speed knock. Also, the Nissan and Toyota engines have virtually the same KLSA but they have very different swirl ratios.

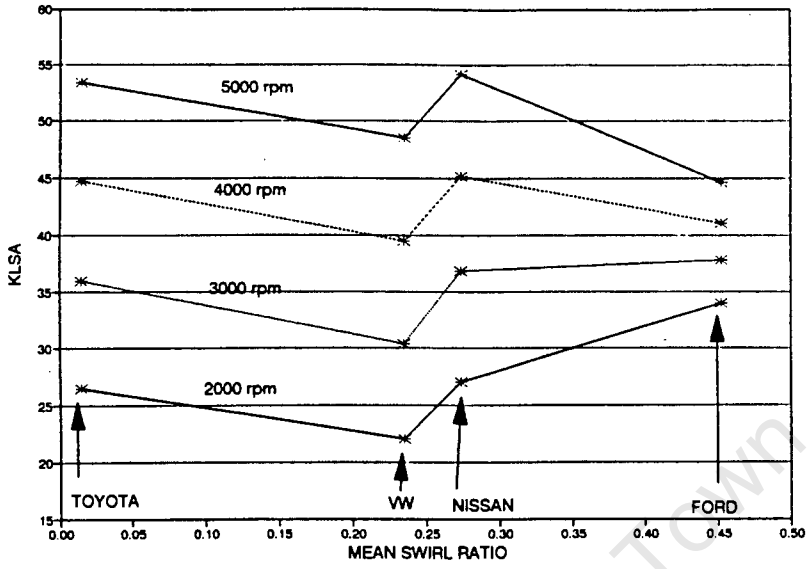

Figure 4.3.2 KLSA data vs Mean Swirl Ratio

From the above graph it is clear that if the entire speed range is taken into account, there is no correlation between swirl ratio and KLSA.

Figure 4.3.3 and 4.3.4 overleaf are bar charts showing a comparison of swirl ratios on the left hand axis and the Knock Limited Spark Advance on the right hand axis, for 97 and 93 octane petrols, and at various engine speeds.

At low engine speeds the KLSA increases with increased swirl ratio with the exception of the Toyota engine which has a very low swirl ratio but a comparatively good KLSA. The good KLSA value for the Toyota engine may be possibly explained by high turbulence levels generated by the colliding inlet jets. As the engine speed increases, the situation almost reverses with the Ford engine, which has the highest swirl ratio, having the lowest KLSA. The Nissan engine appears to have the most favorable KLSA throughout the entire speed range and this may be attributed to the strong presence of barrel swirl detected in this engine as discussed in section 4.2.

Thus it would appear from these results that no significant conclusion can be drawn with regard to the effects of swirl ratio on KLSA. It is most likely that other factors which are known to affect KLSA such as combustion chamber size and shape and spark plug location, have greater influences then swirl ratio and are thus masking the effects of swirl.

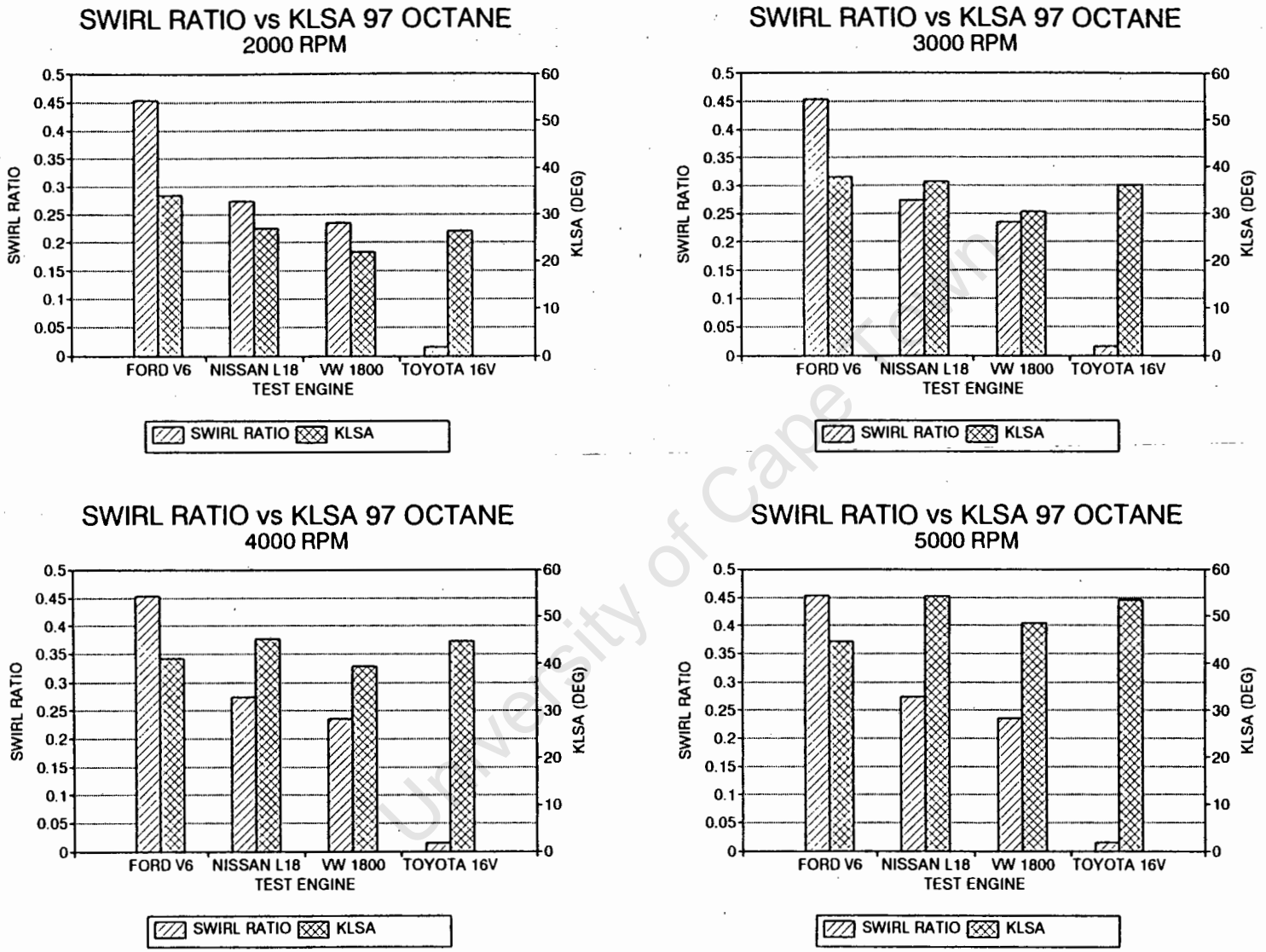

Figure 4.3.3 Swirl Ratio comparison with Knock Limited Spark Advance using 97 octane
* KLSA Data was obtained from ERI report # IER 059

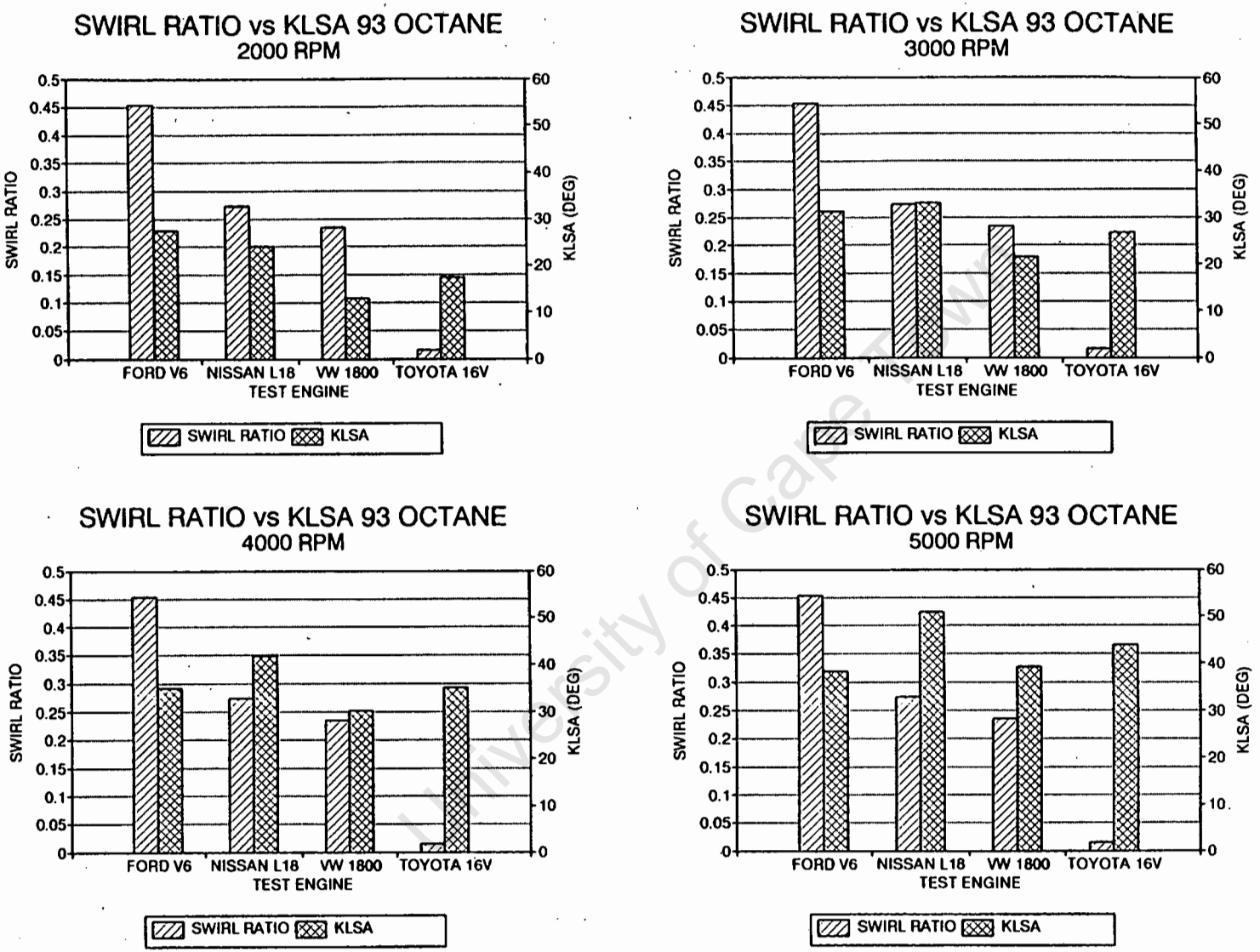

Figure 4.3.4 Swirl Ratio comparison with Knock Limited Spark Advance using 93 octane

* KLSA Data was obtained from ERI report # IER 059

4.4 Swirl Comparison with Deposits

These deposits were found in a Toyota 1300, 3 valve per cylinder engine. It is understood that this vehicle was used as a city taxi and thus only did short trips, with the engine most probably operated at part load condition for most of its life, accounting for the extensive inlet port and valve deposits. Below is a photograph of the inlet valves showing these substantial deposits.

Plate 4.4.1 Inlet valve deposits in a Toyota 1300 multi-valve engine

Overleaf are photographs which compare rubber castings of the inlet ports of this engine, firstly with the deposits intact, and then with the deposits removed.

Plate 4.4.2 Casting of Toyota 1300 inlet port with deposits

Plate 4.4.3 Casting of Toyota 1300 inlet port with deposits removed

As one would expect, the mass flow rate and hence volumetric efficiency decreased with valve deposits, and decreased further with both valve and port deposits. This is illustrated in figure 4.4.1 below.

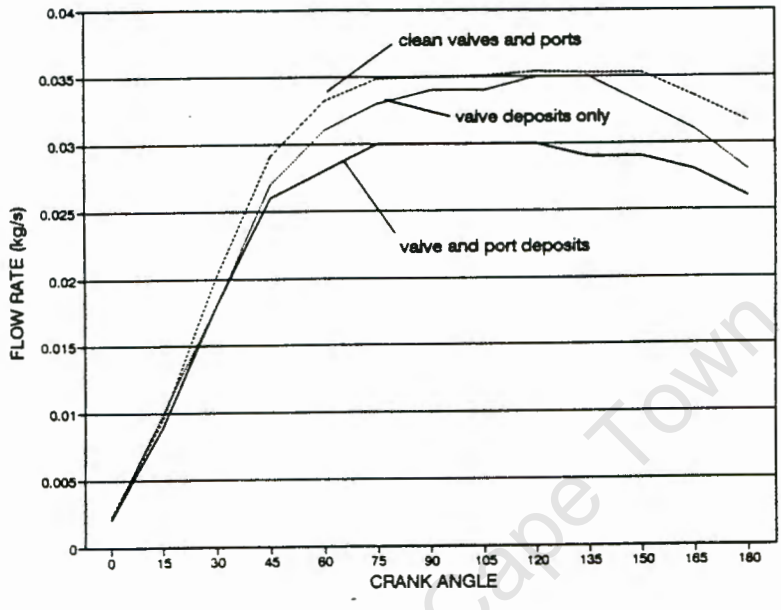

Figure 4.4.1 Flow rate in Toyota 1300 engine with and without deposits

Figure 4.4.2 below compares the difference in swirl ratio with the various deposits, as measured on the steady-flow swirl rig.

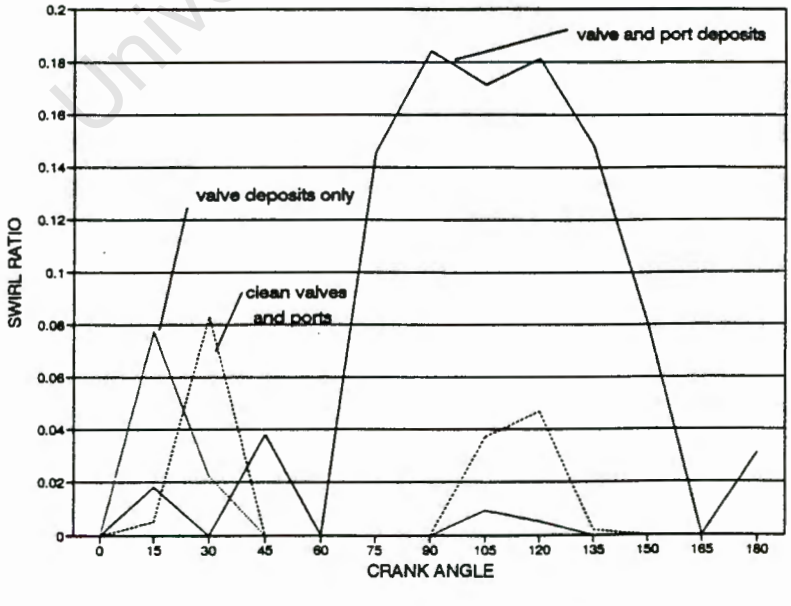

Figure 4.4.2 Swirl ratio of Toyota 1300 engine with and without deposits

The most obvious result from Figure 4.4.2 is that the swirl ratio increases greatly with both valve and port deposits for this particular engine. The distribution of swirl throughout the crank period is erratic for the most part, but there is a consistent occurrence of swirl among the three cases centered around the 110° crank position. At this position both types of deposits cause a large increase in swirl. But, in the case of valve deposits alone, the swirl level decreased. At smaller crank angles, corresponding to low valve lifts, the swirl is lower when both types of deposits are present. Although the swirl level at these positions is similar for valve deposits only and no deposits, there is a phase shift of 15° between the peak swirl values. And in general, at low valve lifts, deposits cause peak swirl values at different crank positions, rather then either accentuating or decreasing the swirl level at a particular location.

It would appear from these results, that swirl level depends on different factors at low valve lifts and at high valve lifts. At low valve lifts, any swirl is caused by jets of high velocity issuing from the valve apertures. At low valve lifts, the flow area consists of the area between the valve perimeter and the valve seat. Thus deposits will not significantly reduce the flow area which would result in increased jet velocities. The pressure drop caused by deposits would be small in comparison to the pressure drop across the valve. Thus at this level, any variation in swirl must come from flow biasing depending on the position of the deposits. This biasing may change at various valve lifts and hence various crank positions.

At high valve lifts the swirl is a result of the increased angular momentum of the incoming flow as initiated by the direction of the inlet port. In this case, the swirl speed may be increased or decreased due to flow biasing which in turn depends on the nature of the deposits. In this case it seems that port deposits which are more irregularly spaced then valve deposits had a positive biasing effect. On the contrary, valve deposits alone had a negative biasing effect which resulted in lower swirl speeds. Another factor resulting in increased swirl ratios with increased deposits, is the change in flow rate. In order to compensate for the increased pressure drop due to deposits, the flow rate is reduced to maintain a constant pressure drop across the valve. As swirl ratio is inversely proportional to flow rate, lower flow rates will reflect higher swirl ratios, for the same paddle speed.

In summary, it can be said that the effect of deposits depends on the nature and location of these deposits. In all cases however, deposits adversely affect the flow rate and volumetric efficiency.

4.5 Dynamometer Comparison of KLSA

4.5.1 Nissan L18 : Deflector plates

The Nissan engine exhibited some peculiar traits which are somewhat difficult to explain.

Firstly it was noted that at all speeds up to 4000 rpm, the KLSA was greater but the torque lower for the low swirl case. Above 4000 rpm the situation reverses, and the KLSA becomes greater and the torque lower for the high swirl case. One would expect that the greater spark advance would produce higher torques, considering that the measured spark advance settings up to 4000 rpm are below MBT timing. Above 4000 rpm, the KLSA timing is greater than MBT timing and this explains why the more advanced timing settings in the high swirl case produce lower torques.

The above issues are clearly illustrated in figures 4.5.1 and 4.5.2.

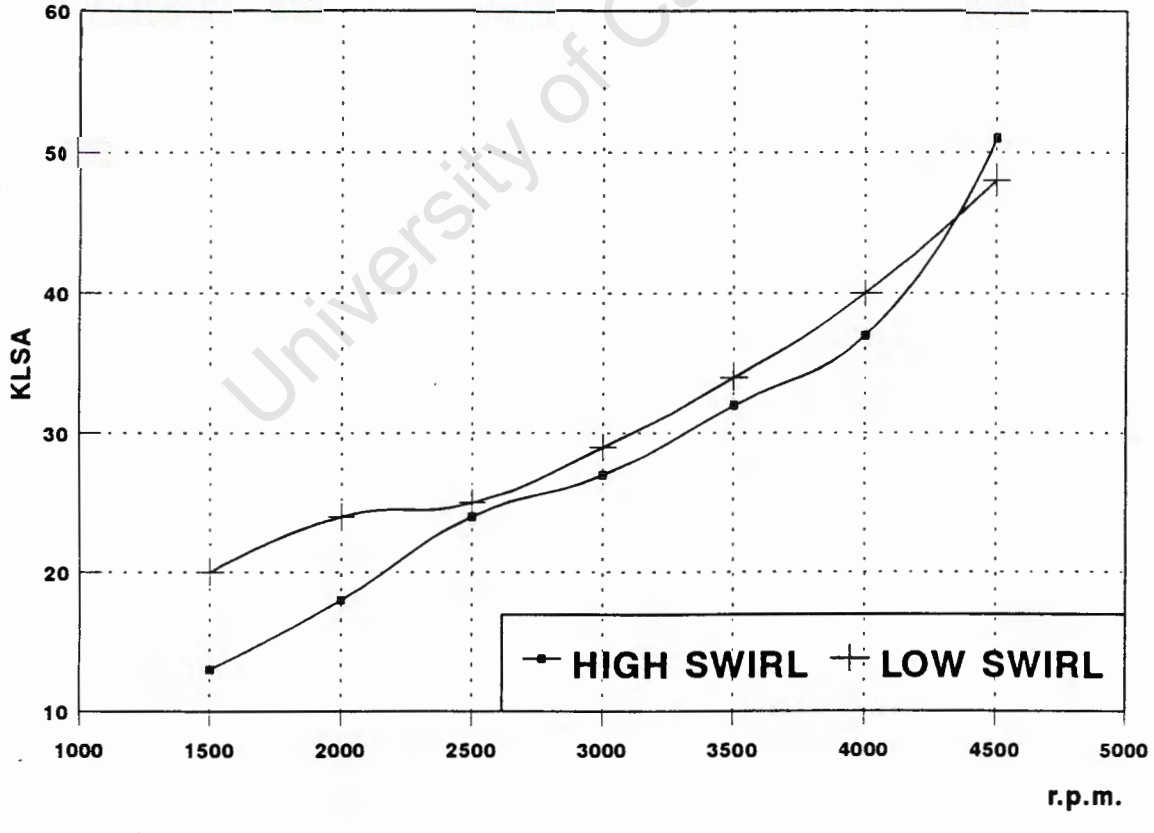

Figure 4.5.1 KLSA Comparison of Nissan L18 engine with deflector plates

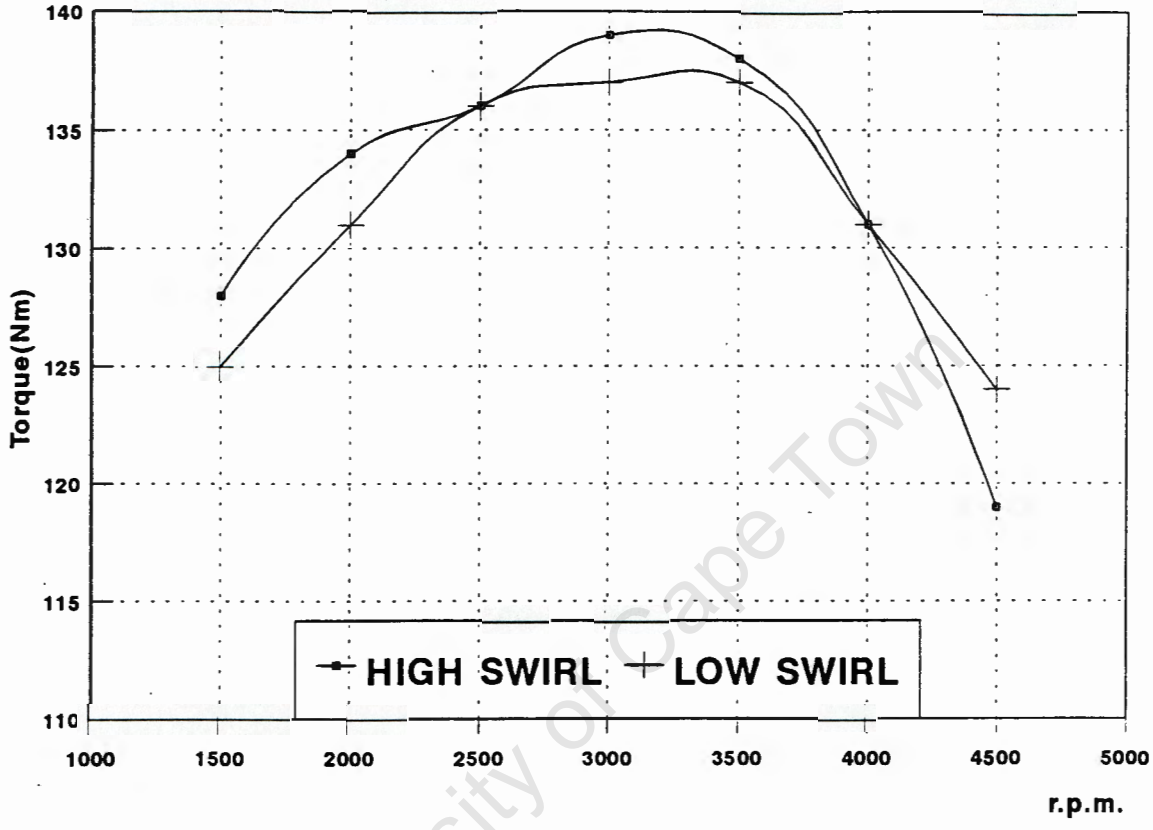

Figure 4.5.2 Torque Comparison of Nissan L18 engine with deflector plates

Secondly, upon examining the recorded pressure traces, it was noted that up to 4000 rpm the low swirl case produced higher peak pressures and a more rapid pressure rise, indicative of faster flame propagation. These factors would normally result in higher torque, and therefore it is puzzling as to why the torque is lower in the low swirl case. Similarly, above 4000 rpm the high swirl case resulted in greater peak pressures and more rapid pressure rise but lower torque. Overleaf is a typical comparison of pressure traces for the low and high swirl cases at low rpm. The pressure traces at other speeds can be found in Appendix C.

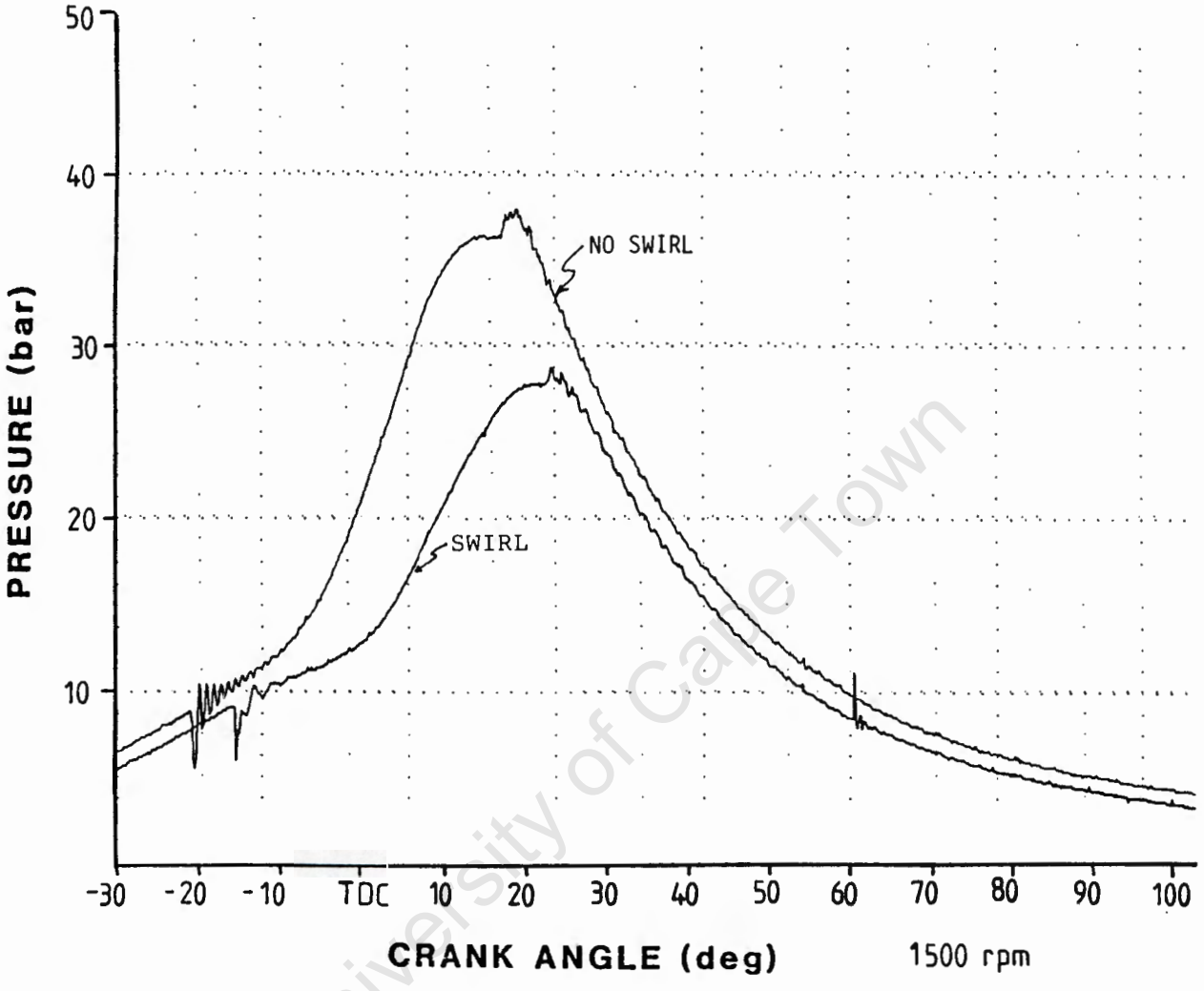

Figure 4.5.3 Pressure trace comparison for Nissan L18 engine at 1500 rpm

4.5.2 Volkswagen : Baffle plates

In this instance, there was a definite increase in KLSA in the high swirl case above the low swirl case. This increase is more dominant at high rpm where the difference in KLSA is about 3 degrees. This can be seen in figure 4.5.4 overleaf.

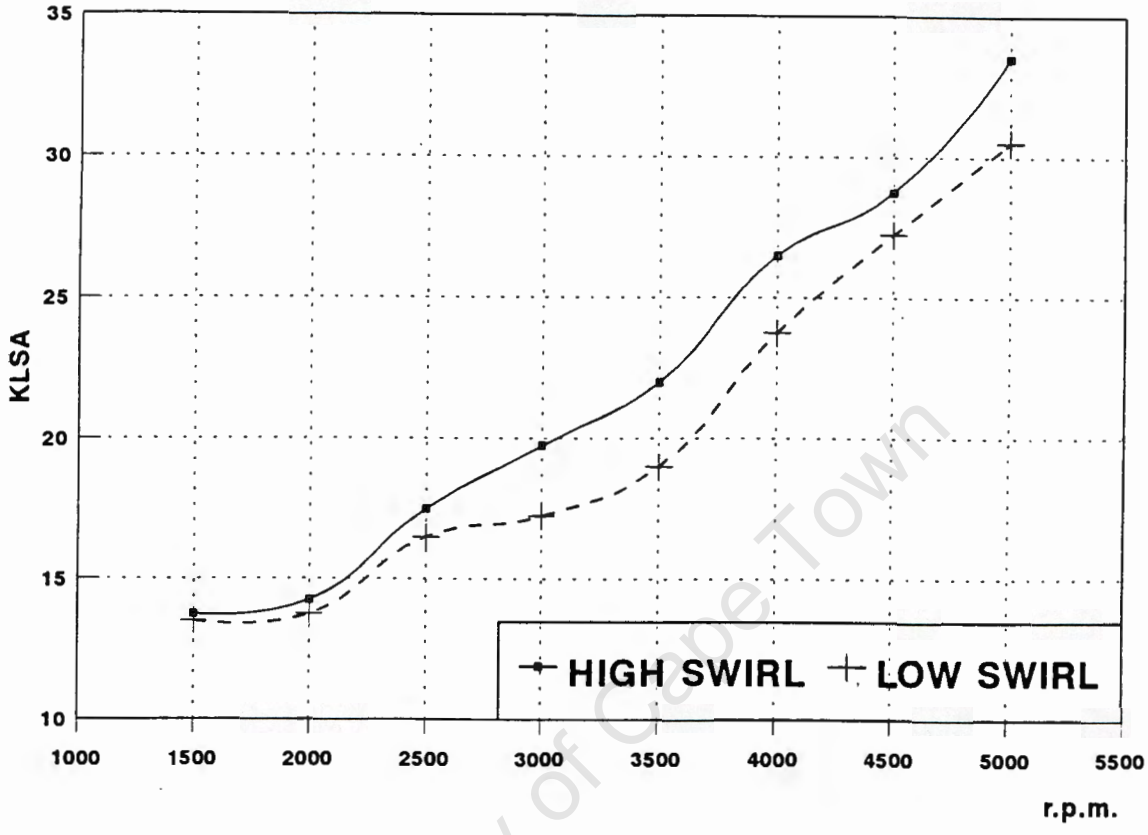

Figure 4.5.4 KLSA Comparison for VW engine with baffle plates

Figure 4.5.5 overleaf is a comparison of torque at the low and high swirl conditions. It can be seen that there is very little difference between the two curves. Although the same amount of throttling is present in each case, one would expect the high swirl case to produce slightly higher torque, considering that the spark timing was slightly more advanced. A check with the MBT timing curve established that for speeds up to 4500 rpm, the measured KLSA timing was well below MBT timing. On the other hand, the inserted baffle plates, which vary the swirl level, may alter engine performance so as to modify the MBT timing curve. It follows that a new MBT timing curve should be measured for both cases of high and low swirl in order to formulate a comparison of this nature.

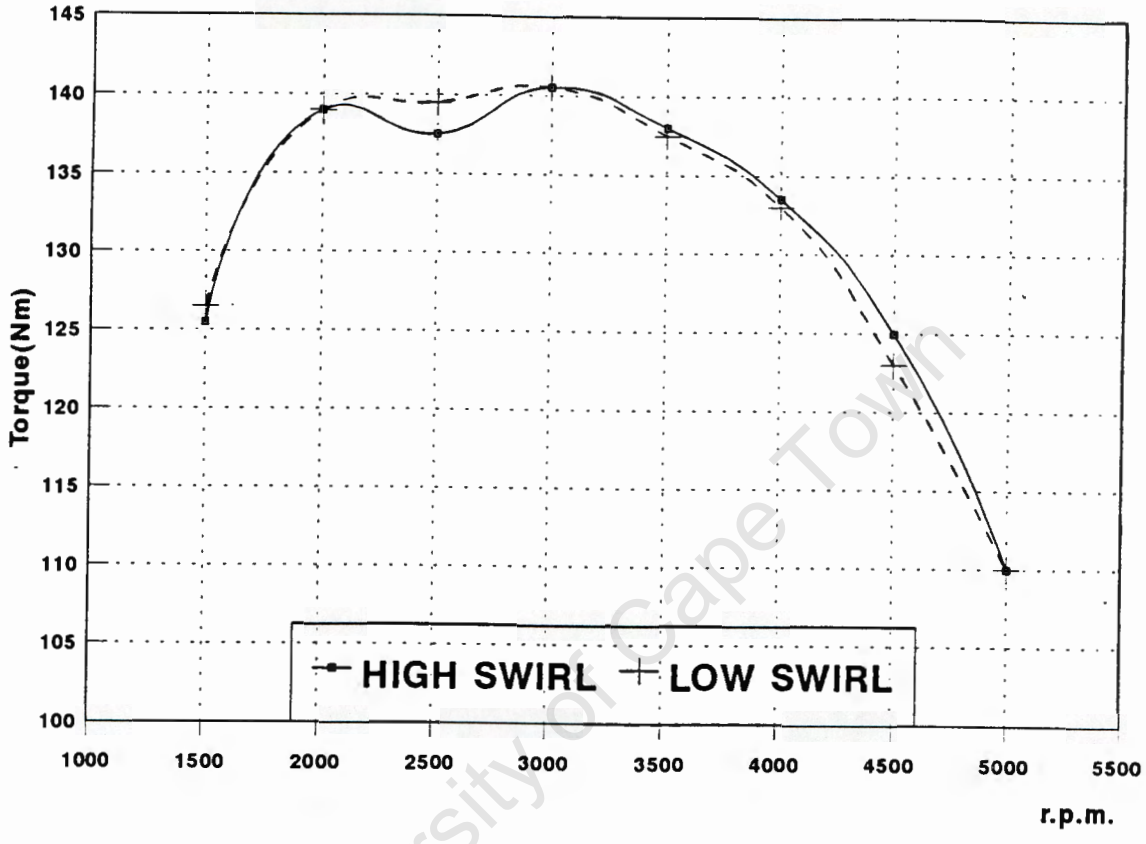

Figure 4.5.5 Torque Comparison of VW engine with baffle plates

Generally, it is apparent from the superimposed pressure traces that the high swirl case produces higher peak pressures and more rapid pressure rise. Overleaf is a comparison of typical pressure traces for the low and high swirl cases at 2500 rpm. Pressure trace comparisons at other speeds can be found in Appendix C.

At every speed, 5 to 8 pressure traces were averaged and the difference between the greatest and lowest peak pressure values were calculated. At all speeds, the high swirl case produced higher peak pressures, and at most speeds, the cycle to cycle variation was less. This comparison is examined in Table 4.5.1 overleaf.

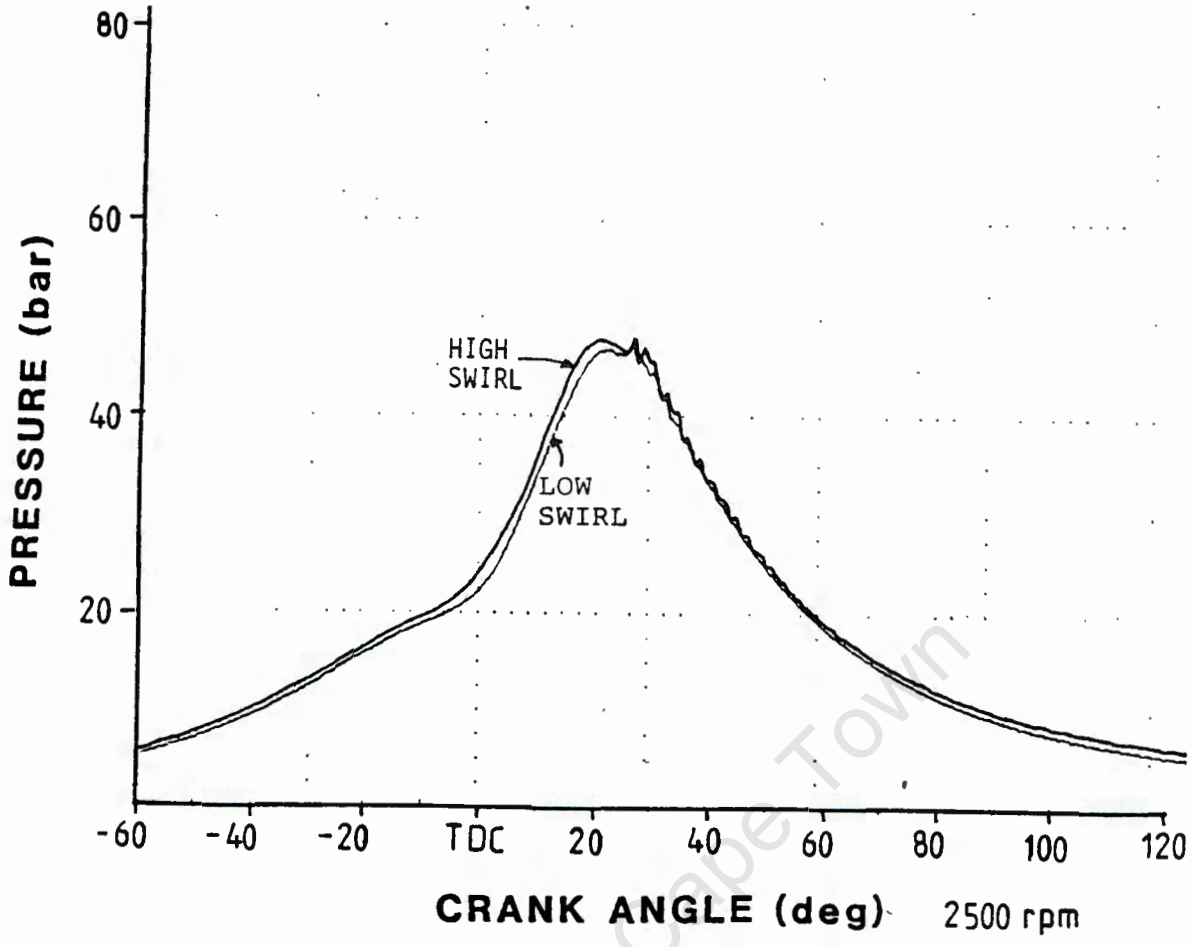

Figure 4.5.6 Pressure trace comparison of VW engine at 2500 rpm

Table 4.5.1 Comparison of peak average pressures

Speed (rpm)	Average Pressure (bar) low swirl	high swirl	Pressure Variation (bar) low swirl	high swirl
1500	38.5	41.2	4.7	3.8
2000	39.5	45.1	3.6	10.0
2500	43.2	44.4	7.5	9.0
3000	39.5	49.8	13.8	10.0
3500	48.6	51.3	8.7	5.13
4000	52.3	55.1	11.5	13.3
4500	56.2	57.3	11.2	10.5
5000	51.7	55.3	11.2	10.0

5. CONCLUSIONS

5.1 Effect of inlet geometry on swirl ratio

It was confirmed by measurement, that the inlet port configuration has a direct bearing on the swirl level generated in standard engines. This made it possible to alter the swirl ratio of standard engines by modifying the inlet port. This was achieved by port inserts, to be discussed later. A Toyota engine with a helical pre-chamber exhibited the highest mean swirl ratio of 0.95 while non-directed ports, as found in the Nissan and VW 1800 engines, have swirl ratios of about 0.25. A Ford V6 engine which has a slight S-bend in the port has a swirl ratio of 0.45. It was found that multiple inlet valve ports have very poor swirl ratios of about 0.015 as found in both the Toyota 1600 and 1300 engines.

5.2 Detection of barrel swirl

A coarse method of detecting barrel swirl was tried, but proved to be ineffectual in characterising the cylinder flow. However, it was demonstrated using this method that the Nissan engine has a "strong" presence of barrel swirl. However, the Toyota multiple inlet valve engines which are reputed to predominantly have barrel swirl, did not exhibit any.

5.3 Swirl Comparison with Knock Limited Spark Advance data

A selection of four commercially available engines with similar bores, but varying combustion chamber shapes, were used in a comparison of their mean swirl ratios and KLSA. It was not possible to find a correlation between swirl ratio and KLSA. This is because the KLSA values increased at different rates amongst the four engines, with increase in engine speed. For example the Ford engine has the highest spark advance at 2000 rpm but exhibits high speed knock, so that it has the lowest KLSA at 5000 rpm. Also, the Toyota 16 valve engine which has a very low swirl ratio, demonstrated higher values of KLSA throughout the speed range then the VW engine which has a moderate swirl ratio. This was attributed to possible high turbulence levels in the Toyota, generated by the interference of the two inlet valves.

It was concluded that other factors such as combustion chamber shape and spark plug location, have a more dominant affect on knock then swirl level.

5.4 Swirl comparison with deposits

It was found that inlet port and valve deposits reduced the volumetric efficiency. However, both types of deposits increased the swirl ratio substantially from that of the normal case. On the other hand, valve deposits alone reduced the swirl ratio from the normal case. Thus it would appear, that anything obstructing the flow will cause an increase or decrease in swirl ratio depending on the direction that these objects bias the flow.

5.5 Dynamometer comparison of KLSA

Dynamometer tests comparing the KLSA of a VW engine fitted with baffle plates arranged to either increase or decrease the swirl demonstrated that in the case of high swirl, the measured KLSA was higher by up to almost 10% at 5000 rpm. At lower speeds this increase was not as great. On the other hand, there was virtually no change in torque, possibly because there was the same amount of throttling in each case. An examination of the engine pressure traces showed that high swirl caused higher peak pressures and more rapid rate of pressure rise. It was concluded that swirl has a beneficial affect on combustion and reduces the tendency to knock. This means that the engine compression ratio can be increased, which will increase the thermal efficiency. Alternatively, a lower octane petrol can be used before knock occurs.

6. REFERENCES

1. Amann C.A. - *A perspective of reciprocating engine diagnostics without lasers*, Progress In Energy and Combustion Science, vol 9 No. 3 pp 239-267.

2. Anonymous - *Measuring combustion chamber parameters: part 2*, Automotive Engineering Journal vol 98 No. 4, April 1990.

3. Anonymous - *Designing Engine Combustion chambers*, E-Lab, April-June 1984, pp 6-8.

4. Anonymous - *Modelling turbulence in engines*, E-Lab, Jan-Mar 1978, pp 4-5.

5. Anonymous - *High Turbulence Engines*, Ford Energy Report, Volume 2, 1987 chapter 11.

6. Bradley D, Hynes J, Lawes M, Shepard C.G.W.- *Limitations to turbulence-enhanced burning rates in lean burn engines*, C46/88 IMechE, 1988.

7. Heywood J.B. - *Internal Combustion Engine Fundamentals*, McGraw-Hill, 1988.

8. Ferguson C.R. - *Internal Combustion Engines*, Applied Thermosciences, Wiley, 1985.

9. Ramos J.I. - *Internal Combustion Engine Modeling*, Hemisphere Publishing Corporation, 1989.

10. Seppen J.J. - *A new method to determine flow phenomena in Internal Combustion Engines*, In Proceedings of the 20th FISITA Congress, May 1984, vol 4, pp 4.17-4.24.

11. Brandstatter W, Johns R.J.R, Wigley G. - *The effect of inlet port geometry on in-cylinder flow structure*, SAE Technical paper series No. 850499, 1985.

12. Lenox H, Scussel A.J. - *The New Ford 2,3L High-Swirl Combustion (HSC) Engine*, SAE Technical paper series No. 831009, 1983.

13. Nagayama I, Araki Y, Iioka Y. - *Effects of Swirl and Squish on S.I. Engine Combustion and Emission*, SAE Technical paper series No. 770217, 1977.

14. Kajiyama K, Nishida K, Murakami A, Arai M, Hiroyasu H. - *An analysis of Swirling Flow in Cylinder for predicting D.I. Diesel Engine Performance*, SAE Technical paper series No. 840518, 1984.

15. Duggal V.K, Kuo T.W, Mukerjee T, Przekwas A.J, Singhal A.K. - *Three-dimensional modelling of In-cylinder processes in D.I. Diesel engines*, SAE Technical paper series No. 840227, 1984.

16. Tanabe S, Hamamoto Y, Ohighashi S. - *Swirl in a four-stroke cycle engine cylinder*, Bulletin of the JSME vol 21 No. 152 Feb, 1978.

17. Marsee F.J, Olree R.M, Hill J.L, Temby A.L. - *Lean burn - A rational approach to Emission Control*, XIX International Fisita Congress, Melbourne Australia Nov 8-12, 1982 vol 1.

18. Arcoumanis C, Whitelaw J.H. - *In-cylinder flow measurements in motored internal combustion engines*, IMechE, 1991 C433/060.

19. Benjamin S.F. - *The development of the GTL 'barrel swirl' combustion system with application to four-valve spark ignition engines*, PI MechE, C54/88.

20. Agnew B, Chan C.L, Tam I.C.K. - *The influence of swirl and fuel type on mass burning rates in spark ignition engines*, PI MechE, C69/88.

21. Wakisaka T, Shimamoto Y, Isshiki Y. - *Induction swirl in a multiple intake valve engine three-dimensional numerical analysis*, PI MechE, C40/88.

22. Kumar S, Ahary M, Lambe S.M, Watson H.C. - *Flame Propagation in a high-speed variable swirl spark ignition engine*, PI MechE, C61/88.

23. Gajendra Babu M.K, Sabharwal R, Sarcar P, Subrahmanyam J.P. - *Studies on the effect of turbulence on the performance characteristics of a spark-ignition engine*, Int Journal of Vehicle Design vol 12, 1991 No. 3 pp 336-344.

24. Gething J.A. - *Performance robbing aspects of intake valve deposits*, SAE Technical paper series No. 872116, 1987.

25. Uzkan T, Borgnakke C, Morel T. - *Characterisation of flow produced by a High-Swirl inlet port*, SAE Technical paper series No. 830266, 1983.

26. Inoue T, Nakanishi K, Noguchi H, Iguchi S. - *The Role of Swirl and Squish in Combustion of the S.I. Engine*, 18th International Congress, Fisita 1980, VDI-Berichte No. 370.

27. Clarke R.H, Dutkiewicz R.K. - *Knock resistance of fuels with decreasing lead levels*, Engineering Research Report No. IER 059, July 1991.

APPENDICES

APPENDIX A

Table A.1 Swirl Ratio Tabulation

ENGINE	SWIRL GENERATOR	MEAN SWIRL RATIO
FORD V6	NONE	0.45
NISSAN 1800	NONE	0.27
VW 1800	NONE	0.24
TOYOTA 1600	NONE	0.02
TOYOTA 22R	HELICAL PORT	0.95
TOYOTA 1300	VALVE/PORT DEPOSITS	0.14
	VALVE DEPOSITS	0.01
	NONE	0.02
NISSAN 1800	SHROUD (DEG.)	
	0	0.60
	30	0.49
	60	0.37
	90	0.27
	120	0.19
	150	0.02
	180	-0.18
NISSAN 1800	DEFLECTOR PLATE	
VW 1600	NONE	0.21
	DEFLECTOR PLATE	1.42
	BAFFLE PLATE HI	1.53
	BAFFLE PLATE LO	-0.03

APPENDIX B

ENGINE DATA

Ford Essex V6

Configuration	:	6 cylinder, 60 deg. V
Valve gear	:	Pushrods, 2 valves per cylinder
Fuel management	:	Single carburetor
Swept Volume	:	2993 cm^3
Bore	:	93.67 mm
Stroke	:	72.42 mm
Compression Ratio	:	9.5 : 1
Standard Spark Timing	:	12° BTDC @ 750 rpm
Combustion Chamber	:	Bowl-in-piston
Maximum Power	:	114 kW @ 5500 rpm
Maximum Torque	:	220 Nm @ 4000 rpm

Nissan L18

Configuration	:	in-line 4 cylinder
Valve gear	:	Single overhead camshaft, 2 valves per cylinder
Fuel management	:	Twin carburetors
Swept Volume	:	1770 cm^3
Bore	:	85.0 mm
Stroke	:	78.0 mm
Compression Ratio	:	9.3 : 1
Standard Spark Timing	:	10° BTDC @ 750 rpm
Combustion Chamber	:	Wedge shape
Maximum Power	:	67 kW @ 5500 rpm
Maximum Torque	:	129 Nm @ 4000 rpm

Volkswagen 1800

Configuration	:	in-line 4 cylinder
Valve gear	:	Single overhead camshaft, 2 valves per cylinder
Fuel management	:	Single carburetor
Swept Volume	:	1781 cm^3
Bore	:	81.0 mm
Stroke	:	86.4 mm
Compression Ratio	:	10 : 1
Standard Spark Timing	:	6^o BTDC @ 850 rpm
Combustion Chamber	:	Bath tub shape
Maximum Power	:	70 kW @ 5200 rpm
Maximum Torque	:	150 Nm @ 3500 rpm

Toyota 4AF 16V

Configuration	:	in-line 4 cylinder
Valve gear	:	Twin overhead camshaft, 4 valves per cylinder
Fuel management	:	Single carburetor
Swept Volume	:	1587 cm^3
Bore	:	81.0 mm
Stroke	:	77.0 mm
Compression Ratio	:	9.5 : 1
Standard Spark Timing	:	10^o BTDC @ 900 rpm
Combustion Chamber	:	Hemispherical shape
Maximum Power	:	70 kW @ 6000 rpm
Maximum Torque	:	135 Nm @ 3600 rpm

APPENDIX C

Engine Pressure Traces

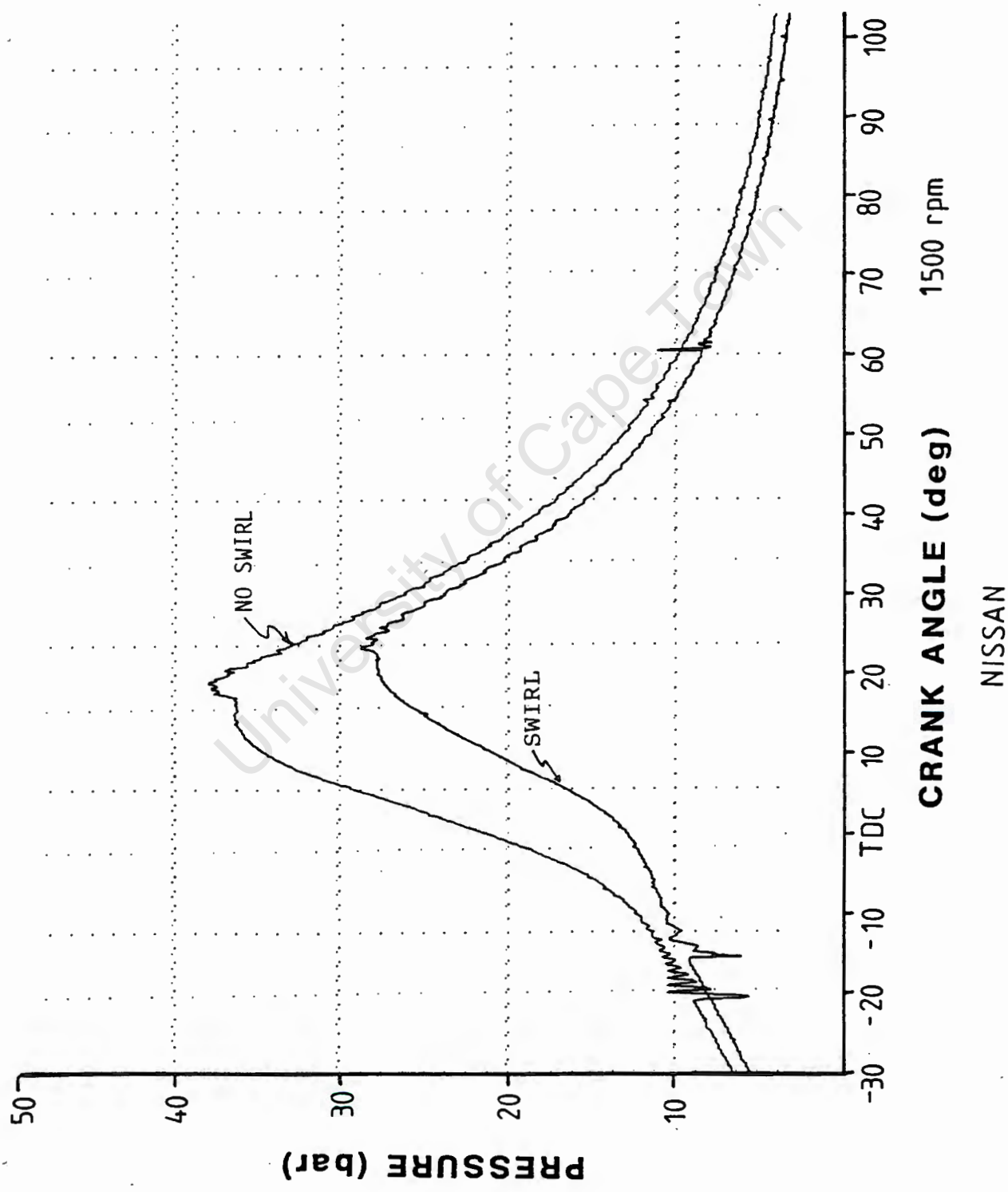

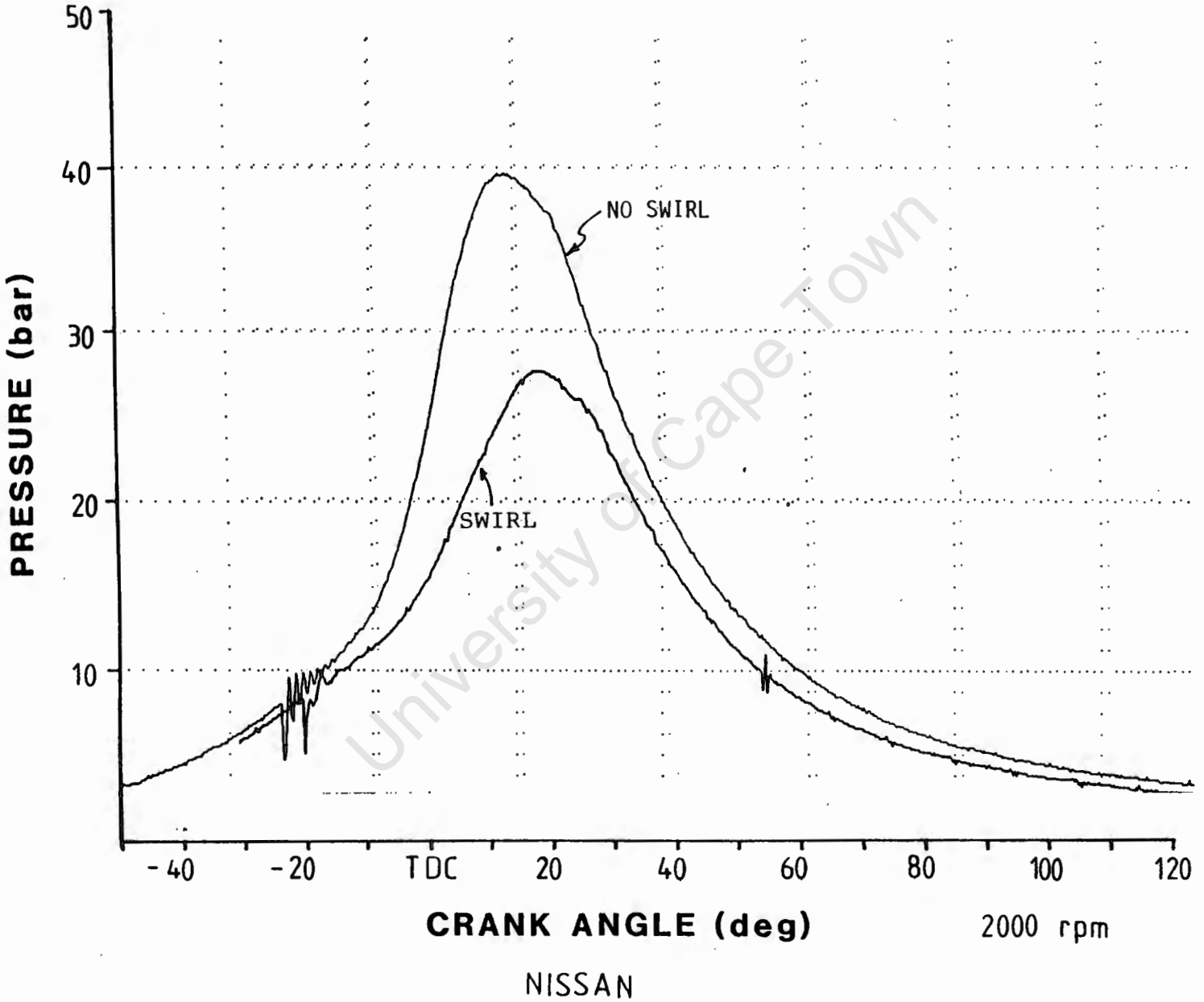

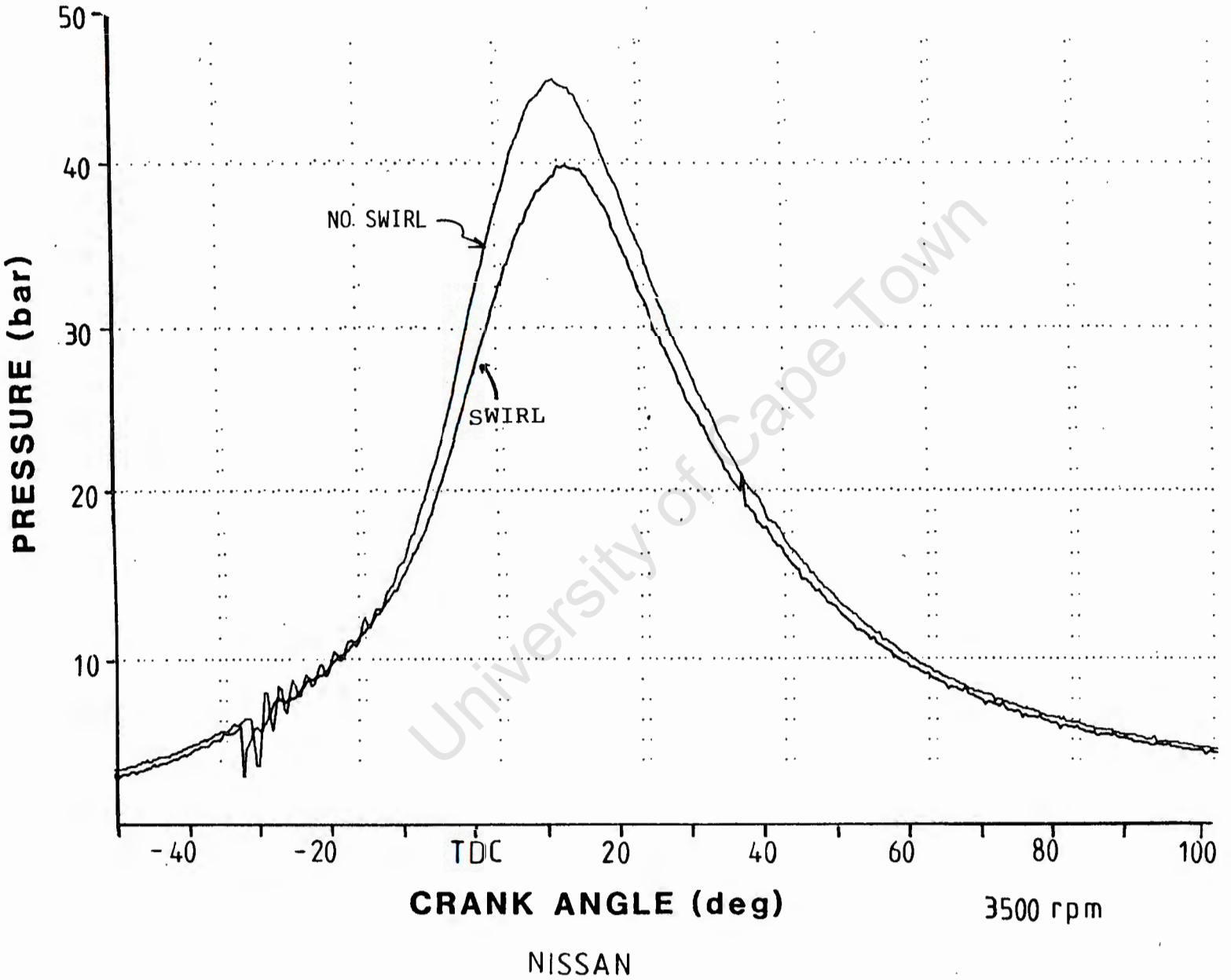

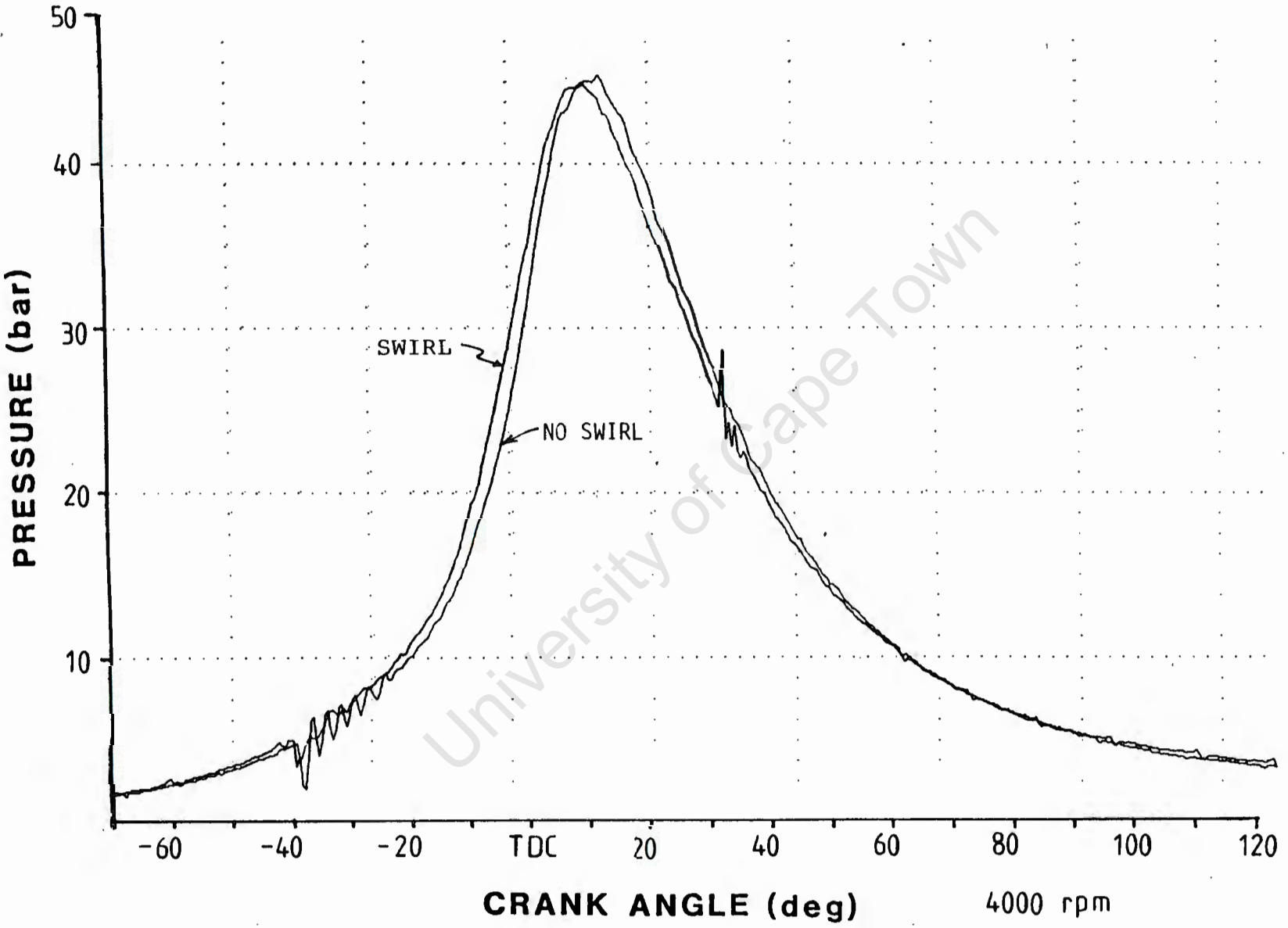

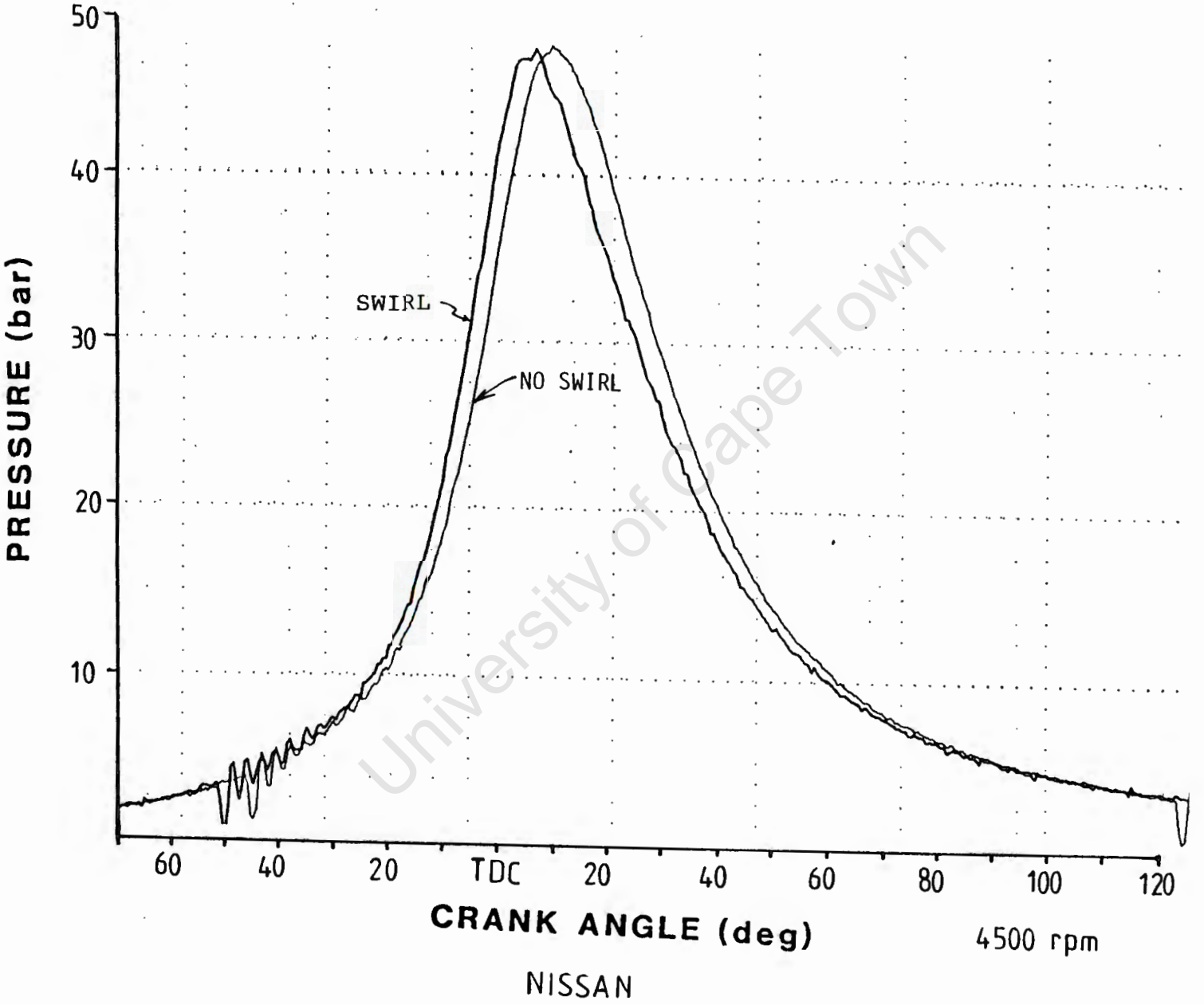

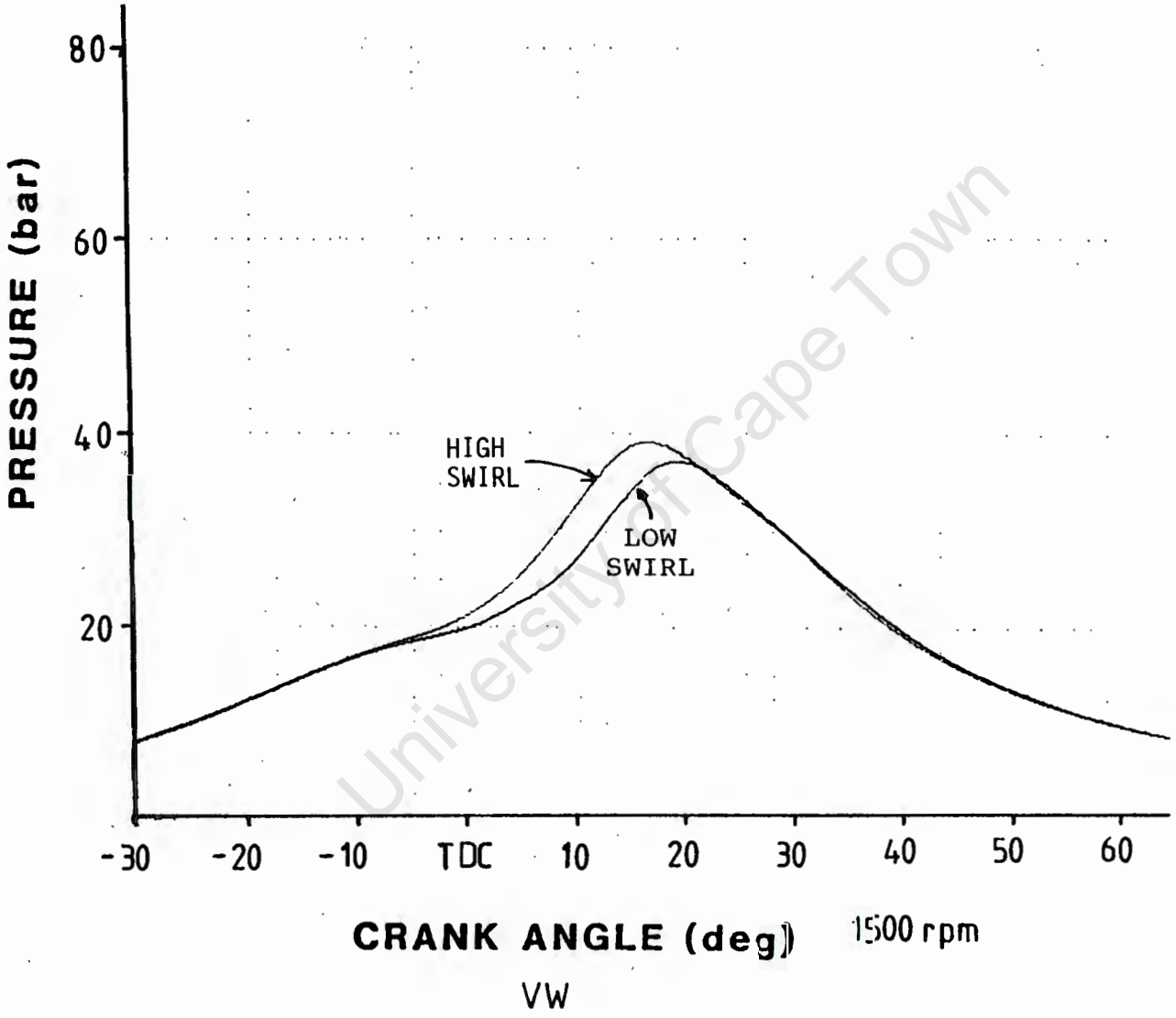

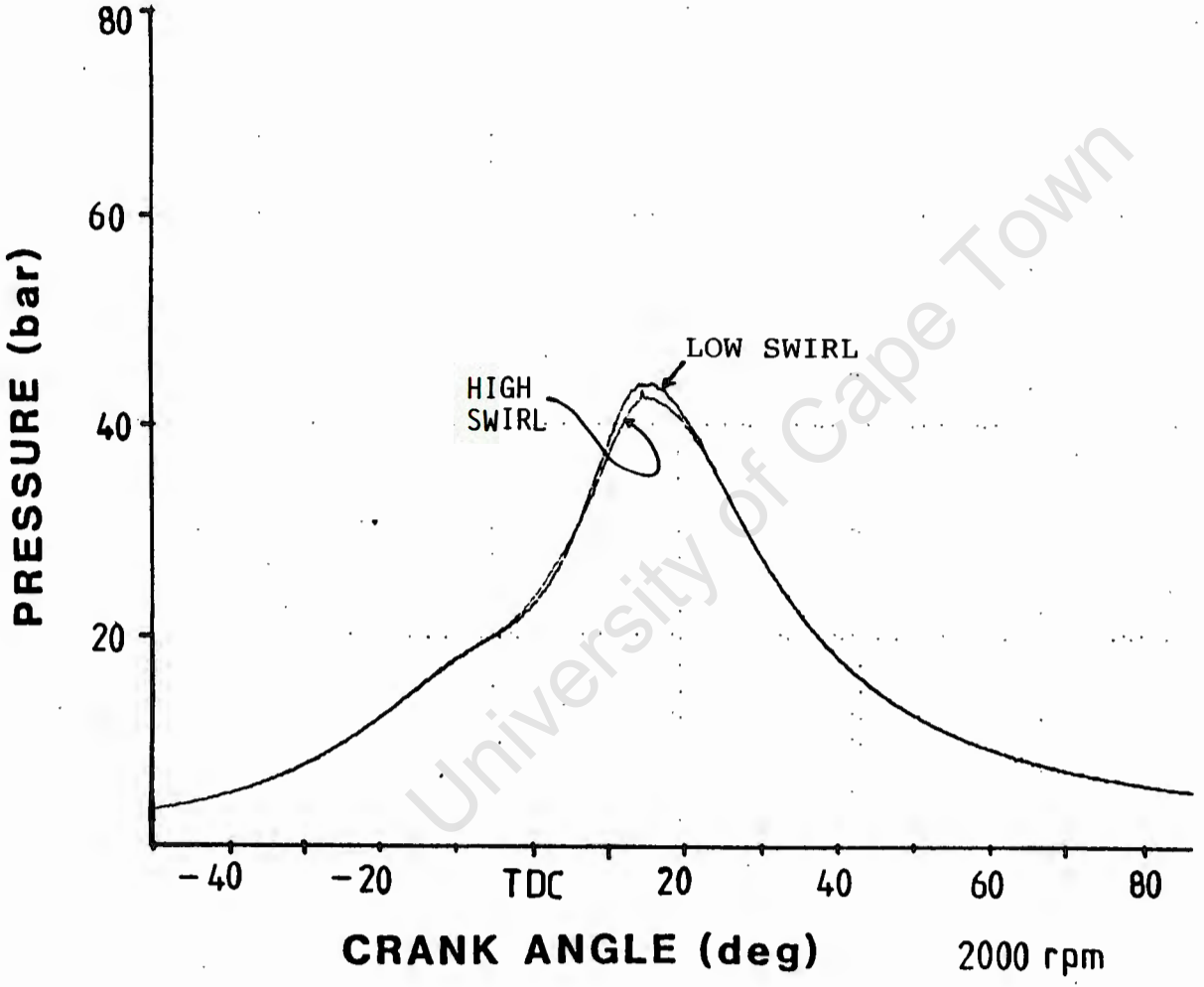

VW

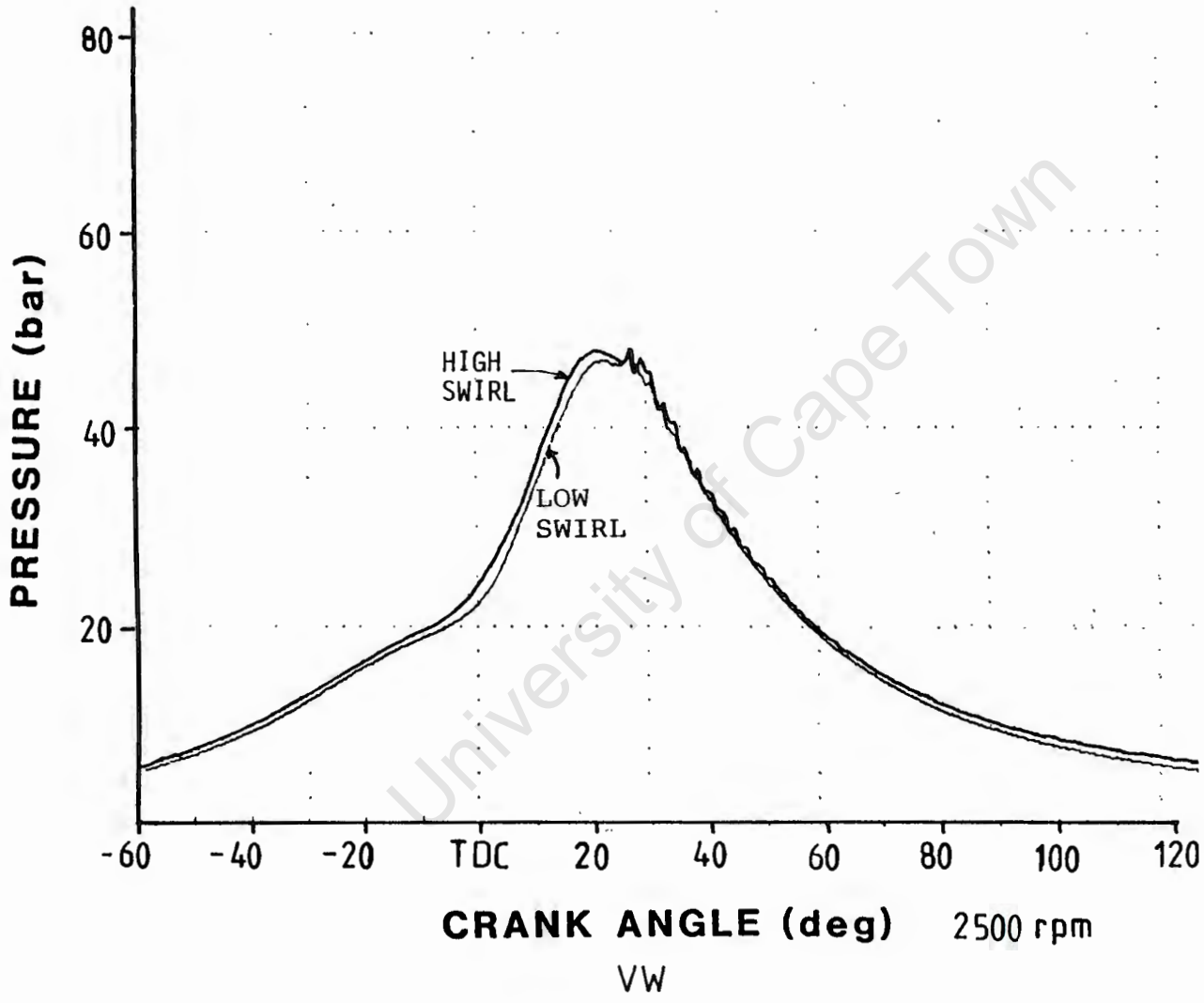

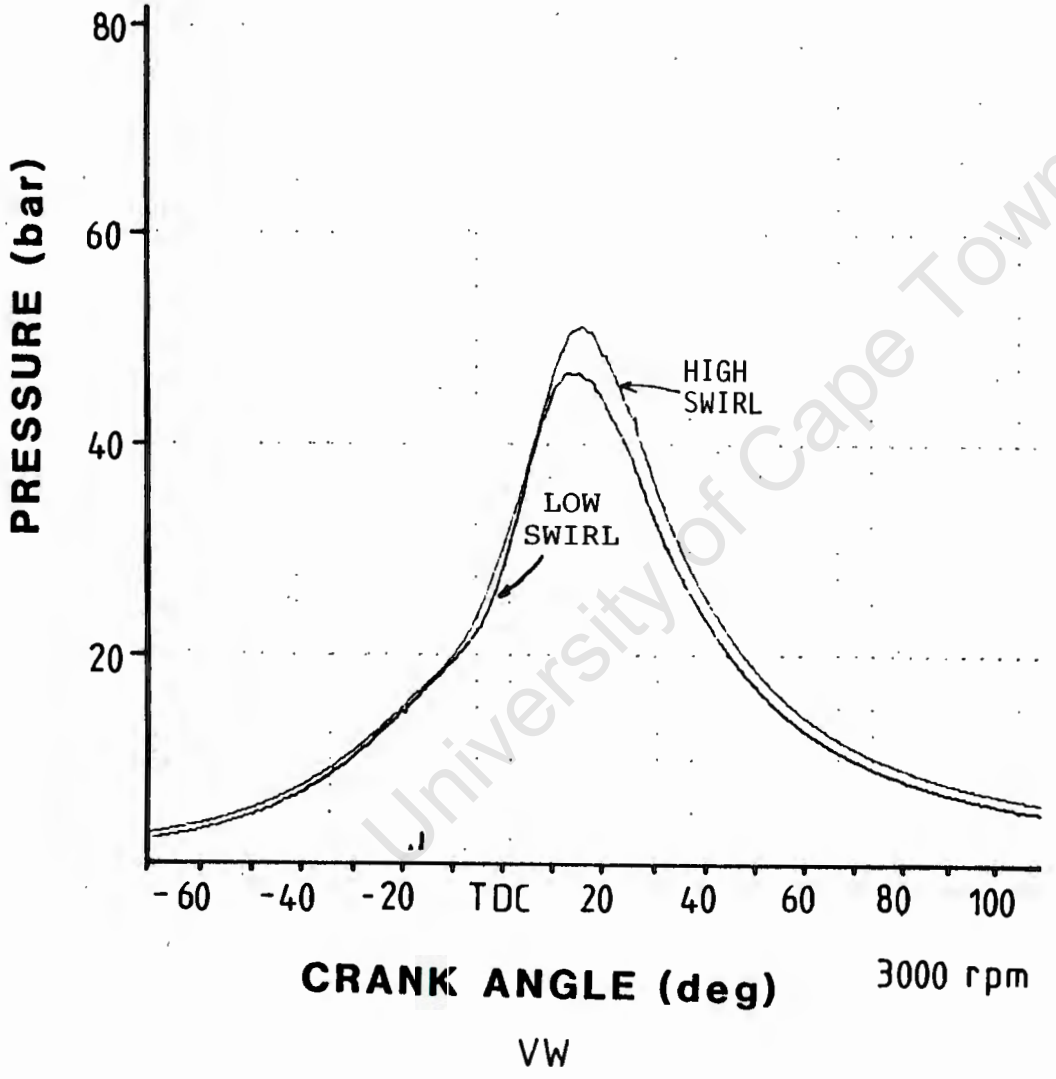

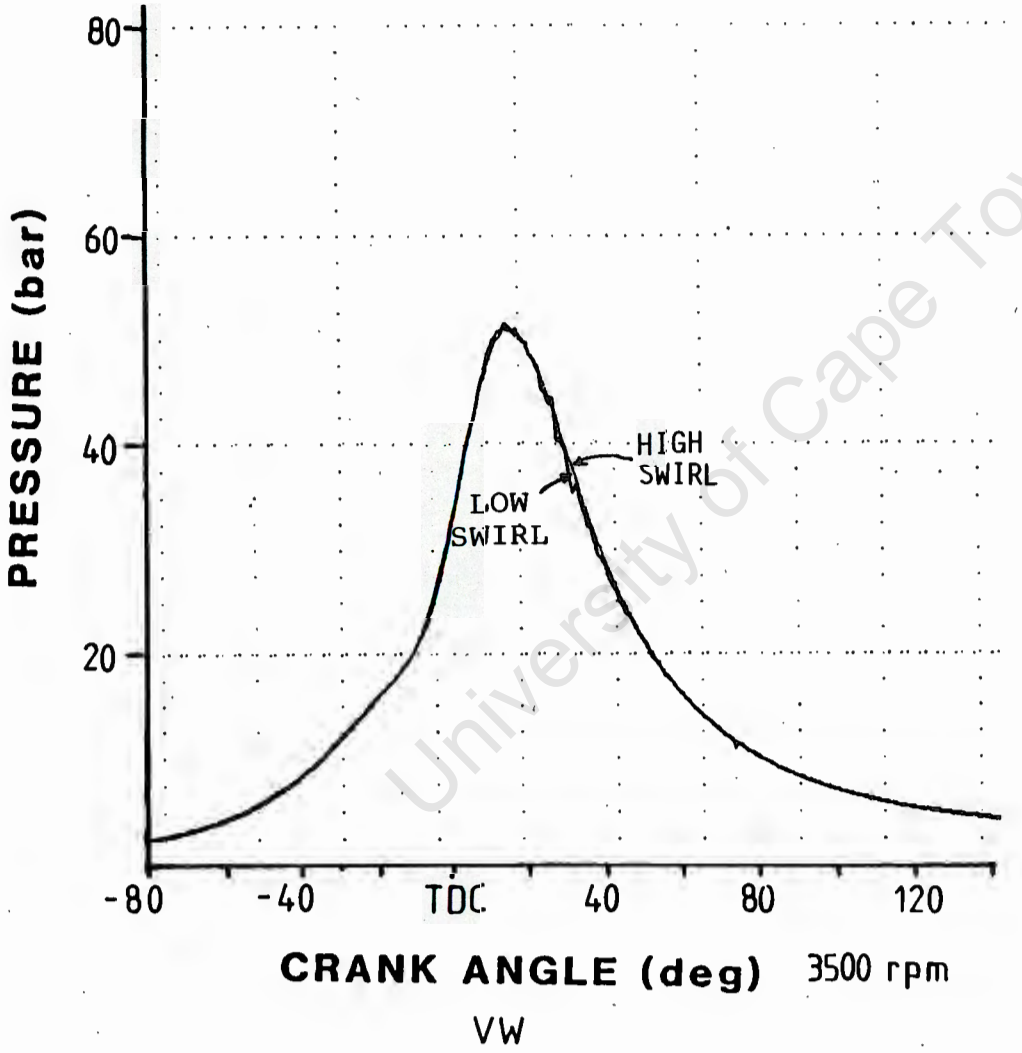

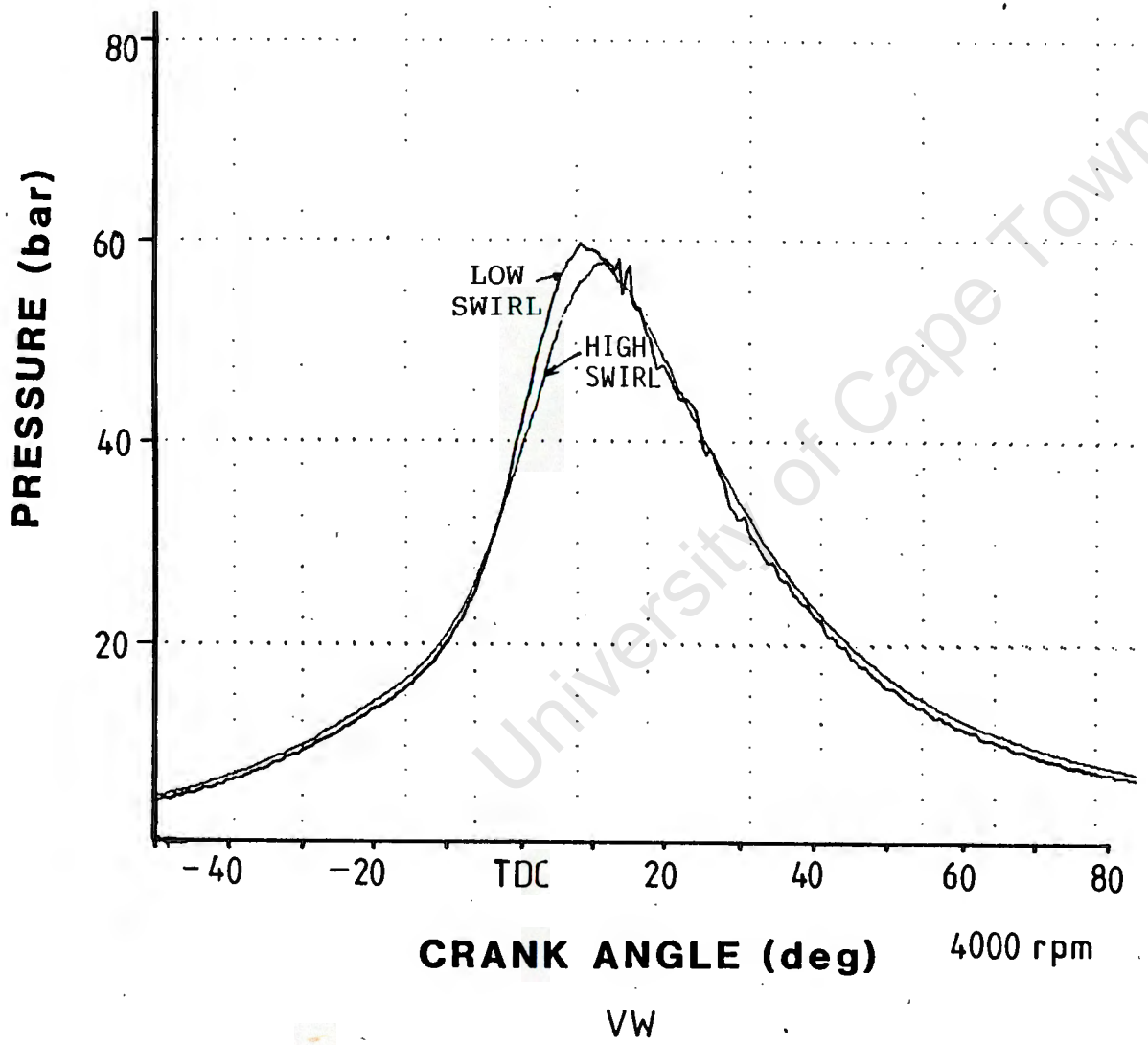

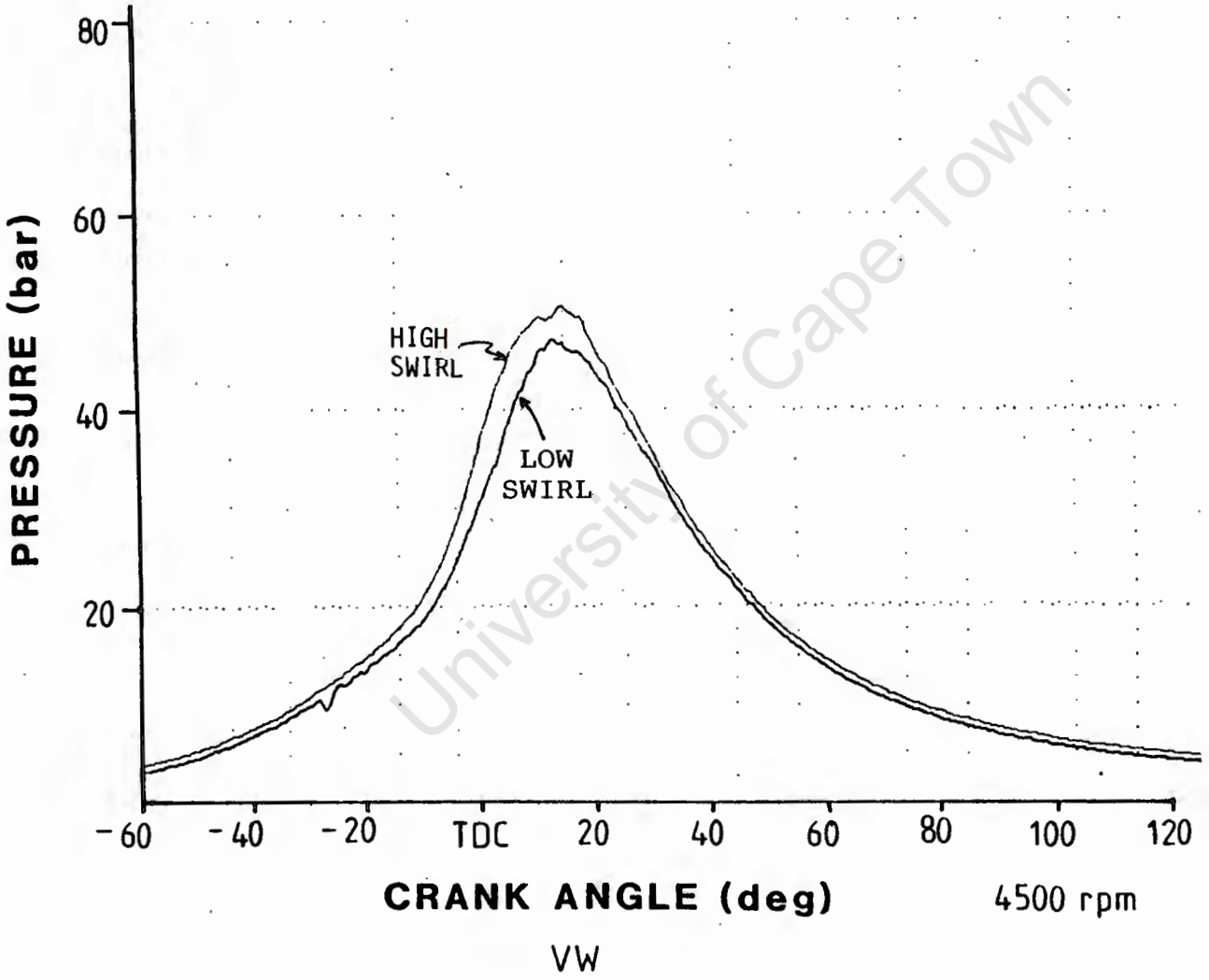

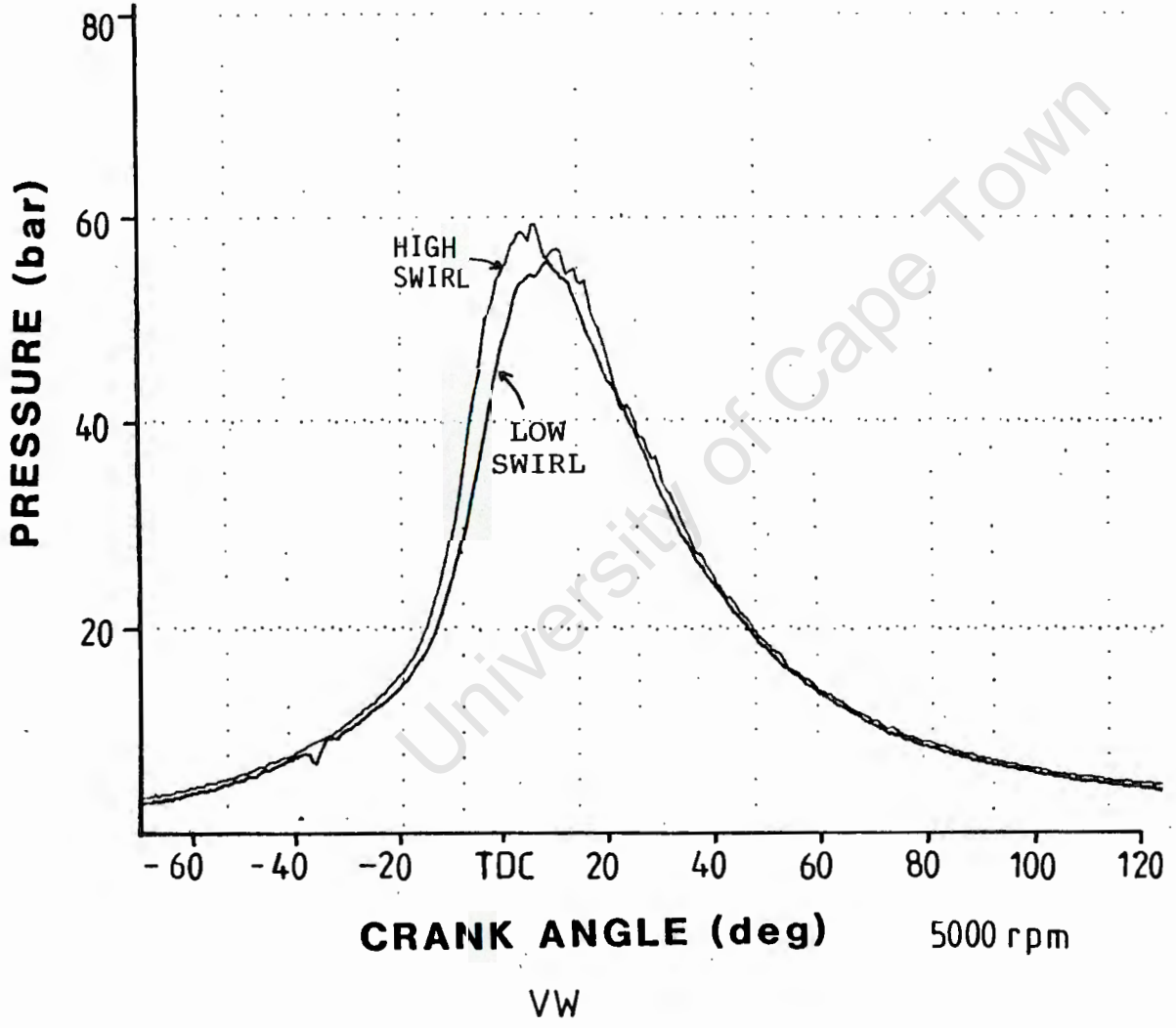

APPENDIX D

AVL Swirl measurement procedure

The test valve lifts are from:

$$h_v = d_v \cdot 0.04 \rightarrow d_v \cdot 0.4$$

where d_v = valve diameter

$= 41 \cdot 0.04 \rightarrow 41 \cdot 0.4$

$= 1.64 \text{ mm} \rightarrow 16.4 \text{ mm}$

incrementing by $41 \cdot 0.04 = 1.64$ mm

The pressure drop across the inlet port is kept constant at 250 mm of water.
The air flowrate is found as follows:

Atmospheric pressure = 102.22 kPa

$P_a - P_1 = 160$ mm $CCl_4 \Rightarrow P_1 = 99.72$ kPa

$P_a - P_2 = 160$ mm $CCl_4 \Rightarrow P_2 = 99.21$ kPa

The air density was determined by fitting a third order polynomial to steam table data.
Air Flowrate:

$$G = C_d \cdot \epsilon \cdot A_o \sqrt{2 \cdot \rho \cdot (P_1 - P_2)} \text{ kg/s}$$

$$= 0.61 \cdot 0.997 \cdot \frac{\pi}{4} \cdot 0.028^2 \sqrt{2 \cdot 1.18 \cdot (99.72 - 99.21) \cdot 1000}$$

$$= 0.0128 \text{ kg/s}$$

The mean swirl ratio is defined as $\omega_{paddle}/\omega_{engine} = rpm_{paddle}/rpm_{engine} = n_d/n$

n is found by equating the mean axial flow velocity in the cylinder c_a with a mean piston speed $c_m = s \cdot n/30$,

hence $c_m = c_a = s \cdot n/30 = G/A_L \cdot \rho$

where A_L = cylinder area

hence $\frac{n_d}{n} = \frac{n_d \cdot \rho \cdot A_L \cdot s}{G \cdot 30}$

$$= \frac{252 \cdot 1.21 \cdot 0.094^2 \pi \cdot 0.07242}{0.037 \cdot 30 \cdot 4}$$

$$= 0.138$$

The ratio between mean and actual piston speed is given by:

$$\frac{c}{c_m} = \frac{\pi}{2}\left(1 + \frac{\lambda \cdot \cos\alpha}{\sqrt{1 - \lambda^2 \cdot \sin^2\alpha}}\right) \cdot \sin\alpha$$

where $\lambda = r/l = 0.253$

i.e. stroke-connecting-rod ratio

$$\frac{c}{c_m} = \frac{\pi}{2}\left(1 + \frac{0.253 \cdot \cos 45}{\sqrt{1 - 0.253^2 \cdot \sin^2 45}}\right) \sin 45$$
$$= 1.312$$

Let Y_n = the product of swirl ratio and speed ratio squared for a particular crank angle

i.e. $Y = (n_d/n) \cdot (c/c_m)^2$

$Y_4 = 0.0986 \cdot 1.312^2$

$= 0.169$

The Y values corresponding to crank angles from 15° to 180° incrementing by 15° are integrated using Simpsons Rule.

Thus in this case the mean swirl ratio is: $(n_d/n)_m = 0.453$

Check on Swirl Ratio calculation error

	P1mm	**P2mm**	**rpm**	**swirl ratio**
actual readings = >	184	505	1194	0.596
possible deviation = >	184	503	1104	0.552

$$\text{\% difference} = \frac{0.596 - 0.552}{0.596}$$
$$= 7.4\ \%$$

or

	P1mm	**P2mm**	**rpm**	**swirl ratio**
actual readings = >	159	180	60	0.117
possible deviation = >	153	187	84	0.128

$$\text{\% difference} = \frac{0.128 - 0.117}{0.128}$$
$$= 8.5\ \%$$

APPENDIX E

Basic programme listing: " SWIRL "

```
10 '*************************************************************************"
20 'THIS PROGRAMME CALCULATES INTERPOLATED VALUES OF SWIRL RATIO FOR CRANK ANG
S CORRESPONDING TO VALVE LIFT. IT THEN CALCULATES A MEAN SWIRL RATIO"
30 '*************************************************************************
40 DIM E(13),Y(13),D(13),C(13)
50 PRINT"ENTER ENGINE TYPE
60 INPUT E$
70 PRINT
80 PRINT"ENTER ENGINE STROKE AND CONNECTING ROD LENGTH
90 INPUT S,L
100 LAMBDA=S/L/2
110 PRINT"ENTER INLET VALVE DIAMETER dv"
120 INPUT DV
130 PRINT
140 PRINT"ENTER VALVE LIFT PROFILE AT 15 DEGREE INTERVALS
150 FOR I=1 TO 13
160 INPUT C(I)
170 PRINT
180 C(I)=C(I)/DV
190 NEXT I
200 PRINT"ARE ENTERED VALUES CORRECT (Y/N)
210 INPUT Q$
220 PRINT
230 IF Q$="N" OR Q$="n" THEN GOTO 140
240 FOR I=1 TO 10
250 A(I)=.04*I
260 NEXT I
270 PRINT"ENTER INSTANTANEOUS SWIRL RATIO FOR THE NORMALISED VALVE LIFT
280 FOR I= 1 TO 10
290 INPUT B(I)
300 PRINT
310 NEXT I
320 PRINT"ARE ENTERED VALUES CORRECT (Y/N)"
330 INPUT Q$
340 IF Q$= "N"  OR Q$="n" THEN GOTO 270
350 '*************************************************************************
360 'COMPARE TEST VALVE LIFTS WITH CORRESPONDING CRANK ANGLE VALVE LIFT
370 FOR I= 1 TO 13
380 FLAG = 0
390 FOR J = 1 TO 10
400 IF C(I)<A(J) THEN GOSUB 810
410 IF C(I)=A(J) THEN GOSUB 810
420 IF FLAG = 1 THEN GOTO 440
430 NEXT J
440 NEXT I
450 '*************************************************************************
460 'THIS CALCULATES THE SPEED RATIO CORRESPONDING TO EACH CRANK ANGLE
470 K=0
480 FOR I= 0 TO 180 STEP 15
490 U=I*.0174532925#
500 K=K+1
510 E(K)= ABS(1.570796*(1+(LAMBDA*COS(U))/(1-(LAMBDA*SIN(U))^2)^.5)*SIN(U))
520 NEXT I
```

```
530 '*****************************************************************
540 'THIS CALCULATES Y VALUES i.e. SWIRL RATIO * SPEED RATIO SQUARED
550 FOR I = 1 TO 13
560 Y(I)=D(I)*E(I)^2
570 NEXT I
580 '*****************************************************************
590 'THIS CALCULATES A MEAN SWIRL RATIO USING SIMPSONS RULE
600 SWIRL=(4*Y(2)+2*Y(3)+4*Y(4)+2*Y(5)+4*Y(6)+2*Y(7)+4*Y(8)+2*Y(9)+4*Y(10)+2*Y
1)+4*Y(12))/36
610 '*****************************************************************
620 'PRINT RESULTS
630 PRINT"RESULTS FOR ";E$;"  ENGINE"
640 PRINT
650 PRINT TAB(6)"SWIRL" TAB(25)"SPEED RATIO" TAB(48)"Y VALUE"
660 PRINT
670 FOR I=1 TO 13
680 PRINT USING "     #.##              ";D(I),E(I),Y(I)
690 NEXT I
700 PRINT
710 PRINT
720 PRINT
730 PRINT " THE MEAN SWIRL RATIO FOR THE ";E$;" ENGINE IS ";SWIRL
740 PRINT
750 PRINT"EXIT (Y/N)
760 INPUT G$
770 PRINT
780 IF G$="Y" OR G$="y" THEN 800
790 GOTO 140
800 END
810 '*****************************************************************
820 'SUBROUTINE CALCULATION FOR THE INTERPOLATED SWIRL RATIOS
830 D(I)=(A(J)-C(I))/(A(J)-A(J-1))*B(J-1)+(1-(A(J)-C(I))/(A(J)-A(J-1)))*B(J)
840 FLAG=1
850 RETURN

40 PRINT
50 PRINT TAB(6)"SWIRL" TAB(25)"SPEED RATIO" TAB(48)"Y VALUE"
60 PRINT
70 FOR I=1 TO 13
80 PRINT USING "     #.##              ";D(I),E(I),Y(I)
90 NEXT I
00 PRINT
10 PRINT
 20 PRINT
 30 PRINT " THE MEAN SWIRL RATIO FOR THE ";E$;" ENGINE IS ";SWIRL
 40 PRINT
 50 PRINT"EXIT (Y/N)
 60 INPUT G$
 70 PRINT
 80 IF G$="Y" OR G$="y" THEN 800
 90 GOTO 140
 00 END
 10 '*****************************************************************
 20 'SUBROUTINE CALCULATION FOR THE INTERPOLATED SWIRL RATIOS
 30 D(I)=(A(J)-C(I))/(A(J)-A(J-1))*B(J-1)+(1-(A(J)-C(I))/(A(J)-A(J-1)))*B(J)
 40 FLAG=1
 50 RETURN
```

Basic programme - mean swirl ratio calculation results

RESULTS FOR FORD V6 ENGINE

SWIRL	SPEED RATIO	Y VALUE
0.00	0.00	0.00
0.00	0.51	0.00
0.00	0.96	0.00
0.10	1.31	0.17
0.23	1.54	0.54
0.38	1.62	0.99
0.51	1.57	1.27
0.57	1.41	1.15
0.57	1.18	0.80
0.49	0.91	0.40
0.31	0.61	0.12
0.19	0.31	0.02
0.05	0.00	0.00

THE MEAN SWIRL RATIO FOR THE FORD V6 ENGINE IS .4534666

APPENDIX F

Example of Swirl Rig Test data sheet

APPENDIX F

SWIRL RIG DATA SHEET - FORD V6

BAROMETRIC PRESSURE 1022.2 HPa 102.22 kPa

INLET TEMPERATURE (To) DRY 19.4 (To) WET 16.2 DEG.C

ENGINE TYPE FORD 3000

BORE 93.67 mm

CONROD 143.3 mm STROKE 72.42 mm r/l= 0.253

DISPLACEMENT 2994.3 cm cubed

NO OF CYLINDERS 6 VALVES/CYL 2

DIAMETER OF LINER 94 mm

CROSS SECTIONAL AREA OF LINER 0.006940 m squared

CHAMBER TYPE BOWL-IN-PISTON

SWIRL TYPE NONE

INNER DIAMETER OF VALVE (dv) 41 mm

hv(in)	hv (mm)	PA-P1 (mm)	PA-P2 (mm)	nd rps/2	nd rpm	P1	P2
0.065	1.64	160	192	0	0	99.72	99.22
0.129	3.28	165	262	0	0	99.64	98.13
0.194	4.92	171	358	0	0	99.55	96.63
0.258	6.56	177	442	2.1	252	99.45	95.31
0.323	8.2	183	499	4.9	588	99.36	94.42
0.387	9.84	184	505	9.95	1194	99.34	94.33
0.452	11.48	184	504	14.4	1728	99.34	94.34
0.517	13.12	NA	NA	NA	NA	NA	NA
0.581	14.76	NA	NA	NA	NA	NA	NA
0.646	16.4	NA	NA	NA	NA	NA	NA

Example of Swirl Rig Test calculation sheet

APPENDIX F

MEAN SWIRL RATIO CALCULATION FOR - FORD V6 ENGINE

			P1-P2/P1	P2/P1 ^ 1/K
ORIFICE DISCHARGE COEFFICIENT	0.61			
AIR COMPRESSIBILITY FACTOR	0.996		0.005	0.996
ORIFICE BORE AREA	6.16E-04	m squared		
AIR VAPOUR PARTIAL PRESSURE	1632.80	Pa		
AIR VAPOUR SATURATION PRESSURE	2251.41	Pa		
AIR RELATIVE HUMIDITY	72.52	%		
AIR DENSITY	1.210	kg/cubic m		

VALVE LIFT / VALVE DIAM	SWIRL RATIO nd/n	FLOW RATE kg/s	AIR DENS. kg/mcub
0.04	0.000	0.013	1.180
0.08	0.000	0.022	1.179
0.12	0.000	0.031	1.178
0.16	0.138	0.037	1.177
0.2	0.296	0.040	1.176
0.24	0.596	0.041	1.176
0.28	0.863	0.041	1.176
0.32	NA	NA	NA
0.36	NA	NA	NA
0.4	NA	NA	NA

CRANK ANGLE	hv	hv/dv	c/cm	nd/n	Y1
0	1.21	0.030	0.000	0.000	0.000
15	2.67	0.065	0.506	0.000	0.000
30	4.38	0.107	0.959	0.000	0.000
45	6.08	0.148	1.312	0.098	0.169
60	7.48	0.182	1.536	0.226	0.534
75	8.64	0.211	1.620	0.376	0.987
90	9.39	0.229	1.571	0.513	1.265
105	9.71	0.237	1.415	0.572	1.145
120	9.7	0.237	1.184	0.570	0.799
135	9.24	0.225	0.909	0.485	0.401
150	8.3	0.202	0.612	0.314	0.118
165	7.11	0.173	0.307	0.191	0.018
180	5.51	0.134	0.000	0.050	0.000

MEAN SWIRL RATIO (nd/n)m => 0.453